

ANL-80-8

Dr. 2552

ANL-80-8

R. 3753

4/23/85 R

**COMMIX-SA-1: A THREE-DIMENSIONAL
THERMOHYDRODYNAMIC COMPUTER PROGRAM
FOR SOLAR APPLICATIONS**

MASTER

by

**W. T. Sha, E. I. H. Lin, R. C. Schmitt,
K. V. Liu, J. R. Hull, J. J. Oras, Jr.,
and H. M. Domanus**



ARGONNE NATIONAL LABORATORY, ARGONNE, ILLINOIS

**Prepared for the U. S. DEPARTMENT OF ENERGY
under Contract W-31-109-Eng-38**

DISTRIBUTION OF THIS DOCUMENT IS UNLIMITED

DISCLAIMER

This report was prepared as an account of work sponsored by an agency of the United States Government. Neither the United States Government nor any agency Thereof, nor any of their employees, makes any warranty, express or implied, or assumes any legal liability or responsibility for the accuracy, completeness, or usefulness of any information, apparatus, product, or process disclosed, or represents that its use would not infringe privately owned rights. Reference herein to any specific commercial product, process, or service by trade name, trademark, manufacturer, or otherwise does not necessarily constitute or imply its endorsement, recommendation, or favoring by the United States Government or any agency thereof. The views and opinions of authors expressed herein do not necessarily state or reflect those of the United States Government or any agency thereof.

DISCLAIMER

Portions of this document may be illegible in electronic image products. Images are produced from the best available original document.

The facilities of Argonne National Laboratory are owned by the United States Government. Under the terms of a contract (W-31-109-Eng-38) among the U. S. Department of Energy, Argonne Universities Association and The University of Chicago, the University employs the staff and operates the Laboratory in accordance with policies and programs formulated, approved and reviewed by the Association.

MEMBERS OF ARGONNE UNIVERSITIES ASSOCIATION

The University of Arizona
Carnegie-Mellon University
Case Western Reserve University
The University of Chicago
University of Cincinnati
Illinois Institute of Technology
University of Illinois
Indiana University
The University of Iowa
Iowa State University

The University of Kansas
Kansas State University
Loyola University of Chicago
Marquette University
The University of Michigan
Michigan State University
University of Minnesota
University of Missouri
Northwestern University
University of Notre Dame

The Ohio State University
Ohio University
The Pennsylvania State University
Purdue University
Saint Louis University
Southern Illinois University
The University of Texas at Austin
Washington University
Wayne State University
The University of Wisconsin-Madison

NOTICE

This report was prepared as an account of work sponsored by an agency of the United States Government. Neither the United States Government or any agency thereof, nor any of their employees, make any warranty, express or implied, or assume any legal liability or responsibility for the accuracy, completeness, or usefulness of any information, apparatus, product, or process disclosed, or represent that its use would not infringe privately owned rights. Reference herein to any specific commercial product, process, or service by trade name, mark, manufacturer, or otherwise, does not necessarily constitute or imply its endorsement, recommendation, or favoring by the United States Government or any agency thereof. The views and opinions of authors expressed herein do not necessarily state or reflect those of the United States Government or any agency thereof.

Printed in the United States of America
Available from
National Technical Information Service
U. S. Department of Commerce
5285 Port Royal Road
Springfield, VA 22161

NTIS price codes
Printed copy: A06
Microfiche copy: A01

ANL-80-8

ARGONNE NATIONAL LABORATORY
9700 South Cass Avenue
Argonne, Illinois 60439

COMMIX-SA-1: A THREE-DIMENSIONAL
THERMOHYDRODYNAMIC COMPUTER PROGRAM
FOR SOLAR APPLICATIONS

by

W. T. Sha, E. I. H. Lin, R. C. Schmitt,
K. V. Liu, J. R. Hull, J. J. Oras, Jr.,
and H. M. Domanus

Components Technology Division

November 1980

DISCLAIMER

This book was prepared as an account of work sponsored by an agency of the United States Government. Neither the United States Government nor any agency thereof, nor any of their employees, makes any warranty, express or implied, or assumes any legal liability or responsibility for the accuracy, completeness, or usefulness of any information, apparatus, product, or process disclosed, or represents that its use would not infringe privately owned rights. Reference herein to any specific commercial product, process, or service by trade name, trademark, manufacturer, or otherwise does not necessarily constitute or imply its endorsement, recommendation, or favoring by the United States Government or any agency thereof. The views and opinions of authors expressed herein do not necessarily state or reflect those of the United States Government or any agency thereof.

DISTRIBUTION OF THIS DOCUMENT IS UNLIMITED

[Signature]

THIS PAGE
WAS INTENTIONALLY
LEFT BLANK

TABLE OF CONTENTS

	<u>Page</u>
ABSTRACT.....	7
I. INTRODUCTION.....	7
II. GOVERNING EQUATIONS	9
A. Relations in Cylindrical Coordinates.....	10
B. Integral Treatment of Singularities.....	11
III. FINITE-DIFFERENCE EQUATIONS AND SOLUTION SCHEME.....	13
A. Finite-difference Equations.....	13
1. The Continuity Equation.....	13
2. The Momentum Equation.....	15
3. The Energy Equation.....	23
4. Computations near $r = 0$	27
5. The Pressure-correction Equation.....	34
B. Solution Procedure.....	35
1. The Modified ICE Scheme.....	35
2. Flow Diagram.....	37
3. Convergence Criterion.....	37
C. Physical System and Parameters.....	37
1. Properties of Water.....	37
2. A Hydraulic Model for Impermeable and Perforated Baffles.....	39
3. Thermal Interactions between Fluid and Structures.....	41
IV. INITIAL AND BOUNDARY CONDITIONS.....	44
A. Initial Conditions.....	44
B. Boundary Conditions.....	44
1. Grouped Fictitious Boundary Cells.....	44
2. Velocity-boundary Conditions.....	46
3. Temperature-boundary Conditions.....	48
V. CODE STRUCTURE.....	50
VI. INPUT DESCRIPTION.....	52

TABLE OF CONTENTS

	<u>Page</u>
VII. SAMPLE PROBLEMS.....	61
A. Heat Discharge from a Simple Cylindrical Storage Tank.....	61
B. Heat Discharge from a VCCB Tank.....	63
VIII. CONCLUDING REMARKS.....	95
 APPENDIXES	
A. A Simple Eddy-diffusivity Turbulence Model.....	96
B. Thermophysical Properties of Water.....	98
C. A Modified Successive Overrelaxation Iteration Scheme.....	102
ACKNOWLEDGMENTS.....	106
REFERENCES.....	106

LIST OF FIGURES

<u>No.</u>	<u>Title</u>	<u>Page</u>
1.	A Typical Computation Cell in a Staggered Cylindrical-coordinate Grid System.....	13
2.	Definitions of Coordinates and Coordinate Increments in the Kth Polar Plane.....	13
3.	Staggered Grid and Degenerate Control Volumes in Cylindrical-coordinate System.....	27
4.	Control Volume for v or p with Stress Components Shown on Surfaces.....	31
5.	Control Volume for u_x and u_y at Center.....	31
6.	A Simplified Flow Chart for COMMIX-SA-1 Execution.....	38
7.	An Example Illustrating COMMIX-SA-1 Numbering Schemes and Grouping of Fictitious Boundary Cells.....	45
8.	Zero Normal-velocity-gradient Boundary Condition.....	47
9.	Velocity at Outflow Boundary Determined by Local Mass Balance....	48
10.	Velocity at Outflow Boundary Determined by Global Mass Balance...	48
11.	Storage-tank Geometry and Finite-difference Grid Layout.....	61
12.	Temperature Profile at Tank Centerline.....	62
13.	Temperature Distribution across Section A-A at $t = 10.7$ s.....	62
14.	Temperature Distribution across Section B-B at $t = 10.7$ s.....	63
15.	Flow Pattern across Section A-A at $t = 10.7$ s; $V_{in} = 1$ m/s.....	63
16.	Storage Tank with Vertical Concentric Cylindrical Baffles and Ring Distributor.....	64
17.	Finite-difference Grid Layout for 15° Sector of VCCB Tank.....	64
18.	Evolution of Temperature Profile during Heat Discharge from a Storage Tank.....	64
B.1.	Density of Water as a Function of Temperature.....	98
B.2.	Viscosity of Water as a Function of Temperature.....	99
B.3.	Specific Heat of Water as a Function of Temperature.....	99
B.4.	Thermal Conductivity of Water as a Function of Temperature.....	100
B.5.	Kinematic Viscosity of Water as a Function of Temperature.....	100
B.6.	Thermal Diffusivity of Water as a Function of Temperature.....	101

LIST OF FIGURES

<u>No.</u>	<u>Title</u>	<u>Page</u>
B.7.	Prandtl Number of Water as a Function of Temperature.....	101
C.1.	Convergence Properties of Various Point-relaxation Methods.....	104
C.2.	Effects of Time-step Size on Convergence Properties of the Jacobi and SOR Methods.....	105

COMMIX-SA-1: A THREE-DIMENSIONAL
THERMOHYDRODYNAMIC COMPUTER PROGRAM
FOR SOLAR APPLICATIONS

by

W. T. Sha, E. I. H. Lin (Principal Investigators),
R. C. Schmitt, K. V. Liu, J. R. Hull,
J. J. Oras, Jr., and H. M. Domanus

ABSTRACT

COMMIX-SA-1 is a three-dimensional, transient, single-phase, compressible-flow, component computer program for thermohydrodynamic analysis. It was developed for solar applications in general, and for analysis of thermocline storage tanks in particular. The conservation equations (in cylindrical coordinates) for mass, momentum, and energy are solved as an initial-boundary-value problem. The detailed numerical-solution procedure based on a modified ICE (Implicit Continuous-Fluid Eulerian) technique is described. A method for treating the singularity problem arising at the origin of a cylindrical-coordinate system is presented. In addition, the thermal interactions between fluid and structures (tank walls, baffles, etc.) are explicitly accounted for. Finally, the COMMIX-SA-1 code structure is delineated, and an input description and sample problems are presented.

I. INTRODUCTION

Successful utilization of solar energy hinges on developing efficient methods of energy collection and storage. Heat-storage components play an important role in solar heating, cooling, agriculture applications, desalination, process-heat systems and electricity generation. Owing to the intermittent and diurnal nature of solar insolation, and to the often-encountered phase lag between energy collection and demand, storage components such as thermocline tanks, rock beds, and salt-gradient solar ponds are required to store the collected thermal energy. The thermal-energy storage efficiency varies from one storage component to the next, depending on design of the component and fluid-flow and heat-transfer processes that occur within it. In order to improve storage design and hence system performance, the thermohydrodynamic responses of the storage components must be understood in detail. This requires analyses of storage behavior using an appropriate detailed thermohydrodynamic model.

The computer code described in this report was developed in response to this need. The computer code is designated COMMIX-SA-1, an acronym derived from COmponent MIXing-Solar Applications-1st version. Although its analytical framework is general and suitable for treatment of a variety of storage components, COMMIX-SA-1 confines its attention to the analysis of heat-storage water tanks with cylindrical geometries, since these are the most commonly used in solar domestic hot-water and space-heating applications at present. Before the development of COMMIX-SA-1, the analytical models available for analyzing water tanks were mostly one-dimensional (i.e., they treated only one space dimension, as in Refs. 2-4, among others) and at best two-dimensional.⁵ The applicability of these models is limited, since three-dimensional effects are often important, especially when storage tanks possess advanced design features. The shortcomings of the one-dimensional models are particularly serious in that these models fail even to account for the effects of tank height-to-diameter ratio and inlet/outlet flow rate. This must not be construed, however, to mean that one-dimensional models are utterly useless; their utility lies in their simplicity and ease of application, provided that the one-dimensional assumption is approximately true. For the purpose of understanding the thermohydrodynamic behavior inside a storage component, and for the sake of identifying and evaluating more advanced storage design, however, a rigorous, flexible, three-dimensional model must be relied upon.

In fact, when the development of COMMIX-SA-1 was first undertaken in FY 1978, the primary objective was to develop a three-dimensional model for investigating flow stratification in thermocline storage tanks.⁶ Subsequently, through parametric studies using COMMIX-SA-1, the objective was broadened to include the study of improved storage-tank designs that give high charge and discharge efficiencies.⁷ Recently, the general analytical framework of COMMIX-SA-1 was further extended for applications to rock beds and salt-gradient solar ponds. Additional development of specific physical models for rock beds and salt-gradient solar ponds is necessary, but the basic framework of COMMIX-SA-1 is fully used. Work in these latter areas will be reported later. For now, we shall restrict our attention to an analysis of cylindrical water tanks.

Development of a rigorous, three-dimensional, thermohydrodynamic computer code is by no means trivial. Fortunately, previous experience and expertise existed at ANL-CT (i.e., Argonne National Laboratory Components Technology Division) from developing the THI3D⁸ and COMMIX-1 (Ref. 9) codes. In particular, the developmental work on COMMIX-SA-1 benefited greatly from an earlier version of COMMIX-1; it also benefited from the effort made toward the development of COMMIX-IHX,¹⁰ i.e., the implementation of cylindrical-coordinate terms. Without these earlier efforts, more manpower and time would have been required to complete COMMIX-SA-1.

The purposes of this report are to:

1. Detail the mathematical formulation underlying the COMMIX-SA-1 code; i.e., present in full the governing partial differential equations, their corresponding finite-difference approximations, the numerical-solution techniques, the initial and boundary conditions, and other auxiliary relations.
2. Describe the structure of COMMIX-SA-1.
3. Provide a set of user input instructions.
4. Present some sample analyses and results.

Together with some relevant discussions on various aspects, we hope to provide needed information about the theoretical and numerical background, and about how one can actually use the computer code to solve practical problems.

II. GOVERNING EQUATIONS

The time-dependent, three-dimensional conservation equations of mass, momentum, and energy governing the fluid-flow and heat-transfer processes can be expressed in integral form. Within a control volume V and enclosing surface S , we have the following equations:

Continuity:

$$\frac{\partial}{\partial t} \iiint_V \rho \, dV = - \oint_S \rho \vec{q} \cdot d\vec{S}. \quad (1)$$

Momentum:

$$\frac{\partial}{\partial t} \iiint_V \rho \vec{q} \, dV = - \oint_S \rho \vec{q} (\vec{q} \cdot d\vec{S}) + \iiint_V \rho \vec{X} \, dV - \iiint_V \vec{R} \, dV + \oint_S (\vec{\sigma} - p \vec{I}) \cdot d\vec{S}. \quad (2)$$

Energy:

$$\begin{aligned} \frac{\partial}{\partial t} \iiint_V \rho h \, dV = & - \oint_S \rho h \vec{q} \cdot d\vec{S} + \frac{\partial}{\partial t} \iiint_V p \, dV + \oint_S p \vec{q} \cdot d\vec{S} \\ & - \iiint_V p(\nabla \cdot \vec{q}) \, dV + \iiint_V \nabla \cdot (K \nabla T) \, dV + \iiint_V (Q + \Phi) \, dV. \end{aligned} \quad (3)$$

Here ρ is the density of the fluid, t is the time, \vec{q} is the velocity vector, p is the pressure, \vec{X} is the body force per unit mass (or specifically gravitational acceleration), \vec{R} is the resistance force (such as caused by baffles),

ℓ is the appropriate length scale associated with \vec{R} , $\vec{\sigma}$ is the viscous stress tensor, I is the identity matrix, h is the enthalpy, T is the temperature, K is the effective thermal conductivity (it may include eddy conductivity due to turbulence), Q is the rate of heat production or removal via heat source or sink, and Φ is the viscous dissipation = $\vec{\sigma} \cdot (\nabla \cdot \vec{q})$.

A. Relations in Cylindrical Coordinates

For problems dealing with cylindrical tanks, it is convenient to solve the problem in cylindrical coordinates r, θ, z for the radial, circumferential, and axial coordinates, respectively, with conjugate velocity coordinates u, v, w . If the divergence theorem is applied to Eqs. 1-3, they can be reduced to partial differential equations in the following forms:

Continuity Equation:

$$\frac{\partial \rho}{\partial t} + \frac{1}{r} \frac{\partial}{\partial r} (\rho r u) + \frac{1}{r} \frac{\partial}{\partial \theta} (\rho v) + \frac{\partial}{\partial z} (\rho w) = 0. \quad (4)$$

Momentum Equations:

r Component of Momentum:

$$\begin{aligned} \frac{\partial}{\partial t} (\rho u) + \frac{1}{r} \frac{\partial}{\partial r} (r \rho u^2) + \frac{1}{r} \frac{\partial}{\partial \theta} (\rho u v) + \frac{\partial}{\partial z} (\rho u w) - \frac{\rho v^2}{r} &= - \frac{\partial p}{\partial r} + \rho g_r \\ - \frac{R_r}{\ell_r} + \frac{1}{r} \frac{\partial}{\partial r} (r \sigma_{rr}) + \frac{1}{r} \frac{\partial \sigma_{r\theta}}{\partial \theta} - \frac{\sigma_{\theta\theta}}{r} + \frac{\partial \sigma_{rz}}{\partial z} &. \end{aligned} \quad (5)$$

θ Component of Momentum:

$$\begin{aligned} \frac{\partial}{\partial t} (\rho v) + \frac{1}{r} \frac{\partial}{\partial r} (r \rho u v) + \frac{1}{r} \frac{\partial}{\partial \theta} (\rho v^2) + \frac{\partial}{\partial z} (\rho w v) + \frac{\rho u v}{r} &= - \frac{1}{r} \frac{\partial p}{\partial \theta} \\ + \rho g_\theta - \frac{R_\theta}{\ell_\theta} + \frac{1}{r^2} \frac{\partial}{\partial r} (r^2 \sigma_{\theta r}) + \frac{1}{r} \frac{\partial \sigma_{\theta\theta}}{\partial \theta} + \frac{\partial \sigma_{\theta z}}{\partial z} &. \end{aligned} \quad (6)$$

z Component of Momentum:

$$\begin{aligned} \frac{\partial}{\partial t} (\rho w) + \frac{1}{r} \frac{\partial}{\partial r} (r \rho u w) + \frac{1}{r} \frac{\partial}{\partial \theta} (\rho v w) + \frac{\partial}{\partial z} (\rho w^2) &= - \frac{\partial p}{\partial z} + \rho g_z \\ - \frac{R_z}{\ell_z} + \frac{1}{r} \frac{\partial}{\partial r} (r \sigma_{zr}) + \frac{1}{r} \frac{\partial \sigma_{z\theta}}{\partial \theta} + \frac{\partial \sigma_{zz}}{\partial z} &. \end{aligned} \quad (7)$$

Energy Equation:

$$\begin{aligned} \frac{\partial}{\partial t}(\rho h) + \frac{1}{r} \frac{\partial}{\partial r}(r \rho u h) + \frac{1}{r} \frac{\partial}{\partial \theta}(\rho v h) + \frac{\partial}{\partial z}(\rho w h) &= \frac{\partial p}{\partial t} + u \frac{\partial p}{\partial r} + \frac{v}{r} \frac{\partial p}{\partial \theta} + w \frac{\partial p}{\partial z} \\ &+ \frac{1}{r} \frac{\partial}{\partial r} \left(K r \frac{\partial T}{\partial r} \right) + \frac{1}{r^2} \frac{\partial}{\partial \theta} \left(K \frac{\partial T}{\partial \theta} \right) + \frac{\partial}{\partial z} \left(K \frac{\partial T}{\partial z} \right) + \dot{Q} + \Phi. \end{aligned} \quad (8)$$

Here R_r , R_θ , and R_z are components of the resistance force R with corresponding lengths l_r , l_θ , and l_z .

The components of the viscous stress tensor in cylindrical coordinates are

$$\sigma_{rr} = \mu \left(2 \frac{\partial u}{\partial r} - \frac{2}{3} \nabla \cdot \vec{q} \right), \quad (9)$$

$$\sigma_{\theta\theta} = \mu \left[2 \left(\frac{1}{r} \frac{\partial v}{\partial \theta} + \frac{u}{r} \right) - \frac{2}{3} \nabla \cdot \vec{q} \right], \quad (10)$$

$$\sigma_{zz} = \mu \left(2 \frac{\partial w}{\partial z} - \frac{2}{3} \nabla \cdot \vec{q} \right), \quad (11)$$

$$\sigma_{r\theta} = \sigma_{\theta r} = \mu \left(\frac{\partial v}{\partial r} - \frac{v}{r} + \frac{1}{r} \frac{\partial u}{\partial \theta} \right), \quad (12)$$

$$\sigma_{\theta z} = \sigma_{z\theta} = \mu \left(\frac{\partial v}{\partial z} + \frac{1}{r} \frac{\partial w}{\partial \theta} \right), \quad (13)$$

$$\sigma_{rz} = \sigma_{rz} = \mu \left(\frac{\partial w}{\partial r} + \frac{\partial u}{\partial z} \right), \quad (14)$$

and

$$\nabla \cdot \vec{q} = \frac{1}{r} \frac{\partial}{\partial r}(r u) + \frac{1}{r} \frac{\partial v}{\partial \theta} + \frac{\partial w}{\partial z}.$$

The viscous dissipation function is given by

$$\begin{aligned} \Phi = 2\mu & \left[\left(\frac{\partial u}{\partial r} \right)^2 + \left(\frac{1}{r} \frac{\partial v}{\partial \theta} + \frac{u}{r} \right)^2 + \left(\frac{\partial w}{\partial z} \right)^2 + \frac{1}{2} \left(\frac{\partial v}{\partial r} - \frac{v}{r} + \frac{1}{r} \frac{\partial u}{\partial \theta} \right)^2 \right. \\ & \left. + \frac{1}{2} \left(\frac{1}{r} \frac{\partial w}{\partial \theta} + \frac{\partial v}{\partial z} \right)^2 + \frac{1}{2} \left(\frac{\partial u}{\partial z} + \frac{\partial w}{\partial r} \right)^2 - \frac{1}{3} (\nabla \cdot \vec{q})^2 \right]. \end{aligned} \quad (15)$$

B. Integral Treatment of Singularities

In several terms of the partial differential equations 4-8, singularities are found along the axis of the cylindrical-coordinate system (i.e., $r = 0$), as

is evident from the presence of the $1/r$ and $1/r^2$ terms. Especially when solved via finite difference, the singularity problem is manifested through terms that appear difficult to evaluate at or near the axis or origin.

Several different methods have been devised to either bypass or deal with the singularity problem, e.g., one that assumes a fictitious rod with radius $\ll 1$ at the center of the cylinder together with vanishing normal velocity or velocity gradient on the rod surface, one that uses quadratic extrapolation at the center, and the method of Kee and McKillop,¹¹ which uses square control-volume and rectangular-coordinate equations at the center. As pointed out in Ref. 12, these methods are too cumbersome or fail to account for the case in which significant crossflow occurs at the center.

The method that evolved during the development of COMMIX-SA-1 originated from these observations:

1. The singularity problem is a mathematical rather than a physical one. Namely, the physical flow field does not contain any singularity, but the singularities arise from the peculiarity of the cylindrical-coordinate system.

2. The difficult terms mentioned above came into being via direct finite-differencing of the partial differential equations 4-8, having in mind primarily a typical six-sided computation cell (or control volume). But the control volumes around the origin degenerate to five-sided ones.

3. The flow velocity at the origin is not well defined in the staggered mesh system under consideration, and much of the difficulty encountered has to do with its evaluation.

The first observation suggests that there might be a natural or satisfactory solution to the problem, because the physical situation demands it. The second observation suggests concentrating on the five-sided control volumes, and perhaps starting, not from the partial differential equations, but from integral forms of the conservation equations. The third observation points out that flow velocity at the origin must be unambiguously computed, because it exists in nonaxisymmetric cases and is needed in evaluating the related terms. Within a selected control volume, we then seek to satisfy the conservation equations in the integral form given by Eqs. 1-3. In terms of these integrals, the axis does not contribute singularities in the sense of the type of physical problems under consideration.

Programming for the computation will account for three ranges:

1. Flow field away from $r = 0$.
2. Flow field near $r = 0$.
3. Flow field at $r = 0$.

III. FINITE-DIFFERENCE EQUATIONS AND SOLUTION SCHEME

A. Finite-difference Equations ($r > 0$) ($i > 1$)

The finite-difference approximations to the governing partial differential equations 4-8 are obtained by using essentially the ICE (Implicit Continuous-fluid Eulerian) technique¹³ in a staggered grid system. A typical computation cell is shown in Fig. 1; computational nodes for pressure, density, enthalpy, and temperature are located at cell center (i, j, k) and those for velocities u , v , and w at centers of cell surfaces ($i \pm 1/2, j, k$), ($i, j \pm 1/2, k$) and ($i, j, k \pm 1/2$), respectively. (The grid system is called staggered because there are four different sets of control volumes: one control volume for pressure, density, enthalpy, and temperature, and one control volume each for u , v , and w .) The relations among nodal points, nodal lines, and the definitions of coordinates and coordinate-increments are illustrated for a typical K th polar plane in Fig. 2. The resulting finite-difference equations are as follows.

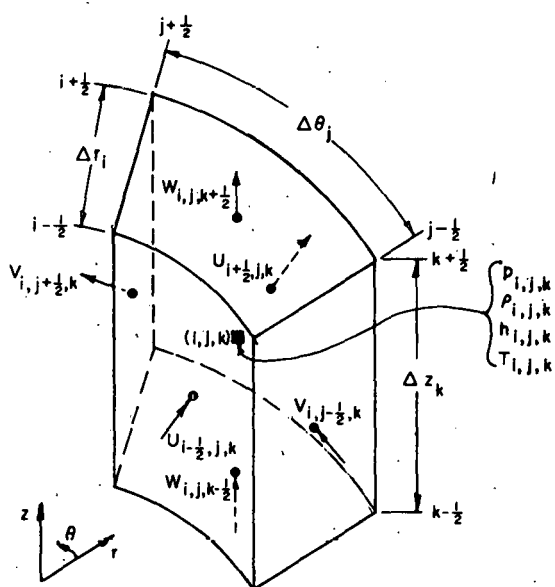


Fig. 1. A Typical Computation Cell in a Staggered Cylindrical-coordinate Grid System

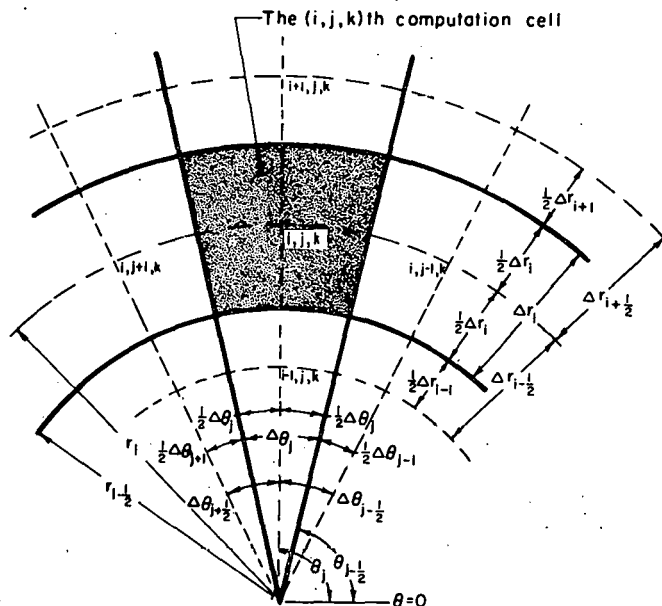


Fig. 2. Definitions of Coordinates and Coordinate Increments in the K th Polar Plane

1. The Continuity Equation

$$D_{i,j,k}^{n+1} = \frac{1}{\Delta t} (\rho_{i,j,k}^{n+1} - \rho_{i,j,k}^n)$$

$$+ \frac{1}{r_i \Delta r_i} [\langle \rho u r \rangle_{i+(1/2), j, k}^{n+1} - \langle \rho u r \rangle_{i-(1/2), j, k}^{n+1}]$$

$$\begin{aligned}
& + \frac{1}{r_i \Delta \theta_j} \left[\langle \rho v \rangle_{i, j+(1/2), k}^{n+1} - \langle \rho v \rangle_{i, j-(1/2), k}^{n+1} \right. \\
& \left. + \frac{1}{\Delta z_k} \left[\langle \rho w \rangle_{i, j, k+(1/2)}^{n+1} - \langle \rho w \rangle_{i, j, k-(1/2)}^{n+1} \right] \right], \quad (16)
\end{aligned}$$

where the angular brackets $\langle \rangle$ denote partial-donor-cell differencing of the enclosed quantity as discussed below, Δt denotes time increment, and D denotes mass residue in a given computation cell. The mass residue is to be reduced by iteration to a small quantity as specified by the convergence criteria (discussed later). The superscript n over a quantity means that the quantity is to be evaluated using values of the pertinent variables for the n th, or "old," or "previous," time step; the superscript $n + 1$ over a quantity means that evaluation of the quantity is to be made using the $(n + 1)$ st step, the "current," or the "latest" values of the pertinent variables.

$$\langle \rho u \rangle_{i+(1/2), j, k}^{n+1} = r_{i+(1/2)} u_{i+(1/2), j, k}^{n+1} \left[(1/2 + \xi_r) \rho_{i, j, k}^{n+1} + (1/2 - \xi_r) \rho_{i+1, j, k}^{n+1} \right], \quad (17)$$

where

$$\xi_r = \alpha \operatorname{sign}[u_{i+(1/2), j, k}^{n+1}] + \beta u_{i+(1/2), j, k}^{n+1} \frac{\Delta t}{\Delta r_{i+(1/2)}};$$

$$\langle \rho v \rangle_{i, j+(1/2), k}^{n+1} = v_{i, j+(1/2), k}^{n+1} \left[(1/2 + \xi_\theta) \rho_{i, j, k}^{n+1} + (1/2 - \xi_\theta) \rho_{i, j+1, k}^{n+1} \right]. \quad (18)$$

where

$$\xi_\theta = \alpha \operatorname{sign}[v_{i, j+(1/2), k}^{n+1}] + \beta v_{i, j+(1/2), k}^{n+1} \frac{\Delta t}{r_i \Delta \theta_{j+(1/2)}};$$

and

$$\langle \rho w \rangle_{i, j, k-(1/2)}^{n+1} = w_{i, j, k-(1/2)}^{n+1} \left[(1/2 + \xi_z) \rho_{i, j, k-1}^{n+1} + (1/2 - \xi_z) \rho_{i, j, k}^{n+1} \right], \quad (19)$$

where

$$\xi_z = \alpha \operatorname{sign}[w_{i, j, k-(1/2)}^{n+1}] + \beta w_{i, j, k-(1/2)}^{n+1} \frac{\Delta t}{\Delta z_{k-(1/2)}}.$$

All other convective flux terms occurring in Eq. 16 and subsequent equations are to be evaluated in a similar manner.

In the equations for ξ_r , ξ_θ , and ξ_z above, α and β are input parameters, by means of which one can control the degree of donor-cell differencing

desired. In general, $0 < \alpha < 1/2$ and $0 < \beta < 1/2$. As is well known, $\alpha = \beta = 0$ gives the standard central differencing scheme, and $\alpha = 1/2$ with $\beta = 0$ gives the upwind differencing or pure donor-cell differencing scheme. In practice, the upwind differencing option is more frequently used as it provides for greater numerical stability.

2. The Momentum Equations

In the finite-difference approximations to the full Navier-Stokes equations as given in Sec. II, $\nabla \cdot \vec{q} = 0$, corresponding to incompressibility, is assumed in evaluating the viscous terms. This is done primarily because of the negligible effect of the term anticipated in the range of COMMIX-SA-1 applications. The addition of the $\nabla \cdot \vec{q}$ term, when found necessary, can be easily implemented. The finite-difference representations of Eqs. 5-7 are given as follows.

a. The r-momentum equation

$$(\rho_{i+(1/2),j,k}^n + \Delta t B_r^n / \ell_r) u_{i+(1/2),j,k}^{n+1} = \overline{(\rho u)}_{i+(1/2),j,k}^n + \Delta t \rho_{i+(1/2),j,k}^n g_r - \frac{\Delta t}{\Delta r_{i+(1/2)}} (p_{i+1,j,k}^{n+1} - p_{i,j,k}^{n+1}), \quad (20)$$

where

$$\begin{aligned} \overline{(\rho u)}_{i+(1/2),j,k}^n &= (\rho u)_{i+(1/2),j,k}^n - \frac{\Delta t A_r^n}{\ell_r} + \frac{\Delta t D^n}{\Delta r_{i+(1/2),j,k}} u_{i+(1/2),j,k}^n \\ &+ \frac{\Delta t}{r_{i+(1/2)} \Delta r_{i+(1/2)}} (\langle \rho u_r^2 \rangle_{i,j,k}^n - \langle \rho u_r^2 \rangle_{i+1,j,k}^n) \\ &+ \frac{\Delta t}{r_{i+(1/2)} \Delta \theta_j} (\langle \rho u v \rangle_{i+(1/2),j-(1/2),k}^n - \langle \rho u v \rangle_{i+(1/2),j+(1/2),k}^n) \\ &+ \frac{\Delta t}{\Delta z_k} (\langle \rho u w \rangle_{i+(1/2),j,k-(1/2)}^n - \langle \rho u w \rangle_{i+(1/2),j,k+(1/2)}^n) \\ &+ \frac{\Delta t}{r_{i+(1/2)}} (\rho v^2)_{i+(1/2),j,k}^n + \Delta t \mu_{i+(1/2),j,k}^n (v_r)_{i+(1/2),j,k}^n, \end{aligned} \quad (21)$$

and

$$\begin{aligned}
 \mu_{i+(1/2), j, k}^n (v_r)_{i+(1/2), j, k}^n &= \frac{1}{\Delta r_{i+(1/2)}} [(\sigma_{rr})_{i+1, j, k}^n - (\sigma_{rr})_{i, j, k}^n] \\
 &+ \frac{1}{r_{i+(1/2)}} (\sigma_{rr})_{i+(1/2), j, k}^n - \frac{1}{2r_{i+(1/2)}} [(\sigma_{\theta\theta})_{i+(1/2), j+(1/2), k}^n + (\sigma_{\theta\theta})_{i+(1/2), j-(1/2), k}^n] \\
 &+ \frac{1}{r_{i+(1/2)} \Delta \theta_j} [(\sigma_{r\theta})_{i+(1/2), j+(1/2), k}^n - (\sigma_{r\theta})_{i+(1/2), j-(1/2), k}^n] \\
 &+ \frac{1}{\Delta z_k} [(\sigma_{rz})_{i+(1/2), j, k+(1/2)}^n - (\sigma_{rz})_{i+(1/2), j, k-(1/2)}^n], \tag{22}
 \end{aligned}$$

where, for $\mu \equiv \mu_{i+(1/2), j, k}^n$,

$$\frac{1}{\mu} (\sigma_{rr})_{i+1, j, k}^n = \frac{2}{\Delta r_{i+1}} [u_{i+(3/2), j, k}^n - u_{i+(1/2), j, k}^n],$$

$$\frac{1}{\mu} (\sigma_{rr})_{i, j, k}^n = \frac{2}{\Delta r_i} [u_{i+(1/2), j, k}^n - u_{i-(1/2), j, k}^n],$$

$$\frac{1}{\mu} (\sigma_{rr})_{i+(1/2), j, k}^n = \frac{2}{\Delta r_{i+(1/2)}} (u_{i+1, j, k}^n - u_{i, j, k}^n),$$

$$\frac{1}{\mu} (\sigma_{\theta\theta})_{i+(1/2), j+(1/2), k}^n = \frac{2}{r_{i+(1/2)} \Delta \theta_j} [v_{i+(1/2), j+1, k}^n - v_{i+(1/2), j, k}^n]$$

$$+ \frac{u_{i+(1/2), j+(1/2), k}^n}{r_{i+(1/2)}},$$

$$\frac{1}{\mu} (\sigma_{\theta\theta})_{i+(1/2), j-(1/2), k}^n = \frac{2}{r_{i+(1/2)} \Delta \theta_{j-(1/2)}} [v_{i+(1/2), j, k}^n - v_{i-(1/2), j-1, k}^n]$$

$$+ \frac{u_{i+(1/2), j-(1/2), k}^n}{r_{i+(1/2)}},$$

$$\begin{aligned}
\frac{1}{\mu}(\sigma_{r\theta})_{i+(1/2), j+(1/2), k}^n &= \frac{1}{r_{i+(1/2)} \Delta\theta_{j+(1/2)}} [u_{i+(1/2), j+1, k}^n - u_{i+(1/2), j, k}^n] \\
&+ \frac{1}{\Delta r_{i+(1/2)}} [v_{i+1, j+(1/2), k}^n - v_{i, j+(1/2), k}^n] - \frac{1}{r_{i+(1/2)}} v_{i+(1/2), j+(1/2), k}^n, \\
\frac{1}{\mu}(\sigma_{r\theta})_{i+(1/2), j-(1/2), k}^n &= \frac{1}{r_{i+(1/2)} \Delta\theta_{j-(1/2)}} [u_{i+(1/2), j, k}^n - u_{i+(1/2), j-1, k}^n] \\
&+ \frac{1}{\Delta r_{i+(1/2)}} [v_{i+1, j-(1/2), k}^n - v_{i, j-(1/2), k}^n] - \frac{1}{r_{i+(1/2)}} v_{i+(1/2), j-(1/2), k}^n, \\
\frac{1}{\mu}(\sigma_{rz})_{i+(1/2), j, k+(1/2)}^n &= \frac{1}{\Delta z_{k+(1/2)}} [u_{i+(1/2), j, k+1}^n - u_{i+(1/2), j, k}^n] \\
&+ \frac{1}{\Delta r_{i+(1/2)}} [w_{i+1, j, k+(1/2)}^n - w_{i, j, k+(1/2)}^n], \\
\frac{1}{\mu}(\sigma_{rz})_{i+(1/2), j, k-(1/2)}^n &= \frac{1}{\Delta z_{k-(1/2)}} [u_{i+(1/2), j, k}^n - u_{i+(1/2), j, k-1}^n] \\
&+ \frac{1}{\Delta r_{i+(1/2)}} [w_{i+1, j, k-(1/2)}^n - w_{i, j, k-(1/2)}^n],
\end{aligned}$$

and A_r^n and B_r^n are associated with the resistant force R_r as appearing in Eq. 5; their evaluations in the context of impermeable and perforated baffles are detailed in Sec. III.C.2. The length scale ℓ_r , unless otherwise warranted, will be replaced by $\Delta r_{i+(1/2)}$. The term involving $D_{i+(1/2), j, k}^n$ in Eq. 21 does not follow directly from Eq. 5, but is introduced on the basis of a consistency argument that mass residue remaining in a computation cell entails a corresponding residual mass flux. It is also introduced as an expedient numerical instrument to facilitate convergence. In the actual coding of COMMIX-SA-1, an option is provided to allow the user to include or not include this term in the calculation.

Convective terms are evaluated by partial donor-cell differencing in a manner similar to that prescribed by Eqs. 17-19. As a further example, we note that, in Eq. 21, the velocity components u , v , and w , which are defined on the cell surfaces, are to convect ρu either into or out of the cell

in question, depending on whether u , v , and w are directed into or out of the cell. Thus,

$$\begin{aligned} \langle \rho uv \rangle_{i+(1/2), j-(1/2), k}^n &= v_{i+(1/2), j-(1/2), k}^n [(1/2 + \xi_\theta)(\rho u)_{i+(1/2), j-1, k}^n \\ &\quad + (1/2 - \xi_\theta)(\rho u)_{i+(1/2), j, k}^n], \end{aligned} \quad (23)$$

where

$$\xi_\theta = \alpha \operatorname{sign}[v_{i+(1/2), j-(1/2), k}^n] + \beta v_{i+(1/2), j-(1/2), k}^n \frac{\Delta t}{r_{i+(1/2)} \Delta \theta_{j-(1/2)}},$$

α and β being as discussed previously.

In the θ - and z -momentum equations, and in the energy equation, which are to follow, u , v , and w will convect ρv , ρw , and ρh , respectively, either into or out of a cell, depending on whether their directions are pointing into or out of the cell. Thus the evaluation of the convective terms in these equations will be done similarly and will not be repeatedly explained. Of course, quantities such as $v_{i+(1/2), j-(1/2), k}^n$ in Eq. 23 must be determined by interpolating the neighboring nodal quantities $v_{i, j-(1/2), k}^n$ and $v_{i+1, j-(1/2), k}^n$, and in a variable-mesh setting this is typically accomplished in the following manner:

$$v_{i+(1/2), j-(1/2), k}^n = \frac{\Delta r_i v_{i+1, j-(1/2), k}^n + \Delta r_{i+1} v_{i, j-(1/2), k}^n}{\Delta r_i + \Delta r_{i+1}},$$

where the definitions of the coordinate increments and the locations of the computational nodes are illustrated in Figs. 2 and 1, respectively.

b. The θ -momentum Equation

$$\begin{aligned} [\rho_{i, j+(1/2), k}^n + \Delta t B_\theta^n / \ell_\theta] v_{i, j+(1/2), k}^{n+1} &= \overline{(\rho v)}_{i, j+(1/2), k}^n + \Delta t \rho_{i, j+(1/2), k}^n g_\theta \\ &\quad - \frac{\Delta t}{r_i \Delta \theta_{j+(1/2)}} (p_{i, j+1, k}^{n+1} - p_{i, j, k}^{n+1}), \end{aligned} \quad (24)$$

where

$$\begin{aligned} \overline{(\rho v)}_{i, j+(1/2), k}^n &= (\rho v)_{i, j+(1/2), k}^n - \frac{\Delta t A_\theta^n}{\ell_\theta} + \Delta t D_{i, j+(1/2), k}^n v_{i, j+(1/2), k}^n \\ &\quad + \frac{\Delta t}{r_i \Delta r_i} [\langle \rho uv \rangle_{i-(1/2), j+(1/2), k}^n - \langle \rho uv \rangle_{i+(1/2), j+(1/2), k}^n] \end{aligned}$$

$$\begin{aligned}
& + \frac{\Delta t}{r_i \Delta \theta_{j+(1/2)}} (\langle \rho v^2 \rangle_{i,j,k}^n - \langle \rho v^2 \rangle_{i,j+1,k}^n) \\
& + \frac{\Delta t}{\Delta z_k} [\langle \rho v w \rangle_{i,j+(1/2),k-(1/2)}^n - \langle \rho v w \rangle_{i,j+(1/2),k+(1/2)}^n] \\
& - \frac{\Delta t}{r_i} (\rho u v)_{i,j+(1/2),k}^n + \Delta t \mu_{i,j+(1/2),k}^n (v_\theta)_{i,j+(1/2),k}^n, \tag{25}
\end{aligned}$$

and

$$\begin{aligned}
& \mu_{i,j+(1/2),k}^n (v_\theta)_{i,j+(1/2),k}^n = \frac{1}{\Delta r_i} [(\sigma_{\theta r})_{i+(1/2),j+(1/2),k}^n \\
& - (\sigma_{\theta r})_{i-(1/2),j+(1/2),k}^n] + \frac{1}{r_i} [(\sigma_{\theta r})_{i,j+1,k}^n + (\sigma_{\theta r})_{i,j,k}^n] \\
& + \frac{1}{r_i} \frac{1}{\Delta \theta_{j+(1/2)}} [(\sigma_{\theta \theta})_{i,j+1,k}^n - (\sigma_{\theta \theta})_{i,j,k}^n] \\
& + \frac{1}{\Delta z_k} [(\sigma_{\theta z})_{i,j+(1/2),k+(1/2)}^n - (\sigma_{\theta z})_{i,j+(1/2),k-(1/2)}^n], \tag{26}
\end{aligned}$$

where, for $\mu \equiv \mu_{i,j+(1/2),k}^n$,

$$\begin{aligned}
& \frac{1}{\mu} (\sigma_{\theta r})_{i+(1/2),j+(1/2),k}^n = \frac{1}{\Delta r_{i+(1/2)}} [v_{i+1,j+(1/2),k}^n - v_{i,j+(1/2),k}^n] \\
& + \frac{1}{r_{i+(1/2)} \Delta \theta_{j+(1/2)}} [u_{i+(1/2),j+1,k}^n - u_{i+(1/2),j,k}^n] \\
& - \frac{1}{r_{i+(1/2)}} v_{i+(1/2),j+(1/2),k}^n
\end{aligned}$$

$$\frac{1}{\mu} (\sigma_{\theta r})_{i-(1/2),j+(1/2),k}^n = \frac{1}{\Delta r_{i-(1/2)}} [v_{i,j+(1/2),k}^n - v_{i-1,j+(1/2),k}^n]$$

$$+ \frac{1}{r_{i-(1/2)} \Delta \theta_{j+(1/2)}} [u_{i-(1/2), j+1, k}^n - u_{i-(1/2), j, k}^n]$$

$$- \frac{1}{r_{i-(1/2)}} v_{i-(1/2), j+(1/2), k}^n$$

$$\frac{1}{\mu} (\sigma_{\theta r})_{i, j+1, k}^n = \frac{1}{\Delta r_i} [v_{i+(1/2), j+1, k}^n - v_{i-(1/2), j+1, k}^n]$$

$$+ \frac{1}{r_i \Delta \theta_{j+1}} [u_{i, j+(3/2), k}^n - u_{i, j+(1/2), k}^n] - \frac{1}{r_i} v_{i, j+1, k}^n,$$

$$\frac{1}{\mu} (\sigma_{\theta r})_{i, j, k}^n = \frac{1}{\Delta r_i} [v_{i, j+(1/2), k}^n - v_{i, j-(1/2), k}^n] + \frac{1}{r_i \Delta \theta_i} [u_{i, j+(1/2), k}^n$$

$$- u_{i, j-(1/2), k}^n] - \frac{1}{r_i} v_{i, j, k}^n,$$

$$\frac{1}{\mu} (\sigma_{\theta \theta})_{i, j+1, k}^n = \frac{2}{r_i \theta_{j+1}} [v_{i, j+(3/2), k}^n - v_{i, j+(1/2), k}^n] - \frac{2u_{i, j+1, k}^n}{r_i},$$

$$\frac{1}{\mu} (\sigma_{\theta \theta})_{i, j, k}^n = \frac{2}{r_i \Delta \theta_j} [v_{i, j+(1/2), k}^n - v_{i, j-(1/2), k}^n] - \frac{2u_{i, j, k}^n}{r_i},$$

$$\frac{1}{\mu} (\sigma_{\theta z})_{i, j+(1/2), k+(1/2)}^n = \frac{1}{\Delta z_{k+(1/2)}} [v_{i, j+(1/2), k+1}^n - v_{i, j+(1/2), k}^n]$$

$$+ \frac{1}{r_i \Delta \theta_{j+(1/2)}} [w_{i, j+1, k+(1/2)}^n - w_{i, j, k+(1/2)}^n],$$

and

$$\frac{1}{\mu} (\sigma_{\theta z})_{i, j+(1/2), k-(1/2)}^n = \frac{1}{\Delta z_{k-(1/2)}} [v_{i, j+(1/2), k}^n - v_{i, j+(1/2), k-1}^n]$$

$$+ \frac{1}{r_i \Delta \theta_{j+(1/2)}} [w_{i, j+1, k-(1/2)}^n - w_{i, j, k-(1/2)}^n].$$

The quantities A_θ^n and B_θ^n are associated with the resistant force R_θ as appearing in Eq. 6; their evaluations in the context of impermeable and perforated baffles will be detailed in Sec. III.C.2. The length scale ℓ_θ , unless otherwise warranted, will be replaced by $r_i \Delta \theta_{i+(1/2)}$. The comments made earlier on the term involving the mass residue D in Eq. 21 apply here as well.

The z-momentum Equation

$$[\rho_{i,j,k+(1/2)}^n + \Delta t B_z^n / \ell_z] w_{i,j,k+(1/2)}^{n+1} = \overline{(\rho w)}_{i,j,k+(1/2)}^n + \Delta t \rho_{i,j,k+(1/2)}^n g_z - \frac{\Delta t}{\Delta z_{k+(1/2)}} (p_{i,j,k+1}^{n+1} - p_{i,j,k}^{n+1}), \quad (27)$$

where

$$\begin{aligned} \overline{(\rho w)}_{i,j,k+(1/2)}^n &= (\rho w)_{i,j,k+(1/2)}^n - \frac{\Delta t A_z^n}{\ell_z} + \Delta t D_{i,j,k+(1/2)}^n w_{i,j,k+(1/2)}^n \\ &+ \frac{\Delta t}{r_i \Delta r_i} [\langle \rho r u w \rangle_{i-(1/2), j, k+(1/2)}^n - \langle \rho r u w \rangle_{i+(1/2), j, k+(1/2)}^n] \\ &+ \frac{\Delta t}{r_i \Delta \theta_j} [\langle \rho v w \rangle_{i, j-(1/2), k+(1/2)}^n - \langle \rho v w \rangle_{i, j+(1/2), k+(1/2)}^n] \\ &+ \frac{\Delta t}{\Delta z_{k+(1/2)}} [\langle \rho w^2 \rangle_{i, j, k}^n - \langle \rho w^2 \rangle_{i, j, k+1}^n] + \Delta t \mu_{i,j,k+(1/2)}^n (v_z)_{i,j,k+(1/2)}^n, \end{aligned} \quad (28)$$

and

$$\begin{aligned} \mu_{i,j,k+(1/2)}^n (v_z)_{i,j,k+(1/2)}^n &= \frac{1}{\Delta r_i} [(\sigma_{zr})_{i+(1/2), j, k+(1/2)}^n - (\sigma_{zr})_{i-(1/2), j, k+(1/2)}^n] \\ &+ \frac{1}{2r_i} [(\sigma_{zr})_{i,j,k+1}^n + (\sigma_{zr})_{i,j,k}^n] + \frac{1}{r_i \Delta \theta_j} [(\sigma_{z\theta})_{i,j,k+(1/2)}^n \\ &- (\sigma_{z\theta})_{i,j-(1/2), k+(1/2)}^n] + \frac{1}{\Delta z_{k+(1/2)}} [(\sigma_{zz})_{i,j,k+1}^n - (\sigma_{zz})_{i,j,k}^n], \end{aligned} \quad (29)$$

where, for $\mu \equiv \mu_{i,j,k+(1/2)}^n$,

$$\frac{1}{\mu}(\sigma_{zr})_{i+(1/2),j,k+(1/2)}^n = \frac{1}{\Delta r_{i+(1/2)}}[w_{i+1,j,k+(1/2)}^n - w_{i,j,k+(1/2)}^n]$$

$$+ \frac{1}{\Delta z_{k+(1/2)}}[u_{i+(1/2),j,k+1}^n - u_{i+(1/2),j,k}^n],$$

$$\frac{1}{\mu}(\sigma_{zr})_{i-(1/2),j,k+(1/2)}^n = \frac{1}{\Delta r_{i-(1/2)}}[w_{i,j,k+(1/2)}^n - w_{i-1,j,k+(1/2)}^n]$$

$$+ \frac{1}{\Delta z_{k+(1/2)}}[u_{i-(1/2),j,k+1}^n - u_{i-(1/2),j,k}^n],$$

$$\frac{1}{\mu}(\sigma_{zr})_{i,j,k+1}^n = \frac{1}{\Delta r_i}[w_{i+(1/2),j,k+1}^n - w_{i-(1/2),j,k+1}^n] + \frac{1}{\Delta z_{k+1}}[u_{i,j,k+(3/2)}^n$$

$$- u_{i,j,k+(1/2)}^n],$$

$$\frac{1}{\mu}(\sigma_{zr})_{i,j,k}^n = \frac{1}{\Delta r_i}[w_{i+(1/2),j,k}^n - w_{i-(1/2),j,k}^n] + \frac{1}{\Delta z_k}[u_{i,j,k+(1/2)}^n$$

$$- u_{i,j,k-(1/2)}^n],$$

$$\frac{1}{\mu}(\sigma_{z\theta})_{i,j+(1/2),k+(1/2)}^n = \frac{1}{r_i \Delta \theta_{j+(1/2)}}[w_{i,j+1,k+(1/2)}^n - w_{i,j,k+(1/2)}^n]$$

$$+ \frac{1}{\Delta z_{k+(1/2)}}[v_{i,j+(1/2),k+1}^n - v_{i,j+(1/2),k}^n],$$

$$\frac{1}{\mu}(\sigma_{z\theta})_{i,j-(1/2),k+(1/2)}^n = \frac{1}{r_i \Delta \theta_{j-(1/2)}}[w_{i,j,k+(1/2)}^n - w_{i,j-1,k+(1/2)}^n]$$

$$+ \frac{1}{\Delta z_{k+(1/2)}}[v_{i,j-(1/2),k+1}^n - v_{i,j-(1/2),k}^n],$$

$$\frac{1}{\mu}(\sigma_{zz})_{i,j,k+1}^n = \frac{2}{\Delta z_{k+1}}[w_{i,j,k+(3/2)}^n - w_{i,j,k+(1/2)}^n],$$

and

$$\frac{1}{\mu}(\sigma_{zz})_{i,j,k}^n = \frac{2}{\Delta z_k}[w_{i,j,k+(1/2)}^n - w_{i,j,k-(1/2)}^n].$$

Again the quantities A_z^n and B_z^n are associated with the resistant force R_z in Eq. 7, and details for their evaluations are given in Sec. III.C.2. Also, the length scale λ_z will be approximated by $\Delta z_{k+(1/2)}$, unless otherwise warranted.

3. The Energy Equation

In the finite-difference approximation to the energy equation, Eq. 8, the viscous dissipation function Φ is omitted, as its effects are deemed negligible in the anticipated range of COMMIX-SA-1 applications. It can, however, be added easily in the coding if future usage of the code so requires. The finite-difference energy equation is given as follows:

$$\begin{aligned}
 (\rho h)_{i,j,k}^{n+1} &= (\rho h)_{i,j,k}^n + \Delta t D_{i,j,k}^{n+1} h_{i,j,k}^n \\
 &+ \frac{\Delta t}{r_i \Delta r_i} [\langle \rho h^n r u^{n+1} \rangle_{i-(1/2),j,k} - \langle \rho h^n r u^{n+1} \rangle_{i+(1/2),j,k}] \\
 &+ \frac{\Delta t}{r_i \Delta \theta_j} [\langle \rho h^n v^{n+1} \rangle_{i,j-(1/2),k} - \langle \rho h^n v^{n+1} \rangle_{i,j+(1/2),k}] \\
 &+ \frac{\Delta t}{\Delta z_k} [\langle \rho h^n w^{n+1} \rangle_{i,j,k-(1/2)} - \langle \rho h^n w^{n+1} \rangle_{i,j,k+(1/2)}] + (p_{i,j,k}^{n+1} - p_{i,j,k}^n) \\
 &+ \frac{\Delta t}{r_i \Delta r_i} [\langle \text{pur} \rangle_{i+(1/2),j,k}^{n+1} - \langle \text{pur} \rangle_{i-(1/2),j,k}^{n+1}] \\
 &+ \frac{\Delta t}{r_i \Delta \theta_j} [\langle \text{pv} \rangle_{i,j+(1/2),k}^{n+1} - \langle \text{pv} \rangle_{i,j-(1/2),k}^{n+1}] \\
 &+ \frac{\Delta t}{\Delta z_k} [\langle \text{pw} \rangle_{i,j,k+(1/2)}^{n+1} - \langle \text{pw} \rangle_{i,j,k-(1/2)}^{n+1}]
 \end{aligned}$$

$$\begin{aligned}
& + \frac{\Delta t p_i^{n+1}}{r_i \Delta r_i} [(u r)_{i-(1/2), j, k}^{n+1} - (u r)_{i+(1/2), j, k}^{n+1}] \\
& + \frac{\Delta t p_i^{n+1}}{r_i \Delta \theta_j} [v_{i, j-(1/2), k}^{n+1} - v_{i, j+(1/2), k}^{n+1}] \\
& + \frac{\Delta t p_i^{n+1}}{\Delta z_k} [w_{i, j, k-(1/2)}^{n+1} - w_{i, j, k+(1/2)}^{n+1}] \\
& + \frac{\Delta t}{r_i \Delta r_i} \left[K_{i+(1/2), j, k}^n \frac{T_{i+1, j, k}^n - T_{i, j, k}^n}{\Delta r_{i+(1/2)}} \right. \\
& \quad \left. - K_{i-(1/2), j, k}^n \frac{T_{i, j, k}^n - T_{i-1, j, k}^n}{\Delta r_{i-(1/2)}} \right] \\
& + \frac{\Delta t}{r_i^2 \Delta \theta_j} \left[K_{i, j+(1/2), k}^n \frac{T_{i, j+1, k}^n - T_{i, j, k}^n}{\Delta \theta_{j+(1/2)}} \right. \\
& \quad \left. - K_{i, j-(1/2), k}^n \frac{T_{i, j, k}^n - T_{i, j-1, k}^n}{\Delta \theta_{j-(1/2)}} \right] \\
& + \frac{\Delta t}{\Delta z_k} \left[K_{i, j, k+(1/2)}^n \frac{T_{i, j, k+1}^n - T_{i, j, k}^n}{\Delta z_{k+(1/2)}} \right. \\
& \quad \left. - K_{i, j, k-(1/2)}^n \frac{T_{i, j, k}^n - T_{i, j, k-1}^n}{\Delta z_{k-(1/2)}} \right] + \Delta t \dot{Q}_{i, j, k}^{n+1}. \tag{30}
\end{aligned}$$

Note that when compressibility is neglected in considering viscous effects, since $\nabla \cdot \vec{q} = 0$, viscous-stress terms in Eqs. 5-7 reduce to,

r Component:

$$\mu v_r = \mu \left[\frac{\partial}{\partial r} \left(\frac{1}{r} \frac{\partial}{\partial r} r u \right) + \frac{1}{r^2} \frac{\partial^2 u}{\partial \theta^2} - \frac{2}{r^2} \frac{\partial v}{\partial \theta} + \frac{\partial^2 u}{\partial z^2} \right],$$

θ Component:

$$\mu v_{\theta} = \mu \left[\frac{\partial}{\partial r} \left(\frac{1}{r} \frac{\partial}{\partial r} rv \right) + \frac{1}{r^2} \frac{\partial^2 v}{\partial \theta^2} + \frac{2}{r^2} \frac{\partial u}{\partial \theta} + \frac{\partial^2 v}{\partial z^2} \right],$$

and

z Component:

$$\mu v_z = \mu \left[\frac{1}{r} \frac{\partial}{\partial r} \left(r \frac{\partial w}{\partial r} \right) + \frac{1}{r^2} \frac{\partial^2 w}{\partial \theta^2} + \frac{\partial^2 w}{\partial z^2} \right].$$

Hence, when away from $r = 0$, simplification of Eqs. 22, 26, and 29 is feasible, and we have, in finite-difference form,

$$\begin{aligned}
 (v_r)_{i+(1/2), j, k}^n &= \frac{1}{\Delta r_{i+(1/2)}} \left\{ \frac{1}{\Delta r_{i+1}} [u_{i+(3/2), j, k}^n - u_{i+(1/2), j, k}^n] \right. \\
 &\quad \left. - \frac{1}{\Delta r_i} [u_{i+(1/2), j, k}^n - u_{i-(1/2), j, k}^n] \right\} \\
 &\quad + \frac{1}{r_{i+(1/2)} \Delta r_{i+(1/2)}} (u_{i+1, j, k}^n - u_{i, j, k}^n) - \frac{u_{i+(1/2), j, k}^n}{[r_{i+(1/2)}]^2} \\
 &\quad + \frac{1}{[r_{i+(1/2)}]^2 \Delta \theta_j} \left\{ \frac{1}{\Delta \theta_{j+(1/2)}} [u_{i+(1/2), j+1, k}^n - u_{i+(1/2), j, k}^n] \right. \\
 &\quad \left. - \frac{1}{\Delta \theta_{j-(1/2)}} [u_{i+(1/2), j, k}^n - u_{i+(1/2), j-1, k}^n] \right\} \\
 &\quad + \frac{1}{\Delta z_k} \left\{ \frac{1}{\Delta z_{k+(1/2)}} [u_{i+(1/2), j, k+1}^n - u_{i+(1/2), j, k}^n] \right. \\
 &\quad \left. - \frac{1}{\Delta z_{k-(1/2)}} [u_{i+(1/2), j, k}^n - u_{i+(1/2), j, k-1}^n] \right\} \\
 &\quad - \frac{2}{[r_{i+(1/2)}]^2 \Delta \theta_j} [v_{i+(1/2), j+(1/2), k}^n - v_{i+(1/2), j-(1/2), k}^n]; \quad (22a)
 \end{aligned}$$

$$\begin{aligned}
 (v_{\theta})_{i, j+(1/2), k}^n &= \frac{1}{\Delta r_i} \left\{ \frac{1}{\Delta r_{i+(1/2)}} [v_{i+1, j+(1/2), k}^n - v_{i, j+(1/2), k}^n] \right. \\
 &\quad \left. - \frac{1}{\Delta r_{i-(1/2)}} [v_{i, j+(1/2), k}^n - v_{i-1, j+(1/2), k}^n] \right\}
 \end{aligned}$$

$$\begin{aligned}
& + \frac{1}{r_i \Delta r_i} [v_{i+(1/2), j+(1/2), k}^n - v_{i-(1/2), j+(1/2), k}^n] \\
& + \frac{1}{r_i^2 \Delta \theta_{j+(1/2)}} \left\{ \frac{1}{\Delta \theta_{j+1}} [v_{i, j+(3/2), k}^n - v_{i, j+(1/2), k}^n] \right. \\
& \left. - \frac{1}{\Delta \theta_j} [v_{i, j+(1/2), k}^n - v_{i, j-(1/2), k}^n] \right\} \\
& + \frac{2}{r_i^2 \Delta \theta_{j+(1/2)}} (u_{i, j+1, k}^n - u_{i, j, k}^n) - \frac{v_{i, j+(1/2), k}^n}{r_i^2} \\
& + \frac{1}{\Delta z_k} \left\{ \frac{1}{\Delta z_{k+(1/2)}} [v_{i, j+(1/2), k+1}^n - v_{i, j+(1/2), k}^n] \right. \\
& \left. - \frac{1}{\Delta z_{k-(1/2)}} [v_{i, j+(1/2), k}^n - v_{i, j+(1/2), k-1}^n] \right\}. \tag{26a}
\end{aligned}$$

and

$$\begin{aligned}
(v_z)_i^n, j, k+(1/2) & = \frac{1}{\Delta r_i} \left\{ \frac{1}{\Delta r_{i+(1/2)}} [w_{i+1, j, k+(1/2)}^n - w_{i, j, k+(1/2)}^n] \right. \\
& \left. - \frac{1}{\Delta r_{i-(1/2)}} [w_{i, j, k+(1/2)}^n - w_{i-1, j, k+(1/2)}^n] \right\} \\
& + \frac{1}{r_i \Delta r_i} [w_{i+(1/2), j, k+(1/2)}^n - w_{i-(1/2), j, k+(1/2)}^n] \\
& + \frac{1}{r_i^2 \Delta \theta_j} \left\{ \frac{1}{\Delta \theta_{j+(1/2)}} [w_{i, j+1, k+(1/2)}^n - w_{i, j, k+(1/2)}^n] \right. \\
& \left. - \frac{1}{\Delta \theta_{j-(1/2)}} [w_{i, j, k+(1/2)}^n - w_{i, j-1, k+(1/2)}^n] \right\} \\
& + \frac{1}{\Delta z_{k+(1/2)}} \left\{ \frac{1}{\Delta z_{k+1}} [w_{i, j, k+(3/2)}^n - w_{i, j, k+(1/2)}^n] \right. \\
& \left. - \frac{1}{\Delta z_k} [w_{i, j, k+(1/2)}^n - w_{i, j, k-(1/2)}^n] \right\}. \tag{29a}
\end{aligned}$$

These simplifications are not applicable for $i = 1$ and $r = 0$.

4. Computations near $r = 0$

In the finite-difference approximations Eqs. 16, 20-22, and 24-30, the singularity problem is manifested through terms that appear difficult to evaluate at or near the origin—for example, the term $\langle \rho u r \rangle_{i-(1/2), j, k}^{n+1}$ in Eq. 16 for $i = 1$; the term $\langle \rho u^2 r \rangle_{i, j, k}^n$ in Eq. 21 for $i = 1$; the terms $u_{i-(1/2), j, k}^n$ and $u_{i, j, k}^n$ in Eq. 22 for $i = 1$; the terms $\langle \rho^n h^n r u^{n+1} \rangle_{i-(1/2), j, k}$, $\langle \rho u r \rangle_{i-(1/2), j, k}^{n+1}$, $\langle u r \rangle_{i-(1/2), j, k}^{n+1}$ and $T_{i-1, j, k}^n$ in Eq. 30, again for $i = 1$; etc. Thus, within the framework of the staggered mesh system used in conjunction with the ICE technique, attention is focused on the p -, u -, v -, and w -control volumes around the center as shown in Fig. 3. Note that these degenerate control volumes fit in the cylindrical staggered grid naturally, leaving no region in the flow domain where the balance of mass, momentum, or energy may not be ensured. Within these control volumes, we then seek to satisfy the conservation equations, particularly in integral forms.

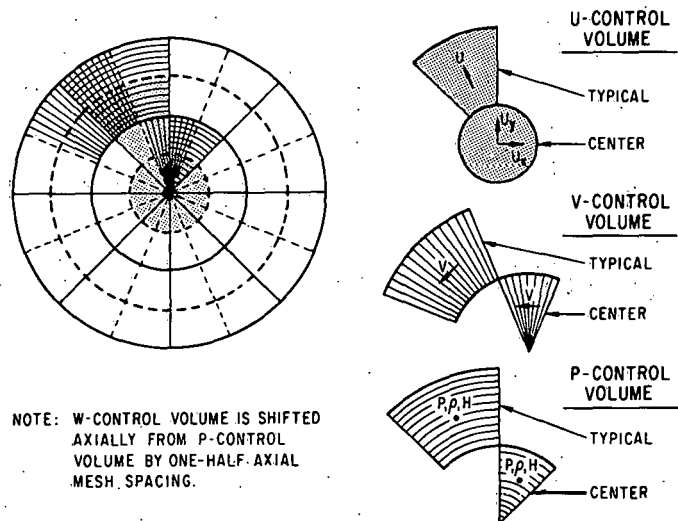


Fig. 3

Staggered Grid and Degenerate Control Volumes in Cylindrical-coordinate System

When Eqs. 1-3 are expanded, in accordance with the ICE technique, for the degenerate five-sided control volumes shown in Fig. 3, and when the resulting finite-difference equations are recast in the forms of Eqs. 16, 20-22, and 24-30, we obtain the following for $i = 1$, whence all quantities with subscript $i-(1/2)$ drop out.

a. Continuity Equation for $i = 1$

$$\begin{aligned}
 D_{i, j, k}^{n+1} = & \frac{1}{\Delta t} (\rho_{i, j, k}^{n+1} - \rho_{i, j, k}^n) + \frac{1}{r_i \Delta r_i} [\langle \rho u r \rangle_{i+(1/2), j, k}^{n+1} \\
 & + \frac{1}{r_i \Delta \theta_j} [\langle \rho v \rangle_{i, j+(1/2), k}^{n+1} - \langle \rho v \rangle_{i, j-(1/2), k}^{n+1}] \\
 & + \frac{1}{\Delta z_k} [\langle \rho w \rangle_{i, j, k+(1/2)}^{n+1} - \langle \rho w \rangle_{i, j, k-(1/2)}^{n+1}]] \quad (31)
 \end{aligned}$$

b. The r-momentum Equation for $i = 1$. (This equation remains the same as given by Eqs. 20-22, since it does not contain $i - (1/2)$ terms.)

$$[\rho_{i+(1/2), j, k}^n + \Delta t B_r^n / \ell_r] u_{i+(1/2), j, k}^{n+1} = \overline{(\rho u)}_{i+(1/2), j, k}^n + \Delta t \rho_{i+(1/2), j, k}^n g_r$$

$$- \frac{\Delta t}{\Delta r_{i+(1/2)}} (p_{i+1, j, k}^{n+1} - p_{i, j, k}^{n+1}), \quad (32)$$

where

$$\begin{aligned} \overline{(\rho u)}_{i+(1/2), j, k}^n &= (\rho u)_{i+(1/2), j, k}^n - \frac{\Delta t A_r^n}{\ell_r} + \Delta t D_{i+(1/2), j, k}^n u_{i+(1/2), j, k}^n \\ &+ \frac{\Delta t}{r_{i+(1/2)} \Delta r_{i+(1/2)}} (\langle \rho u^2 \rangle_{i, j, k}^n - \langle \rho u^2 \rangle_{i+1, j, k}^n) \\ &+ \frac{\Delta t}{r_{i+(1/2)} \Delta \theta_j} [\langle \rho u v \rangle_{i+(1/2), j-(1/2), k}^n - \langle \rho u v \rangle_{i+(1/2), j+(1/2), k}^n] \\ &+ \frac{\Delta t}{\Delta z_k} [\langle \rho u w \rangle_{i+(1/2), j, k-(1/2)}^n - \langle \rho u w \rangle_{i+(1/2), j, k+(1/2)}^n] \\ &+ \frac{\Delta t}{r_{i+(1/2)}} (\rho v^2)_{i+(1/2), j, k}^n + \Delta t \mu_{i+(1/2), j, k}^n (v_r)_{i+(1/2), j, k}^n, \end{aligned} \quad (33)$$

and

$$\begin{aligned} \mu_{i+(1/2), j, k}^n (v_r)_{i+(1/2), j, k}^n &= \frac{1}{\Delta r_{i+(1/2)}} [(\sigma_{rr})_{i+1, j, k}^n - (\sigma_{rr})_{i, j, k}^n] \\ &+ \frac{1}{r_{i+(1/2)}} (\sigma_{rr})_{i+(1/2), j, k}^n - \frac{1}{2r_{i+(1/2)}} [(\sigma_{\theta\theta})_{i+(1/2), j+(1/2), k}^n \\ &+ (\sigma_{\theta\theta})_{i+(1/2), j-(1/2), k}^n] + \frac{1}{r_{i+(1/2)} \Delta \theta_j} [(\sigma_{r\theta})_{i+(1/2), j+(1/2), k}^n \\ &- (\sigma_{r\theta})_{i+(1/2), j-(1/2), k}^n] + \frac{1}{\Delta z_k} [(\sigma_{rz})_{i+(1/2), j, k+(1/2)}^n \\ &- (\sigma_{rz})_{i+(1/2), j, k-(1/2)}^n]. \end{aligned}$$

c. The θ -momentum Equation for $i = 1$. Because of zero area at $i = (1/2)$, Eqs. 24-26 reduce to

$$[\rho_{i, j+(1/2), k}^n + \Delta t B_\theta^n / \ell_\theta] v_{i, j+(1/2), k}^{n+1} = \overline{(\rho v)}_{i, j+(1/2), k}^n + \Delta t \rho_{i, j+(1/2), k}^n g_\theta$$

$$- \frac{\Delta t}{r_i \Delta \theta_{j+(1/2)}} (p_{i, j+1, k}^{n+1} - p_{i, j, k}^{n+1}), \quad (35)$$

where

$$\begin{aligned}
 \overline{(\rho v)}_{i,j+(1/2),k}^n &= (\rho v)_{i,j+(1/2),k}^n - \frac{\Delta t A_\theta^n}{\ell_\theta} + \Delta t D_{i,j+(1/2),k}^n v_{i,j+(1/2),k}^n \\
 &+ \frac{\Delta t}{r_i \Delta r_i} [-\langle \rho r u v \rangle_{i+(1/2),j+(1/2),k}^n] \\
 &+ \frac{\Delta t}{r_i \Delta \theta_{j+(1/2)}} (\langle \rho v^2 \rangle_{i,j,k}^n - \langle \rho v^2 \rangle_{i,j+1,k}^n) \\
 &+ \frac{\Delta t}{\Delta z_k} [\langle \rho v w \rangle_{i,j+(1/2),k-(1/2)}^n - \langle \rho v w \rangle_{i,j+(1/2),k+(1/2)}^n] \\
 &- \frac{\Delta t}{r_i} (\rho u v)_{i,j+(1/2),k}^n + \Delta t (v_\theta)_{i,j+(1/2),k}^n u_{i,j+(1/2),k}^n
 \end{aligned} \tag{36}$$

and

$$\begin{aligned}
 u_{i,j+(1/2),k}^n (v_\theta)_{i,j+(1/2),k}^n &= \frac{1}{\Delta r_i} (\sigma_{\theta r})_{i+(1/2),j+(1/2),k}^n \\
 &+ \frac{(\sigma_{\theta r})_{i,j+1,k}^n + (\sigma_{\theta r})_{i,j,k}^n}{r_i} + \frac{1}{r_i \Delta \theta_{j+(1/2)}} [(\sigma_{\theta \theta})_{i,j+1,k}^n - (\sigma_{\theta \theta})_{i,j,k}^n] \\
 &+ \frac{1}{\Delta z_k} [(\sigma_{\theta z})_{i,j+(1/2),k+(1/2)}^n - (\sigma_{\theta z})_{i,j+(1/2),k-(1/2)}^n].
 \end{aligned} \tag{37}$$

d. The z-momentum Equation for $i = 1$. Because of zero area at $i = (1/2)$, Eqs. 27-29 reduce to

$$\begin{aligned}
 [\rho_{i,j,k+(1/2)}^n + \Delta t B_z^n / \ell_z] w_{i,j,k+(1/2)}^{n+1} &= \overline{(\rho w)}_{i,j,k+(1/2)}^n + \Delta t \rho_{i,j,k+(1/2)}^n g_z \\
 &- \frac{\Delta t}{\Delta z_{k+(1/2)}} (p_{i,j,k+1}^{n+1} - p_{i,j,k}^{n+1}),
 \end{aligned} \tag{38}$$

where

$$\begin{aligned}
 \overline{(\rho w)}_{i,j,k+(1/2)}^n &= (\rho w)_{i,j,k+(1/2)}^n - \frac{\Delta t A_z^n}{\ell_z} + \Delta t D_{i,j,k+(1/2)}^n w_{i,j,k+(1/2)}^n \\
 &+ \frac{\Delta t}{r_i \Delta r_i} [-\langle \rho r u w \rangle_{i+(1/2),j,k+(1/2)}^n] \\
 &+ \frac{\Delta t}{r_i \Delta \theta_j} [\langle \rho v w \rangle_{i,j-(1/2),k+(1/2)}^n - \langle \rho v w \rangle_{i,j+(1/2),k+(1/2)}^n]
 \end{aligned}$$

$$\begin{aligned}
& + \frac{\Delta t}{\Delta z_{k+(1/2)}} (\langle \rho w^2 \rangle_{i,j,k}^n - \langle \rho w^2 \rangle_{i,j,k+1}^n) \\
& + \Delta t (v_z)_{i,j,k+(1/2)}^n u_{i,j,k+(1/2)}^n
\end{aligned} \tag{39}$$

and

$$\begin{aligned}
u_{i,j,k+(1/2)}^n (v_z)_{i,j,k+(1/2)}^n &= \frac{1}{\Delta r_i} (\sigma_{zr})_{i+(1/2),j,k+(1/2)}^n + \frac{(\sigma_{zr})_{i,j,k+(1/2)}^n + (\sigma_{zr})_{i,j,(k-(1/2))}^n}{2r_i} \\
& + \frac{1}{r_i \Delta \theta_j} [(\sigma_{z\theta})_{i,j+(1/2),k+(1/2)}^n - (\sigma_{z\theta})_{i,j-(1/2),k+(1/2)}^n] \\
& + \frac{1}{\Delta s_{k+(1/2)}} [(\sigma_{zz})_{i,j,k+1}^n - (\sigma_{zz})_{i,j,k}^n].
\end{aligned} \tag{40}$$

e. Energy Equation for $i = 1$. Equation 30 reduces to

$$\begin{aligned}
(\rho h)_{i,j,k}^{n+1} &= (\rho h)_{i,j,k}^n + \Delta t D_{i,j,k}^{n+1} h_{i,j,k}^n + \frac{\Delta t}{r_i \Delta r_i} [-\langle \rho h^n n ru^{n+1} \rangle_{i+(1/2),j,k}] \\
& + \frac{\Delta t}{r_i \Delta \theta_j} [\langle \rho h^n n v^{n+1} \rangle_{i,j-(1/2),k} - \langle \rho h^n n v^{n+1} \rangle_{i,j+(1/2),k}] \\
& + \frac{\Delta t}{\Delta z_k} [\langle \rho h^n n w^{n+1} \rangle_{i,j,k-(1/2)} - \langle \rho h^n n w^{n+1} \rangle_{i,j,k+(1/2)}] \\
& + (p_{i,j,k}^{n+1} - p_{i,j,k}^n) + \frac{\Delta t}{r_i \Delta r_i} [\langle pur \rangle_{i+(1/2),j,k}^{n+1}] \\
& + \frac{\Delta t}{r_i \Delta \theta_j} [\langle pv \rangle_{i,j+(1/2),k}^{n+1} - \langle pv \rangle_{i,j-(1/2),k}^{n+1}] \\
& + \frac{\Delta t}{\Delta z_k} [\langle pw \rangle_{i,j,k+(1/2)}^{n+1} - \langle pw \rangle_{i,j,k-(1/2)}^{n+1}] \\
& + \frac{\Delta t p_{i,j,k}^{n+1}}{r_i \Delta r_i} [-(ur)_{i+(1/2),j,k}^{n+1}] + \frac{\Delta t p_{i,j,k}^{n+1}}{r_i \Delta \theta_j} [v_{i,j-(1/2),k}^{n+1} - v_{i,j+(1/2),k}^{n+1}] \\
& + \frac{\Delta t p_{i,j,k}^{n+1}}{\Delta z_k} [w_{i,j,k-(1/2)}^{n+1} - w_{i,j,k+(1/2)}^{n+1}] \\
& + \frac{\Delta t}{r_i \Delta r_i} \left[K_{i+(1/2),j,k}^n \frac{T_{i+1,j,k}^n - T_{i,j,k}^n}{\Delta r_{i+(1/2)}} \right]
\end{aligned}$$

$$\begin{aligned}
 & + \frac{\Delta t}{r_i^2 \Delta \theta_j} \left[K_{i, j+(1/2), k}^n \frac{T_{i, j+1, k}^n - T_{i, j, k}^n}{\Delta \theta_{j+(1/2)}} \right. \\
 & \quad \left. - K_{i, j-(1/2), k}^n \frac{T_{i, j, k}^n - T_{i, j-1, k}^n}{\Delta \theta_{j-(1/2)}} \right] \\
 & + \frac{\Delta t}{\Delta z_k} \left[K_{i, j, k+(1/2)}^n \frac{T_{i, j, k+1}^n - T_{i, j, k}^n}{\Delta z_{k+(1/2)}} \right. \\
 & \quad \left. - K_{i, j, k-(1/2)}^n \frac{T_{i, j, k}^n - T_{i, j, k-1}^n}{\Delta z_{k-(1/2)}} \right] + \Delta t Q_{i, j, k}^{n+1}. \tag{41}
 \end{aligned}$$

Note that Eqs. 37 and 40 were obtained with the aid of Fig. 4, and the components of the stress tensor are related to the velocity gradients through the standard constitutive equations for Newtonian fluid with the Stokes hypothesis. The determination of flow velocity at the center requires calculation of its two components, conveniently chosen here as perpendicular ones u_x and u_y , as shown in Fig. 3 for the cylindrical control volume. The stress components acting on the surfaces of this control volume are shown in Fig. 5. By applying Eq. 2 to this control volume for both the x and y directions, we obtain the following two momentum equations, from which u_x and u_y can be determined.

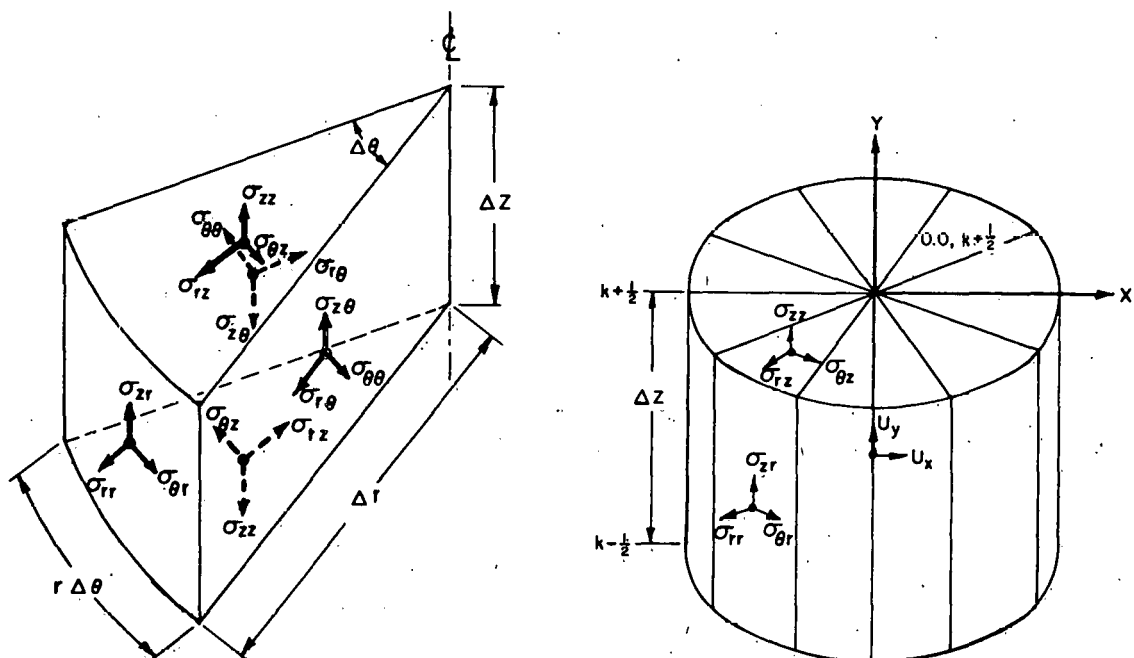


Fig. 4. Control Volume for v or p with Stress Components Shown on Surfaces; $i = 1$

Fig. 5. Control Volume for u_x and u_y at Center

f. The u_x -momentum Equation for $r = 0$. From Eq. 2, in reference to Fig. 5, we get

$$\rho_{0,0,k}^n (u_x)^{n+1} = \overline{(\rho u_x)}_{0,0,k} + \Delta t \rho_{0,0,k}^n g_x - \frac{\Delta t}{\pi r_1} \sum_{\theta_1}^{\theta_n} p_{1,j,k}^{n+1} \cos \theta \Delta \theta, \quad (42)$$

where

$$\begin{aligned} \overline{(\rho u_x)}_{0,0,k} &= (\rho u_x)_{0,0,k}^n + \Delta t D_{0,0,k}^n (u_x)_{0,0,k}^n \\ &\quad - \frac{\Delta t}{\pi r_1} \sum_{\theta_1}^{\theta_n} \langle \rho u_x^{n+1} u^{n+1} \cos \theta \rangle_{1,j,k} \Delta \theta - \frac{\Delta t}{\pi r_1} \sum_{\theta_1}^{\theta_n} \langle \rho u_x^{n+1} v^{n+1} \sin \theta \rangle_{1,j,k} \Delta \theta \\ &\quad - \frac{\Delta t}{\Delta z_k} [\langle \rho u_x^{n+1} w^{n+1} \rangle_{0,0,k+(1/2)} - \langle \rho u_x^{n+1} w^{n+1} \rangle_{0,0,k-(1/2)}] + \Delta t (v_x)_{0,0,k}^{n+1} \end{aligned} \quad (43)$$

and

$$\begin{aligned} (v_x)_{0,0,k}^{n+1} &= \frac{1}{\pi r_1} \sum_{\theta_1}^{\theta_n} (\sigma_{rr})_{1,j,k}^{n+1} \cos \theta \Delta \theta + \frac{1}{\pi r_1} \sum_{\theta_1}^{\theta_n} (\sigma_{r0})_{1,j,k}^{n+1} \sin \theta \Delta \theta \\ &\quad + \frac{1}{2\pi \Delta z_k} \sum_{\theta_1}^{\theta_n} [(\sigma_{rz})_{1/2,j,k+(1/2)}^{n+1} - (\sigma_{rz})_{1/2,j,k-(1/2)}^{n+1}] \cos \theta \Delta \theta \\ &\quad + \frac{1}{2\pi \Delta z_k} \sum_{\theta_1}^{\theta_n} [(\sigma_{\theta z})_{1/2,j,k+(1/2)}^{n+1} - (\sigma_{\theta z})_{1/2,j,k-(1/2)}^{n+1}] \sin \theta \Delta \theta. \end{aligned} \quad (44)$$

g. The u_y -momentum Equation for $r = 0$. Similarly, the y component, as defined, is given by Fig. 2 as

$$\rho_{0,0,k}^n (u_y)^{n+1} = \overline{(\rho u_y)}_{0,0,k} + \Delta t \rho_{0,0,k}^n g_y - \frac{\Delta t}{\pi r_1} \sum_{\theta_1}^{\theta_n} p_{1,j,k}^{n+1} \sin \theta \Delta \theta, \quad (45)$$

where

$$\begin{aligned}
 \overline{(\rho u_y)}_{0,0,k}^n &= (\rho u_y)_{0,0,k}^n + \Delta t D_{0,0,k}^n (u_y)_{0,0,k}^n \\
 &- \frac{\Delta t}{\pi r_1} \sum_{\theta_1}^{\theta_n} \langle \rho u_u^{n+1} u^{n+1} \sin \theta \rangle_{1,j,k} \Delta \theta \\
 &- \frac{\Delta t}{\pi r_1} \sum_{\theta_1}^{\theta_n} \langle \rho u_u^{n+1} v^{n+1} \cos \theta \rangle_{1,j,k} \Delta \theta - \frac{\Delta t}{\Delta z_k} [\langle \rho u_y^{n+1} w^{n+1} \rangle_{0,0,k+(1/2)} \\
 &- \langle \rho u_y^{n+1} w^{n+1} \rangle_{0,0,k-(1/2)}] + \Delta t (v_y)_{0,0,k}^{n+1}, \tag{46}
 \end{aligned}$$

and

$$\begin{aligned}
 (v_y)_{0,0,k}^{n+1} &= \frac{1}{\pi r_1} \sum_{\theta_1}^{\theta_n} (\sigma_{rr})_{1,j,k}^{n+1} \sin \theta \Delta \theta + \frac{1}{\pi r_1} \sum_{\theta_1}^{\theta_n} (\sigma_{r\theta})_{1,j,k}^{n+1} \cos \theta \Delta \theta \\
 &+ \frac{1}{2\pi \Delta z_k} \sum_{\theta_1}^{\theta_n} [(\sigma_{rz})_{1/2,j,k+(1/2)}^{n+1} - (\sigma_{rz})_{1/2,j,k-(1/2)}^{n+1}] \sin \theta \Delta \theta \\
 &+ \frac{1}{2\pi \Delta z_k} \sum_{\theta_1}^{\theta_n} [(\sigma_{\theta z})_{1/2,j,k+(1/2)}^{n+1} - (\sigma_{\theta z})_{1/2,j,k-(1/2)}^{n+1}] \cos \theta \Delta \theta. \tag{47}
 \end{aligned}$$

In Eqs. 42-47, $\theta_1 + \dots + \theta_n = 2\pi$. Note that, except for Eqs. 42-47, which require a modest amount of additional coding, very little coding effort is needed to incorporate the modifications into Eqs. 16, 20-22, and 24-30 to resolve the singularity problem; the modifications can be easily identified by comparing these equations with Eqs. 31-41. What these formulations have achieved to a large measure is that they justify the elimination of most of the difficult terms mentioned at the beginning of this section. Of course, they also provide for the recipes to correctly evaluate the viscous terms in connection with the degenerate five-sided control volumes, and to determine unambiguously the flow velocity at the origin of a cylindrical-coordinate system; $w_{0,0,k}$ and $T_{0,0,k}$ are given by averages of values at $i = 1$. The stresses at $r = 0$ can be computed in an analogous manner when needed.

5. The Pressure-correction Equation

The accuracy of the computed pressure field determines that of the computed velocities and, in turn, the magnitude of the mass residue (or mass imbalance) in each computation cell. The mass residue D as defined by Eq. 16 must be minimized by successively adjusting the pressure field. This is accomplished by means of the Newton-Raphson scheme with a relaxation parameter ω :

$$\Delta \tilde{p}_{i,j,k}^{n+1} = -\omega D_{i,j,k}^{n+1} \left| \frac{\partial D_{i,j,k}^{n+1}}{\partial p_{i,j,k}^{n+1}} \right|, \quad (48)$$

$$p_{i,j,k}^{n+1} = \tilde{p}_{i,j,k}^{n+1} + \Delta \tilde{p}_{i,j,k}^{n+1}. \quad (49)$$

The tilde (~) over pressure p here indicates that the pressure field is being corrected within the same $(n + 1)$ st time step, and that \tilde{p} represents the latest iterative value of p available before the correction as specified by Eqs. 48 and 49.

To derive a relation for $\partial D / \partial p$, Eqs. 20, 24, and 27 are first substituted in Eq. 16, and the partial derivatives then computed. The result is

$$\begin{aligned} \frac{\partial D_{i,j,k}^{n+1}}{\partial p_{i,j,k}^{n+1}} &= \frac{1}{\Delta t} \frac{\partial p_{i,j,k}^{n+1}}{\partial p_{i,j,k}^{n+1}} + \frac{\Delta t}{r_i \Delta r_i} \left[\frac{r_{i+(1/2)}}{\Delta r_{i+(1/2)}} \frac{1}{1 + (B_r^*)_{i+(1/2),j,k}} \right. \\ &+ \frac{r_{i-(1/2)}}{\Delta r_{i-(1/2)}} \frac{1}{1 + (B_r^*)_{i-(1/2),j,k}} \left. \right] + \frac{\Delta t}{r_i \Delta \theta_j} \left[\frac{1}{r_i \Delta \theta_{j+(1/2)}} \frac{1}{1 + (B_\theta^*)_{i,j+(1/2),k}} \right. \\ &+ \frac{1}{r_i \Delta \theta_{j-(1/2)}} \frac{1}{1 + (B_\theta^*)_{i,j-(1/2),k}} \left. \right] + \frac{\Delta t}{\Delta z_k} \left[\frac{1}{\Delta z_{k+(1/2)}} \frac{1}{1 + (B_z^*)_{i,j,k+(1/2)}} \right. \\ &+ \frac{1}{\Delta z_{k-(1/2)}} \frac{1}{1 + (B_z^*)_{i,j,k-(1/2)}} \left. \right], \end{aligned} \quad (50)$$

where

$$\left. \begin{aligned} (B_r^*)_{i+(1/2),j,k} &= [\Delta t / \rho_{i+(1/2),j,k}^n] (B_r^n / \ell_r)_{i+(1/2),j,k}, \\ (B_\theta^*)_{i,j+(1/2),k} &= [\Delta t / \rho_{i,j+(1/2),k}^n] (B_\theta^n / \ell_\theta)_{i,j+(1/2),k}, \\ (B_z^*)_{i,j,k+(1/2)} &= [\Delta t / \rho_{i,j,k+(1/2)}^n] (B_z^n / \ell_z)_{i,j,k+(1/2)}, \end{aligned} \right\} \quad (51)$$

etc.

B_r^n , ℓ_r , ..., etc., are as defined earlier, related to the resistant forces such as arising from baffles. In the absence of such forces, the right-hand sides of Eqs. 51 vanish; and further, if uniform mesh is used, Eq. 50 reduces to

$$\frac{\partial D_{i,j,k}^{n+1}}{\partial p_{i,j,k}^{n+1}} = \frac{1}{\Delta t} \frac{\partial \rho_{i,j,k}^{n+1}}{\partial p_{i,j,k}^{n+1}} + 2\Delta t \frac{1}{(\Delta r_i)^2} + \frac{1}{(r_i \Delta \theta_j)^2} + \frac{1}{(\Delta z_k)^2} . \quad (52)$$

Note that for the degenerate five-sided control volumes next to the singular point $r = 0$, $\partial D/\partial p$ is derived from Eq. 31, and the result is the same as Eq. 50, except with the term involving index $i - (1/2)$ dropped. The same remark also applies to the computation cell that is next to a solid boundary, where the mass-imbalance equation takes a form similar to Eq. 31.

B. Solution Procedure

1. The Modified ICE Scheme

The solution procedure of a well-defined problem follows essentially the ICE scheme.¹³ Typically, after reading input and completing initialization, COMMIX-SA-1 enters the time-step loop. First, energy equation 30 is solved to obtain enthalpy, and temperature and density are computed using the equation of state (i.e., water properties, Sec. III.C). Note that during the very first time step, this computational step ensures that all field variables (i.e., ρ , h , and T) are thermodynamically compatible; during subsequent time steps, however, solving the energy equation at this point is equivalent to solving it at the end of the previous time step. Next, the explicit terms in the momentum equations are evaluated, using Eqs. 21, 22, 25, 26, 28, and 29; these terms are denoted as $(\rho u)^n$, $(\rho v)^n$, and $(\rho w)^n$, which combine the convective and viscous terms, and whose values will remain unchanged throughout all the iterations within the given time step.

At this point, the iteration process starts, the objective being calculation of an acceptably accurate pressure field, which in turn will yield an acceptably accurate velocity field, which, finally, will reduce all the cell mass residues to an acceptable level. This acceptable level is determined by the convergence criteria, which are controlled by the users through input of two parameters (see Sec. III.B.3). Specifically, as COMMIX-SA-1 enters the iteration loop (which is embedded in the time-step loop), the mass residue of a cell is first computed using Eq. 16. Immediately following this, the pressure in that cell is corrected by using Eqs. 37 and 39, and the velocity components entering or leaving this cell are computed by using Eqs. 20, 24, and 27. This completes the adjustment in this cell, and the same operation is repeated for the next cell and all the rest within the flow domain of interest.

Velocities stored in the fictitious boundary cells are updated as needed after each complete sweep according to the appropriate boundary conditions. (See Sec. IV for more detail.) A complete sweep of all computational

cells defines an iteration. At the end of an iteration, a check is made to see if any of the cell mass residues exceeded the specified maximum. If so, the next iteration is performed; but if not (i.e., if none of the cell mass residues exceeded the specified maximum), we say the iteration has converged. Usually, the iteration process would continue until either convergence is reached or the number of iterations is equal to the maximum allowed by the user. (The user must, of course, exercise good judgment in specifying the allowable maximum number of iterations in order to obtain meaningful results.)

Note that during the iterations described above, the latest values for all the variables must be used where $n + 1$ appears as the superscript in the finite-difference equations. Also, the relaxation parameter ω , Eq. 37, must be assigned a value between 1 and 2, i.e., $1 < \omega < 2$, because the iterative method described above is the successive overrelaxation (SOR) technique.

With respect to the convergence rate, experience has shown the SOR technique to be superior to the Jacobi and Gauss-Seidel techniques. These techniques are compared in Appendix C. COMMIX-SA-1 offers all three as options. In addition, COMMIX-SA-1 offers another option, which, under certain circumstances, affords an even better convergence rate than the SOR technique. This technique performs the pressure correction and velocity updating only in cells in which the computed mass residue exceeds the prescribed maximum. This is unlike the SOR, Jacobi, and Gauss-Seidel techniques, which perform the pressure correction and velocity updating in all cells during each iteration. In practice, COMMIX-SA-1 uses a cell index IMASS to signal whether continuity is satisfied in each cell. During the first iteration in a given time step, each cell is assigned IMASS = 9, so that mass residue is computed for each cell. If the computed mass residue for a cell turns out to be less than what the convergence criterion requires, then COMMIX-SA-1 immediately sets IMASS = 0 for that cell. For cells whose computed mass residues exceed the criterion, COMMIX-SA-1 sets IMASS = 9 for those cells and their immediate neighboring cells. Thus, during the subsequent iterations, mass residue is computed only for cells with index IMASS = 9, and the pressure is corrected and velocities updated only for cells in which the newly computed mass residues still exceed the criterion. Obviously, in situations in which the flow field changes only locally from one time step to the next, this technique can speed up the iteration process considerably. Indeed, when stratification is well maintained in the thermal storage, this technique has been shown to reduce the computation by nearly sixfold over the SOR technique.

The above description of the solution procedure indicates that the energy equation is solved outside the iteration loop. In practice, however, COMMIX-SA-1 also allows stronger coupling of the energy equation with other conservation equations; namely, options are provided in the code to include the energy-equation calculations at every N th iteration (N being a user input parameter, ranging from 1 to the maximum number of iterations allowed in a given time step).

Upon exit from the iteration loop, COMMIX-SA-1 proceeds to the next time step and repeats the time-step loop operations as described above. Time advancement would continue until the end of a transient event, or until a steady state is obtained if such is the objective of the calculation. In most of the problems concerning solar applications, however, transient calculations are required.

2. Flow Diagram

The solution procedure as described in Sec. 1 above is summarized in a computational flow diagram (Fig. 6). This diagram is intended only to convey the computational logic and important computational steps. Readers are referred to the coding itself for details, additional options, etc.

3. Convergence Criterion

The criterion used in determining whether the pressure-velocity iteration converges is given in terms of mass residue. Convergence is considered to be reached if the absolute value of the computed mass residue in all the computation cells is less than

$$D_{\text{conv}} = \epsilon_1 \left(\text{Max}_{i,j,k} \left\{ \rho_{i,j,k}^n \left[\frac{|u_{i+(1/2),j,k}^n| + |u_{i-(1/2),j,k}^n|}{2\Delta r_i} \right. \right. \right. \\ \left. \left. \left. + \frac{|v_{i,j+(1/2),k}^n| + |v_{i,j-(1/2),k}^n|}{2r_i \Delta \theta_j} + \frac{|w_{i,j,k+(1/2)}^n| + |w_{i,j,k-(1/2)}^n|}{2\Delta z_k} \right] \right\} + \epsilon_2 \right). \quad (53)$$

In other words, convergence is reached if and only if

$$|D_{i,j,k}^{u+1}| < D_{\text{conv}} \text{ for all } i, j, k.$$

In Eq. 53, ϵ_1 and ϵ_2 are user-input parameters. Their proper magnitudes depend on the magnitude of the velocity field, as is clear from Eq. 53. Commonly used values are $\epsilon_1 = 10^{-3}$ and $\epsilon_2 = 10^{-6}$. But the user is advised to perform a number of experimentations to determine values best suited for the problems under consideration.

C. Physical System and Parameters

1. Properties of Water

The water-properties package as used in COMMIX-SA-1 is the result of cumulative effort by many individuals in performing experiments, curve fitting,

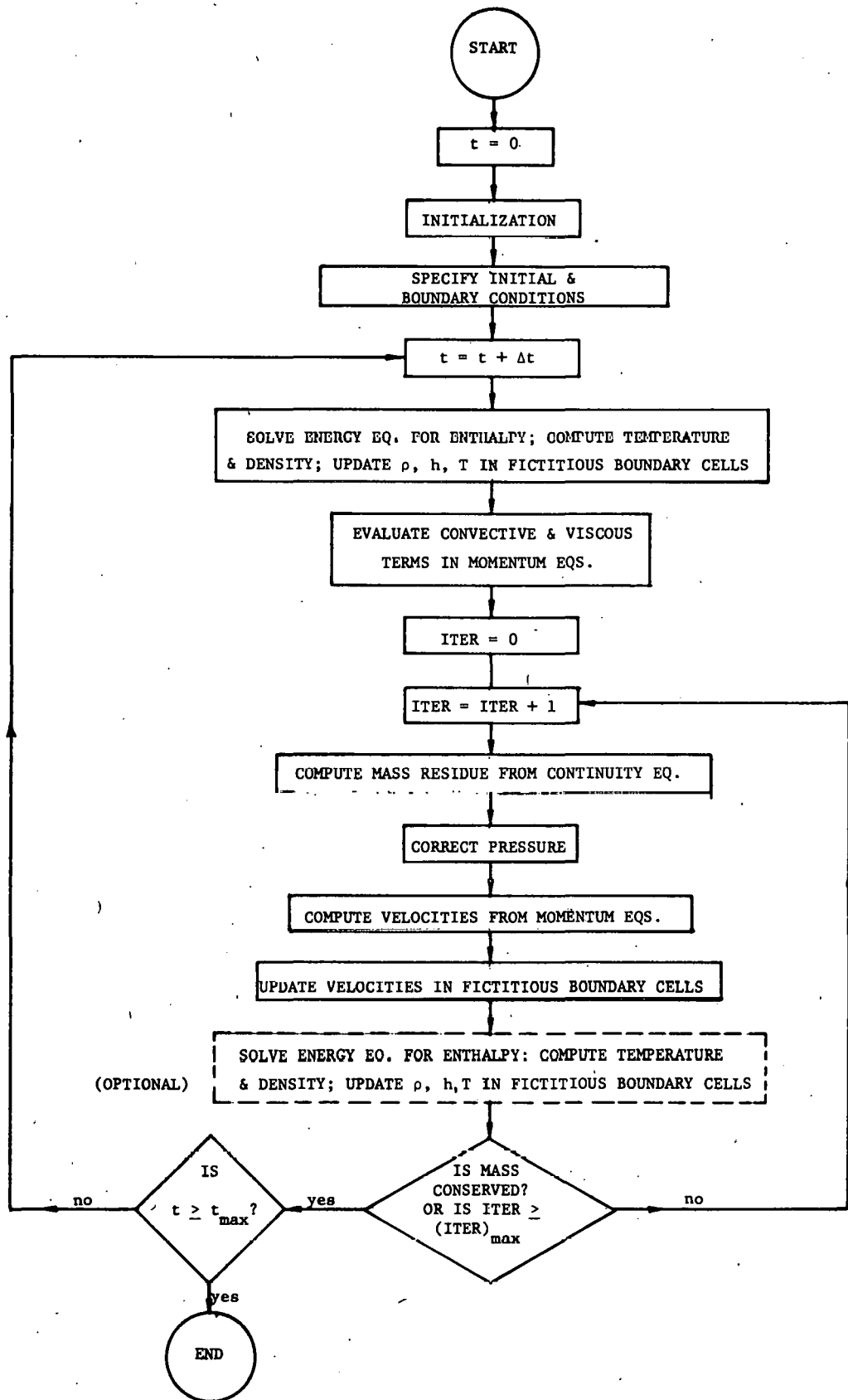


Fig. 6. A Simplified Flow Chart for COMMIX-SA-1 Execution

and computer coding. The works of Keenan et al.,¹⁴ Jordan,¹⁵ the Brookhaven National Laboratory thermal-hydraulics group, and others have contributed directly or indirectly to this final product. The package consists of a collection of subroutines and function subprograms that evaluate the thermophysical properties of water. Appendix B contains some plots of these properties for the temperature range 0-100°C, which is of interest with sensible heat-storage tanks.

2. A Hydraulic Model for Impermeable and Perforated Baffles

The presence of baffles in a flow field alters the flow pattern, influences the extent of turbulent mixing, and affects the heat-transfer process. In the design of heat-storage tanks, where thermal stratification is to be preserved or enhanced, baffles, if properly placed, can have a significant beneficial impact. In COMMIX-SA-1, baffles are represented by nonlinear velocity-dependent resistant forces, which are incorporated in the momentum equations, e.g., R_r , R_θ , and R_z in Eqs. 4, 5, and 6, respectively. Specifically, these resistant forces take the form

$$R_r = (1/2)f\rho|u|u, \quad (54)$$

$$R_\theta = (1/2)f\rho|v|v, \quad (55)$$

and

$$R_z = (1/2)f\rho|w|w, \quad (56)$$

where f represents the friction factor associated with the baffle plates. In the finite-difference representations of the momentum equations, the resistant forces 54-56 are linearized in the following sense:

$$R_r^{n+1} = A_r^n + B_r^n u^{n+1}, \quad (57)$$

$$R_\theta^{n+1} = A_\theta^n + B_\theta^n v^{n+1}, \quad (58)$$

and

$$R_z^{n+1} = A_z^n + B_z^n w^{n+1}, \quad (59)$$

where, as before, the superscripts n and $n + 1$ indicate previous and current time steps, respectively, and where the A 's and B 's are defined as follows.

For impermeable baffles,

$$\left. \begin{aligned} A_r^n &= A_\theta^n = A_z^n = 0, \\ \text{and} \\ B_r^n &= B_\theta^n = B_z^n = \text{a large positive number (say } 10^{25}). \end{aligned} \right\} \quad (60)$$

For perforated baffles,

$$\left. \begin{aligned} A_r^n &= -(1/2)f\rho^n|u^n|u^n, \\ A_\theta^n &= -(1/2)f\rho^n|v^n|v^n, \\ A_z^n &= -(1/2)f\rho^n|w^n|w^n, \\ B_r^n &= f\rho^n|u^n|, \\ B_\theta^n &= f\rho^n|v^n|, \\ B_z^n &= f\rho^n|w^n|. \end{aligned} \right\} \quad (61)$$

and

$$B_z^n = f\rho^n|w^n|.$$

The friction factor f is given by¹⁴

$$\left. \begin{aligned} f &= f_0 \lambda_a \text{ if } t/d < 0.8; \\ \text{or} \\ f &= f_{0.8} \lambda_b \text{ if } t/d > 0.8, \end{aligned} \right\} \quad (62)$$

where t is the baffle-plate thickness, d is the perforated-hole diameter, f_0 and $f_{0.8}$ are functions of the porosity (α), and λ_a and λ_b are correction factors dependent upon α and t/d . (For details of these correlations, see Ref. 16.)

Note that for impermeable baffles, the B 's in COMMIX-SA-1 are assigned an arbitrarily large number, e.g., 10^{25} , the consequence of which is that the calculated velocities practically vanish where the impermeable baffles are located. For perforated baffles, Eqs. 61 lead to reduced velocities depending on the perforation parameters. Of course, when no baffles are present, the A 's and B 's are simply zeros.

3. Thermal Interactions between Fluid and Structures

a. Baffle Heat-transfer Model. The thermal conductivity of baffles is accounted for in the energy equation. Namely, in Eq. 30, the appropriate K's will be substituted by suitable values for the baffles. Thus, the effects of conducting, "low-conducting," and "nonconducting" baffles can be readily compared.⁷ Also, baffles of both finite and infinitesimal thicknesses can be easily simulated. For baffles with finite thicknesses, several computation cells may be arranged to span the thicknesses, if desired. For baffles of sufficiently small thicknesses, the computation cell surfaces are usually made coincident with the baffles, and except for "low-conducting" or "nonconducting" baffles, the thermal effect of thin baffles may be conveniently ignored.

b. Tank-wall Heat-transfer Model. The following model accounts for the convective heat transfer between the storage-tank wall and the contained fluid, as well as for the heat loss from the wall to the ambient. Usually, the wall thickness, d , is small, as is the temperature variation within the wall. Hence we choose to deal with the mean wall temperature, $T_w(t)$. In other words, we neglect heat conduction within the wall so that our attention is confined to the heat exchange between the fluid and the wall, and between the wall and its surrounding environment. Such a simplification will greatly facilitate computation and reduce the computer storage requirement while still allowing the essential physical processes to be represented.

We consider a wall element having a volume V and heat-transfer area A with the fluid on one side and the surrounding environment on the other. The energy balance for this wall element can be written

$$\rho_w c_w V \frac{dT_w}{dt} = -h_f A (T_w - T_f) - h_a A (T_w - T_a), \quad (63)$$

where

ρ_w = density of wall,

c_w = specific heat of wall,

T_f = fluid temperature,

T_a = ambient temperature,

h_f = fluid-side heat-transfer coefficient,

and

h_a = ambient heat-transfer coefficient.

In general, T_f , T_a , h_f , and h_a are functions of time; h_f is given by¹⁷

$$h_f = Nu \frac{k_f}{L} = 0.664 Pr^{1/3} Re_L^{1/2} \frac{k_f}{L}, \quad Pr > 0.5, \quad (64)$$

where

L = tank depth,

k_f = thermal conductivity of fluid,

Nu = Nusselt number,

Pr = Prandtl number,

and

Re_L = Reynolds number based on tank depth.

We determine h_a by tank-insulation thickness and thermal properties as well as the ambient conditions.

Defining

$$\tau_f = \frac{\rho_w C_w V}{h_f A} \quad (65)$$

and

$$\tau_a = \frac{\rho_w C_w V}{h_a A}, \quad (66)$$

we can rewrite Eq. 63 as

$$\frac{dT_w}{dt} + \left(\frac{1}{\tau_f} + \frac{1}{\tau_a} \right) T_w = \frac{T_f}{\tau_f} + \frac{T_a}{\tau_a}. \quad (67)$$

With the initial condition taken to be

$$T_w(0) = T_{w0}, \quad (68)$$

Eq. 8 has the solution

$$T_w(t) = \exp \left[- \int_0^t \left(\frac{1}{\tau_f} + \frac{1}{\tau_a} \right) dt' \right] \left\{ \int_0^t \left(\frac{T_f}{\tau_f} + \frac{T_a}{\tau_a} \right) \exp \left[\int_0^{t'} \left(\frac{1}{\tau_f} + \frac{1}{\tau_a} \right) dt'' \right] dt' + T_{w0} \right\}. \quad (69)$$

If $T_w(t_1)$ is the wall temperature at $t = t_1$, then at $t = t_1 + \Delta t$, the wall temperature is given by

$$T_w(t_1 + \Delta t) = T_w(t_1) \exp \left[-\left(\frac{1}{\tau_f} + \frac{1}{\tau_a} \right) \Delta t \right] + \frac{T_f(t_1) \tau_a + T_a(t_1) \tau_f}{\tau_f + \tau_a} \left\{ 1 - \exp \left[-\left(\frac{1}{\tau_f} + \frac{1}{\tau_a} \right) \Delta t \right] \right\}, \quad (70)$$

provided that T_f , T_a , τ_f , and τ_a can be treated as constants during the time interval Δt .

Equation 70 can also be written as

$$T_w(t_1 + \Delta t) = T_w(t_1) \exp[-(Bi_f + Bi_a) \alpha \Delta t / d^2] + \frac{T_f(t_1) Bi_f + T_a(t_1) Bi_a}{Bi_f + Bi_a} \left\{ 1 - \exp[-(Bi_f + Bi_a) \alpha \Delta t / d^2] \right\}, \quad (71)$$

where

$d = V/A$ = wall thickness,

$\alpha = k_w / (\rho_w C_w)$ = thermal diffusivity of wall,

$Bi_f = h_f d / k_w$ = fluid-side Biot modulus,

$Bi_a = h_a d / k_w$ = ambient-side Biot modulus,

and

k_w = thermal conductivity of wall.

The dimensionless number $\alpha \Delta t / d^2$ in Eq. 71 is sometimes referred to as the Fourier modulus.

In the COMIX-SA-1 calculations, Eq. 70 or 71 is invoked at each time step to update temperatures in the fictitious boundary cells when the option to consider effect of tank-wall heat capacity is used (see Sec. IV). In addition, the total heat loss (H_ℓ) from the storage tank to the ambient is computed according to

$$H_\ell = \int_{t_1}^{t_2} \phi \int_A h_a (T_w - T_a) dA dt \quad (72)$$

for any given time interval $t_2 - t_1$.

IV. INITIAL AND BOUNDARY CONDITIONS

A. Initial Conditions

Initial conditions for pressure, temperature, and the three velocity components are specified through input for the whole flow domain (default value is zero). Initial values for density and enthalpy are computed from equations of state, using the initial values for pressure and temperature. Since initial conditions can greatly affect computational efficiency, they should be specified judiciously. To reduce input effort, COMMIX-SA-1 automatically performs a pressure initialization to account for hydrostatic head in the presence of the gravitational field. A restarting option is provided in COMMIX-SA-1. In this case, the initial conditions are the values of the state variables at the previous iteration before the restarting.

B. Boundary Conditions

1. Grouped Fictitious Boundary Cells

Fictitious boundary cells (FBC's) are a layer of computation cells outside of and adjacent to the flow domain of interest that are used to facilitate treatment of boundary conditions. They have been used previously, e.g., in the KACHINA code,¹⁸ and have afforded some computational conveniences. COMMIX-SA-1, in anticipation of complex boundary conditions arising from practical applications, takes a further step to group the FBC's according to types of boundary conditions. Since updating of variables in the FBC's occurs in every iteration, such grouping has realized a substantial saving in computation time.

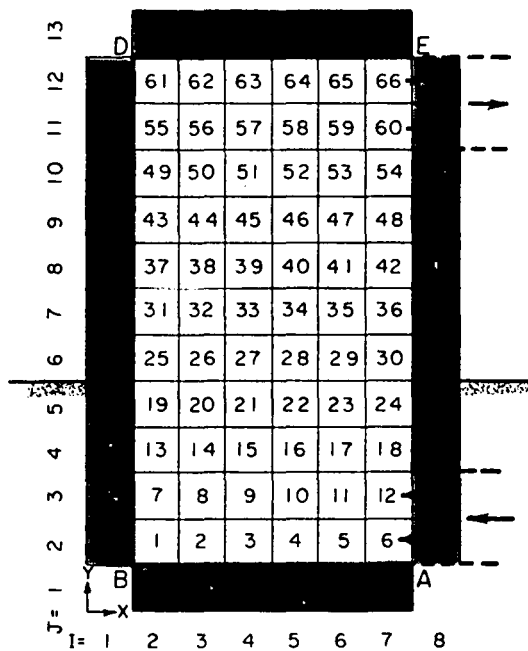
Grouping of FBC's in COMMIX-SA-1 is preceded by a certain ordering (or numbering) of all the computation cells. At the outset of a computational run, COMMIX-SA-1 constructs a three-dimensional array $MS(I,J,K)$ which maps all the three-tuples (I,J,K) into integers MS .

The number-assigning process normally starts with interior cells (i.e., computation cells within the flow domain), in increasing order of I , then J , then K , and continues on to cover all the FBC's. Upon completion of the process, each cell will have two identifications, i.e., (I,J,K) and MS , which are one-to-one correspondent. (The one-to-one correspondence does not apply where the flow domain has a concave corner, i.e., where the FBC has more than one adjacent interior cell. In this case, additional arrays are created to accommodate the additional neighbors. The details for dealing with this situation can be found in subroutines GEOM and CONCAV.)

The (I,J,K) system has the distinct advantage that a given cell (I,J,K) can readily identify its neighbors; namely, cells $(I \pm 1, J, K)$, $(I, J \pm 1, K)$ and $(I, J, K \pm 1)$. Computational sweeps during iterations in COMMIX-SA-1 go by the (I,J,K) system. On the other hand, the one-dimensional MS system has

advantages in connection with storage and with grouping of the FBC's. The efficient boundary-condition updating technique of COMMIX-SA-1 relies on the MS system.

After the MS(I,J,K) array is constructed, and the adjacent interior cell of each FBC identified, the MS numbers of FBC's having the same type of boundary conditions are gathered together to form a group, a running index being also assigned to keep track of the group members. When variables stored in the FBC's must be updated (e.g., when velocities in the FBC's are to be updated in each iteration), COMMIX-SA-1 sweeps through the FBC's group by group, updating only the group members that require it, and leaving the others unaltered. An example is provided in the following to further explain this method.



Shaded cells are fictitious boundary cells
 Numbers in cells are MS-numbers
 Adiabatic boundaries: AB, BC, EF, and GH
 Constant temperature boundaries: CD, DE, FG, and HA
 Solid wall and no-slip boundaries: AB, BD, DE, and FH
 Constant flow boundary: AH
 $\partial u / \partial x = 0$ boundary: EF

Fig. 7. An Example Illustrating COMMIX-SA-1 Numbering Schemes and Grouping of Fictitious Boundary Cells

required, temperatures in the FBC's of the adiabatic group will be set equal to those in the corresponding adjacent interior cells (see Sec. IV.B.3 below), and no changes need to be made on temperatures for the constant-temperature group, as they will remain as initialized.

As shown in Fig. 7, a two-dimensional flow domain is surrounded by solid walls, which are no-slip boundaries; inflow is at constant velocity and temperature, and the outflow velocity and temperature are to be determined by the specified $\partial u / \partial x = 0$ and adiabatic conditions, respectively. Boundaries AB, BC, and GH are heavily insulated; hence, adiabatic conditions are assigned. Boundaries CD, DE, and FG are in direct contact with ambient, which is at constant temperature. A 2-D flow problem is chosen here merely for the convenience of illustration. In Fig. 7, the FBC's are shown shaded, and the numbers in the cells represent their MS numbers, which are established by the procedure just described. The (I,J)-MS correspondences in this case are MS(4,3) = 14, MS(9,6) = 47, etc. Grouping of the FBC's is as stated in Fig. 7. For example, the group for adiabatic conditions consists of cells 67, 68, 69, 70, 71, 72, 73, 75, 77, 78, 79, 80, 92, and 94, and the group for constant temperature consists of cells 74, 76, 81-91, 93, and 95-100. When updating of variables in FBC's is

The advantages of using grouped FBC's in treating boundary conditions are summarized as follows:

a. The governing finite-difference equations can be coded, regardless of boundary conditions. Furthermore, new types of boundary conditions can easily be added without affecting the governing finite-difference equations.

b. The variables in the FBC's are properly updated. Therefore, when they are referenced in the finite-difference equations during computation, the desired boundary conditions are automatically satisfied without any testing of boundary-condition type.

c. Grouping of FBC's and updating by groups reduce computation time substantially. In fact, many groups of FBC's need not even be updated throughout the solution process, e.g., the constant-temperature group mentioned above.

2. Velocity-boundary Conditions

COMMIX-SA-1 provides for options to treat the following types of velocity-boundary conditions.

a. Free-slip Boundary. The boundary exerts no drag on the flow. It can also represent an axis or plane of symmetry. The velocities along the boundary are to equal those in the adjacent interior cells (AIC's). Hence, one or two of the following apply (depending on information supplied at program input, which is used in FBC's grouping):

$$U_{FBC} = U_{AIC},$$

$$V_{FBC} = V_{AIC},$$

or

$$W_{FBC} = W_{AIC}.$$

Note that the Δr , $\Delta\theta$, and Δz dimensions of the FBC's must equal those of their corresponding AIC's.

b. No-slip Boundary. The boundary exerts resistance on the flow, and flow velocity at the boundary is equal to zero. One or two of the following apply:

$$U_{FBC} = -U_{AIC},$$

$$V_{FBC} = -V_{AIC},$$

or

$$W_{FBC} = -W_{AIC}.$$

c. Zero Normal-velocity-gradient Boundary. This type of boundary condition is usually used to determine the velocity at the outflow boundary, where transverse flow is not significant. Some velocities are located at cell surfaces, and since $u_{i+(1/2),j,k}$ is stored at (i,j,k) , $w_{i,j,k-(1/2)}$ is stored at $(i,j,k-1)$, etc., the velocities to be determined may or may not be stored in FBC's. However, the normal velocity at the boundary is set equal to that at the adjacent interior node (AIN); i.e.,

$$U_B = U_{AIN},$$

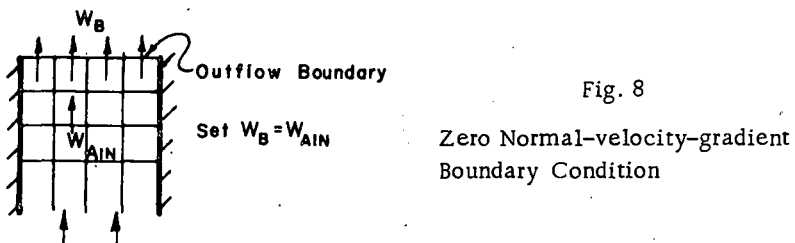
or

$$V_B = V_{AIN},$$

or

$$W_B = W_{AIN}.$$

See Fig. 8 for an illustration.



d. Transient Velocity Boundary. When the normal velocity at the boundary is a given function of time $f(t)$ (specified at program input), COMMIX-SA-1 sets

$$U_B = f(t),$$

or

$$V_B = f(t),$$

or

$$W_B = f(t),$$

whichever is applicable. Note that different functions are allowed at different locations. Again, U_B , V_B , and W_B may or may not be stored in FBC's. Also note that although constant velocity boundary is a special case of this, it is advantageous, in treating such a case, to let the boundary velocity remain constant as initialized, so that no boundary-condition updating is needed.

e. Boundary Velocity Determined by Local Mass Balance. When outflow velocity needs to be determined where velocities in the perpendicular directions are not negligible (Fig. 9), a zero normal-velocity-gradient boundary condition is not suitable. Under such circumstances, the outflow velocity (U_B in Fig. 9) may be determined by local mass balance, i.e., by invoking the continuity equation 16 for the cell in question. Boundary-velocity updating by this method is more time-consuming than for the other boundary types described above. The user is advised to ascertain the suitability of this method by numerical experimentation.

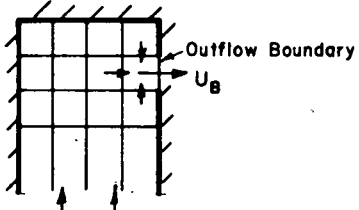


Fig. 9. Velocity at Outflow Boundary Determined by Local Mass Balance

f. Boundary Velocity Determined by Global Mass Balance. An alternative to the local-mass-balance method is one of global mass balance. As shown in

Fig. 10, the inlet velocity U_{in} is prescribed, and the outflow velocity U_B is determined by the continuity relation that both U_B and U_{in} must satisfy. Another option is also available in COMMIX-SA-1, and that is: When applicable, U_B and U_{in} can be both specified through input as constant or time-dependent velocities.

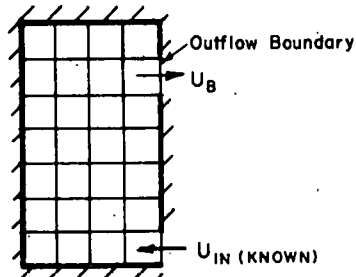


Fig. 10

Velocity at Outflow Boundary Determined by Global Mass Balance

3. Temperature-boundary Conditions

The following options for temperature-boundary conditions are provided for in COMMIX-SA-1.

a. Constant-temperature Boundary. Temperatures stored in the FBC's remain constant as initialized, and no FBC updating is necessary for this type of boundary condition.

b. Adiabatic Boundary. When no heat flux is allowed through the boundary (e.g., when the boundary is ideally insulated), temperature, enthalpy, and density in the FBC's are set equal to those in the corresponding AIC's:

$$T_{FBC} = T_{AIC},$$

$$h_{FBC} = h_{AIC},$$

and

$$\rho_{FBC} = \rho_{AIC}.$$

c. Transient Temperature Boundary. When the boundary temperature is a specified function of time $g(t)$ (different functions are allowed for different locations), temperatures in the FBC's are set according to

$$T_{FBC} = g(t),$$

and enthalpies and densities in the FBC's are computed using the updated temperatures and the initialized pressures.

d. Constant-heat-flux Boundary. When a constant heat flux q is specified at the boundary, temperatures in the related FBC's are computed by

$$T_{FBC} = T_{AIC} + q\delta/K,$$

where a positive q indicates heat flux directed into the flow domain; δ is equal to δr , $r\Delta\theta$, or Δz , depending on whether the boundary surface is perpendicular to the r , θ , or z axis; and K represents the best estimate of local thermal conductivity. Again, enthalpies and densities in the FBC's are calculated via the equations of state by using the updated temperatures and the initialized pressures.

With transient heat-flux boundaries, q will be specified as a function of time, but the updating procedure remains the same as described above.

e. Boundary with Heat Capacity. The wall heat-transfer model described in Sec. III.C.3.b is used to compute the wall temperature and the fluid-side heat-transfer coefficient. Heat gain or loss to the AIC and ambient are computed by $h_f(T_w - T_f)dA$ and $h_a(T_w - T_a)dA$, respectively. (See Sec. III.C.3.b for notation.) Heat gain or loss at the AIC so computed is then treated as the heat source in the energy equation. Consequently, temperature, enthalpy, and density in the FBC's are set equal to those in the AIC's.

V. CODE STRUCTURE

COMMIX-SA-1 was written for the IBM 360 and 370 series. However, care has been taken to facilitate its adaptation to other computing machines. The code uses a modular structure, with each subroutine constructed to perform certain well-defined task(s). Having been coded with practical applications in mind, COMMIX-SA-1 possesses a great degree of generality and flexibility, allowing for easy changes and modifications to be made by future users. Each subroutine in the code contains COMMON blocks, which consist of variables whose dimensions can be adjusted by the users to suit the sizes of problems on hand. The subroutines (or function subprograms) are listed below with brief remarks indicating their functions.

<u>Subroutine Name</u>	<u>Remarks</u>
MAIN	Commanding routine
INPUT	Input
ICNEW	Initialization
GEOM	Geometry and boundary
CONCAV	Conditions set up
	<u>Boundary Conditions Updating</u>
BCFIEL	Temperature, enthalpy, and density
BCFLOW	Velocities
BCFLOK	Velocity by local mass balance
	<u>Momentum Equations</u>
UMOM	u: momentum
VMOM	v: momentum
WMOM	w: momentum
	<u>Continuity Equation</u>
MASSCO	Mass residue
DELP	Derivatives of mass residue with respect to pressure
	<u>Velocity Evaluation</u>
NEWVEL	Cell-surface velocities
CENVEL	Center velocity
REGBAL	Regional mass-balance option
ENERGY	Energy equation
CUTOFF	Convergence criteria
RESIST	Baffle resistance

Water Properties

CPL	Specific heat
VISCL	Viscosity
THCL	Conductivity
HLIQ	Enthalpy
TLIQ	Temperature
DROLPH	Derivative of density with respect to pressure
ROLIQ	Density
POLY	Auxiliary
SNDS	Auxiliary
S	Auxiliary

GETF

FITIT

ICSSCU

LISTIN

OUTPUT

PLANE

TABLES

ARIN

CLEAR

FINI

RSET

WRITRS

Function Fitting and InterpolationOutputUtility

VI. INPUT DESCRIPTION

COMIX - S A

* * A Three-Dimensional Thermohydrodynamic Computer Program
* * for Solar Applications

developed by

Analytical Modeling Section
Components Technology Division
Argonne National Laboratory

under sponsorship of

Systems Development Division
Office of Solar Applications
Office of Assistant Secretary
Conservation and Solar Applications
United States Department of Energy

contact **phone**

J. R. Hull	312-972-8580
H. C. Schmitt	312-972-5914
W. T. Sha	312-972-5910

at

Building 308
Argonne National Laboratory
9700 South Cass Avenue
Argonne, Illinois 60439

Version 4.9

October 7, 1980

Subroutines appear either in alphabetical order or the following semi-logical order:

Subroutine	Remark		
MAIN	Controlling routine		
CUTOFF	Convergence criteria		
INPUT	ICNEW	Input and initialization	
RESIST	Computes baffle resistance		
GEOM	CONCAV	Set up geometry	
BCFIEL	BCFLOW	BCFLOK	Boundary conditions
UMOM	VMOM	WMOM	Momentum equation
MASSCO	DELP	Continuity equation	
NEWVEL	CENVEL	REGBAL	Velocity evaluation
ENERGY	Energy equation		
CPL	VISCI	THCL	Water properties
HLIQ	TLIQ	DBOLPH	
ROLIQ	POLY	SNDS	
S			
GETF	FITIT	ICSSCU	Transient function
LISTIN	OUTPUT	PIANE	Output
TABLES			
APIN	CLEAR	FINI	Miscellaneous utility routines
RSET	WRITRS		

Storage for the problem size dependent variables is allocated in four of the COMMON blocks. The minimum dimensions are defined by the following variables:

I	The number of cells (rings) in the radial direction including fictitious boundary cells.
J	The number of cells (sectors) in the circumferential direction including fictitious boundary cells.
K	The number of cells in the axial direction including two layers of fictitious boundary cells.
IJK	IJK.
MBC	The user can assign the total number of fictitious boundary cells for the problem. Upon completion of initialization the exact value required is printed.
NBU1	The number of fictitious boundary cells (or adjacent interior cells) in each boundary-condition group.
NBU2	Without a precise calculation, the user can assign conservatively the total number of fictitious boundary cells for the problem. Upon completion of initialization the exact values required will be printed.
...	...
NBF5	...

```

COMMON /IARRAY/  MS(I,J,K),  IFIELD( IJK), IFLOWU( IJK),
1 IFLOWV( IJK), IFLLOWW( IJK), IT      (100), NIT      (100),
2 NDT      (100), NTPLOT( 50), ISTPR( 50),
3 NTHPR ( 50), NEND ( 25), NLAST ( 25), IM      ( 15), IP      ( 15),
4 JM      ( 15), JP      ( 15), KM      ( 15), KP      ( 15), IB      (MBC),
5 LBU1 (NBU1), LBU2 (NBU2), LBU3 (NBU3), LBU4 (NBU4), LBV1 (NBV1),
6 LBV2 (NBV2), LBV3 (NBV3), LBV4 (NBV4), LBW1 (NBW1), LBW2 (NBW2),
7 LBW3 (NBW3), LBW4 (NBW4), LBF1 (NBF1), LBF2 (NBF2), LBF3 (NBF3),
8 JBU2 (NBU2), JBV2 (NBV2), JBW2 (NBW2), LBU5I(NBU5), LBU5J(NBU5),
9 LBU5K(NBU5), LBV5I(NBV5), LBV5J(NBV5), LBV5K(NBV5), LBW5I(NBW5),
A LBW5J(NBW5), LBW5K(NBW5), LBW6 (NBU6), LBV6 (NBV6), LBW6 (NBW6),
B LBF4 (NBF4), LBF5 (NBF5), TAEND
COMMON /FLOW /
1 UL      ( IJK), VI      ( IJK), WL      ( IJK),
2 ULRP   ( IJK), VLUP   ( IJK), WLFP   ( IJK),
3 AXTX   ( IJK), AXTY   ( IJK), AZTZ   ( IJK),
4 BXTX   ( IJK), BYTY   ( IJK), BZTZ   ( IJK), FLEND
COMMON /FIELD /
1 HL      ( IJK), HLTI   ( IJK), QDOT   ( IJK),
2 TL      ( IJK), ROI    ( IJK), ROLT   ( IJK), RKL    ( IJK),
3 DL      ( IJK), THI    ( IJK), RBETA  ( IJK), TWALL(NBF5),  FIEND
COMMON /RVEC/ THETA ( J), DY      ( J), DZ      ( K), DX      ( I),
1 X       ( I), DT      (100), CVVEL  ( 15), CHF     (  4), TPPNT  ( 50),
2 TVAL   ( 50), FVAL   ( 50), YCOEF   ( 50), CCUEF(50,3), DAA    (NBF5),
3 TCHF   (NBF1), DXYZ (NBF1), UOOX   (  K), UOOY   (  K), ROO    (  K),
4 RUOOX  (  K), RUOOY  (  K), WOO    (  K), DXYZ1(NBF5), RVEEND

```

* * * * *

The input data for CCMIX-SA consists of three parts:

RESTART FLAG

This parameter must be in column 4.

NAMELIST /STUFF/

This namelist contains input parameters.

SUPPLEMENTARY ARRAY INITIALIZATION CARDS

These cards allow for initialization of arrays. It contains two groups of cards, each terminated by a card containing 'END' in columns 1-3.

* * * * *

* * * * *

Default values are indicated either by an asterisk or a value in parentheses after the variable description.

* * * * * * * * * * *
* RESTART FLAG *
* * * * * * * * * * *

IFRES 0--New case with no restart written (*).
1--New case with restart written to tape 16.
2--Restart of previous run read from tape 15 with no restart written.
3--Restart of previous run read from tape 15 with The restart option uses two Argonne system routines called TLEFT and LOCF. TLEFT returns the amount of time left in the current run in units of 0.01 seconds. LOCF returns the absolute address of the variable passed as the argument. Minor modifications are probably necessary to implement this on other systems.

* * * * * * * * * * *
* NAMELIST /STUFF/ *
* * * * * * * * * * *

***** SPACE AND TIME GEOMETRY *****

ND 2--Two dimensional analysis. (R-Z PLANE).
3--Three dimensional analysis.
ICORD 1--CYLINDRICAL COORDINATE SYSTEM
2--RECTANGULAR COORDINATE SYSTEM
NOTE: IF RECTANGULAR COORDINATES ARE USED, SET XMIN.GE.DX(1) AND ISEC.EQ.1
IBAR The number of computational cells (rings) in the radial direction within the flow domain.
JBAR The number of computational cells (sectors) in the circumferential direction within the flow domain.
KBAR The number of computational cells in the axial direction within the flow domain.
IT(1) The number of iterations for time step 1 through time step NIT(1).

IT(I) The number of iterations for time step $NIT(I-1)+1$ through time step $NIT(I)$.
NIT(I) The last time step with $IT(I)$ iterations per step.
DT(1) The time step size for steps 1 through $NDT(1)$ in seconds.
DT(I) The time step size for steps $NDT(I-1)+1$ through time step $NDT(I)$ in seconds.
NDT(I) The last time step with a time step size of $DT(I)$.
IFNRG 0--Energy equation not solved.
 1--Energy equation solved at beginning of time step loop.
 2--Energy equation solved at end of time step loop.
 -N--Energy equation solved every N th iteration.

***** OUTPUT *****

Array output is done in Subroutine OUTPUT which is called once after initialization and according to the array TPRNT. $TPRNT(1) > 0.0$ --TPRNT can contain up to 50 values of time at which OUTPUT is called.
 =0.0--OUTPUT is called after initialization and before termination.
 <0.0--OUTPUT is called every $TPRNT(1)$ seconds.
 NOTE. To obtain output every time step, set $TPRNT(1)$ such that $ABS(TPRNT(1))$ is less than the time step size.

The arrays which are printed out at the calls to OUTPUT are coded into the values of ISTPR and NTHPR.

ISTPR Up to 50 coded values which specify the arrays to be printed in the first call to OUTPUT.
NTHPR Up to 50 coded values which specify the arrays to be printed after the first call to OUTPUT.

Each value of ISTPR and NTHPR is a signed five digit integer of the form 'VVPLL' which is coded according to the following rules:

S + Only the plane specified by 'VVPLL' is printed.
 NOTE. Plus is assumed and need not be specified.
 - All planes (LL) between 'VVPLL' and the next 'VVPLL' specified in ISTPR or NTHPR are printed.
VV 01--DL is printed. 02--UL is printed.
 03--VI is printed. 04--WL is printed.
 05--P is printed. 06--TL is printed.
 07--HL is printed. 08--ROL is printed.
 09--THL is printed. 10--IFIELD is printed.
 11--IFLOWU is printed. 12--IFLOWV is printed.
 13--IFLOWW is printed.
P 1--An I plane is printed.
 2--A J plane is printed.
 3--A K plane is printed.
LL Specific plane to be printed. If S is +, only one plane is indicated. If S is -, the 'LL' values in the current and next values of ISTPR or NTHPR indicate the range of planes to be printed.
IPLOT -1--No plot tape is written (*).
 0--Only the first and last time steps are written to the plot tape on tape 76.
 N--Every N th time step is written to the plot tape on tape 76.

***** TRANSIENT DRIVING FUNCTIONS *****

All transient driving functions are input into the following three variables. Each function is defined by a user specified set of points. Cubic spline fit coefficients are then generated in subroutine FITIT. Fifty equally spaced values are printed to allow the user to check the adequacy of the input distribution. Ten to fifteen values with points concentrated at rapidly changing Y values should be adequate.

TVAL The independent variable (X values) for the transient functions.
 FVAL The dependent variable (Y values) for the transient functions. The first value of the second function immediately follows the last value of the first function. The same pattern must be followed for all subsequent functions. The endpoints, or beyond, of the range of values used in the transient functions must be input as the fitting routine does not extrapolate. Discontinuities are indicated by specifying the same X coordinate twice with the same or different Y coordinate values.
 NEND(N) The number of points in the Nth transient function.

***** RUN TIME CRITERIA *****

The convective flux calculation is programmed in a form that combines both centered and donor-cell properties depending on the values of AO and BO. Both values must be between 0.0 and 0.5. When AO=0.5 and BO=0.0, the donor-cell approach is used. When AO=0.0 and BO=0.0, central differencing is used.

AO	A parameter used in convective flux differencing (0.5).
BO	A parameter used in convective flux differencing (0.0).
TUREC	Turbulent conductivity, W/m-K (0.0).
TURBV	Turbulent viscosity, kg/m-s (0.0).
EPS1	Convergence criteria parameter (0.0001).
EPS2	Convergence criteria parameter (0.000001).
GX	Gravitational constant in R direction, m/s**2 (0.0).
GY	Gravitational constant in THETA direction, m/s**2 (0.0).
GZ	Gravitational constant in Z direction, m/s**2 (-9.8).
THETAZ	Angle between gravity vector and axis of cylinder (OR Z-AXIS) IN DEGREES (0.0)
OMEGA	Under or over relaxation factor (1.5).
ITRSKM	0--SOR iteration scheme 1--local mass imbalance correction scheme 2--Jacobi iteration scheme (see subroutine MASSCO)
NT	Time step number (1).
T	Time in seconds (0.0).
MAXNT	The maximum number of time steps allowed in this run (100).
IFRMB	0--Do not perform a regional mass balance calculation. 1--Perform a regional mass balance calculation.

IRBLO *
 IRBHI *
 JRBLO * the I, J, and K index limits within which the regional
 JRBHI * mass balance calculation is performed
 KRBLO *
 KRBHI *
 CVVEL Constant value velocities, m/s. See Flow variable
 markers type -(100+n).
 ISEC This parameter is set according to the degree of
 symmetry present in the problem under study. ISEC is
 used inside the program to control calculation of center
 velocities. Four values are defined.
 0--A full circular cylinder is analyzed. The center
 velocities U00X and U00Y are computed (*).
 1--A sector (not half of a cylinder) is analyzed. The
 center velocities U00X and U00Y are zero.
 NOTE: WHEN RECTANGULAR COORDINATES ARE USED, SET
 ISEC.EQ.1
 2--Half of a circular cylinder is analyzed. The center
 velocities U00X and U00Y are zero.
 -2--Half of a circular cylinder is analyzed. The center
 velocities U00X are non zero and the center
 velocities U00Y are zero.
 XMIN The radius of the inner cylindrical boundary. This value
 is zero when analyzing an entire cylindrical flow domain
 with no central hole. It is a positive value when an
 annular flow domain is being analyzed.
 NOTE: WHEN RECTANGULAR COORDINATES ARE USED, SET
 XMIN.GE.DX(1)
 CHF(N) Constant heat flux in the flow domain through the N th
 surface, J/m**2-s. The following surface correspondence
 applies:
 1--Inner surface 2--Outer surface
 3--Top surface 4--Bottom surface
 To facilitate treatment of boundary conditions a layer of
 fictitious boundary cells surrounding the flow domain is
 employed. Input of the variables DX, DY, DZ, IFLD, IPIM,
 IFLV, and IFIW must be specified with consideration of these
 fictitious cells.
 DX(I) The sizes of computational cells in the R-direction, m.
 The size of a fictitious cell, if one is present, must
 be equal to that of the adjacent interior cell.
 DY(J) The sizes of computational cells in the THETA-direction,
 m.
 DZ(K) The sizes of computational cells in the Z-direction, m.
 BAPR Baffle resistance parameter (1.0E+25) kg/m**3.
 Note that this parameter is irrelevant in cases
 where no baffles are present.
 IBAF 0--No perforated baffles present in flow domain (*).
 1--Perforated baffles present in flow domain.
 RIDL 0.0--The effect of mass residue is not considered in the
 momentum and energy equations.
 1.0--The effect of mass residue is considered in the
 momentum and energy equations.
 ICONPR 1--Print out information after each iteration.
 0--Do not print information after each iteration (*).

The following four parameters are used with the tank wall heat capacity model.

TAMB Ambient temperature, deg C.
 HAMB Ambient heat transfer coefficient, (W/m**2-deg C.)
 WTHIC Thickness of tank wall, m.
 TDEP Tank depth, m.

 TIMEND Termination of this job begins at JOBTIME-TIMEND
 seconds where JOBTIME is the time specified for the
 job on the JOB card.

* * * * * * * * * * * * * * *
 * SUPPLEMENTARY ARRAY *
 * INITIALIZATION CARDS *
 * * * * * * * * * * * * * * *

This section of input allows the variables listed below to be initialized. It must contain two groups of cards each group followed by a card containing 'END' in columns one through four. The first group must contain the initialization of the field variable marker, IFLD. If no initialization is required (eg., restart cases) only the 'END' card is required. The second group must contain initialization for all variables except IFLD and must also be followed by an 'END' card.

KEY	Variable	KEY	Variable
IPLD	- Field variable marker.	IFLU	- U velocity marker.
IPLV	- V velocity marker.	IFLW	- W velocity marker.
UL	- U velocity (m/s).	VL	- V velocity (m/s).
WL	- W velocity (m/s).	P	- Pressure (N/m**2).
HL	- Enthalpy (J/kg).	TL	- Temperature (deg C).
ROL	- Density (kg/m**3).	THL	- Void fraction (%).

A suffix of T on these variables indicates updated values for TIME=N+1. No suffix indicates old variables at TIME=N

All input cards in this set are of the following format:

A4	KEY	Variable name key from table above.
F10.3	RVAL	Value to be stored.
6I4	I1,I2	I index limits.
	J1,J2	J index limits.
	K1,K2	K index limits.

The field variable marker, IFLD, conveys information about the cells. The following are acceptable cell types: (see subroutine BCFLOW for associated variables)

- 7--Fictitious boundary cell with wall heat capacity.
- 6--Fictitious boundary cell with adiabatic condition.
- 5--Fictitious boundary cell with constant heat flux.
- 4--Fictitious boundary cell with CONSTANT temperature.

- (300+N) -- Pictitious boundary cell with transient temperature whose values are obtained from the Nth transient function
 - whose values are obtained from the Nth transient function.
- 2--Totally outside the domain of interest.
- 1--Outside but adjacent to the flow domain boundary (pictitious boundary cell).
- 1--Inside and adjacent to the flow domain boundary (adjacent interior cell).
- 2--Totally inside the domain of interest.
- 5--Cell filled with a conducting baffle.

Flow variable markers (velocity markers IFLU, IFLV, and IFLW) provide the means for defining boundary condition types. The following are acceptable boundary condition types:

- (200+N) -- Transient velocity with values obtained from the Nth transient function.
- (100+N) -- Constant value velocity with value obtained from CVVEL(N).
- 4--Free slip wall.
- 3--Velocity derivative equal to 0.0.
- 1--No flow boundary. No velocity calculation is performed. This can be used to indicate solid walls or surfaces outside the domain of interest.
- 0--No slip wall.
- 1--Free flow surface.
- 2--Velocity is computed by doing a local mass balance.
- 3--Nonconducting solid baffle.
- 4--Velocity is computed by doing a global mass balance.
- 5--Conducting solid baffle.
- 6--Conducting perforated baffle.

IFLU is used to define the boundary condition type of surfaces between cell (I,J,K) and cell (I+1,J,K).
 IFLV is used to define the boundary condition type of surfaces between cell (I,J,K) and cell (I,J+1,K).
 IFLW is used to define the boundary condition type of surfaces between cell (I,J,K) and cell (I,J,K+1).
 To specify free slip or no slip boundary condition the type must be entered into the (I+1,J,K) or (I,J+1,K), or (I,J,K+1) location of IFLU, IFLV, or IFLW. For all other boundary conditions, the type must be entered into the (I,J,K) location.

* * * * *

VII. SAMPLE PROBLEMS

Two sample problems are presented to illustrate how to use COMMIX-SA-1, what sort of problems it can analyze, and what kind of results one can expect from it. Both problems concern heat discharge from a cylindrical storage tank; however, different geometries and flow conditions cause quite different flow and thermal behavior.

A. Heat Discharge from a Simple Cylindrical Storage Tank⁶

A cylindrical heat-storage water tank, 1 m in diameter and 2 m high, was considered. The tank was isothermal at 57.2°C. Throughout the demand cycle, hot water was drawn out from the top of the tank and cold water at 15.6°C was pumped in near the bottom of the tank. Figure 11 shows the elevation and top view of the tank along with the finite-difference grid layout. Five radial, 12 circumferential, and 10 axial divisions were used for this tank; hence, $\Delta r = 0.1$ m, $\Delta\theta = 30^\circ$, and $\Delta z = 0.2$ m.

The fictitious boundary cells (shown shaded in Fig. 11) were used to facilitate treatment of boundary conditions. The inlet velocity of the cold makeup water was taken to be 1 m/s.

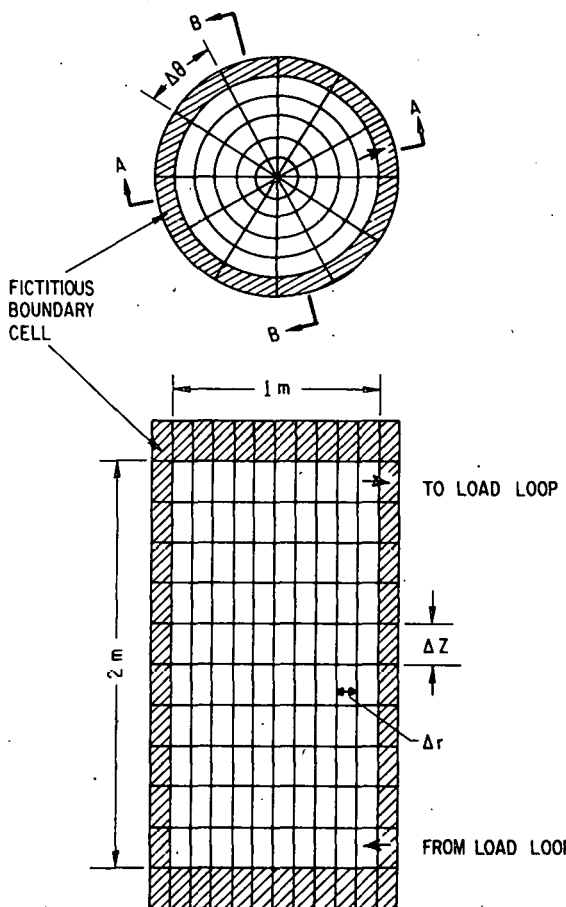


Fig. 11. Storage-tank Geometry and Finite-difference Grid Layout

B-B (see Fig. 11), respectively, at time $t = 10.7$ s. Section A-A is the vertical plane that contains the tank axis and the inlet and outlet ports; Section B-B is perpendicular to Section A-A. Entering horizontally from the inlet port, the stream of cold water progressed through the center of the tank and

Figure 12 shows the calculated temperature profile at four different times during the transient. This figure indicates that the cold lower portion of the tank is separated from the hot upper portion by a thermocline (i.e., a region of steep temperature gradient), and that the thermocline moves upwards with slowly increasing thickness as time progresses. The thermocline thickness varies from 0.3 to 0.4 m, approximately, in the early stage of the demand event as shown in Fig. 12.

The three-dimensional nature of the temperature field in the storage tank is illustrated by Figs. 13 and 14, which show the temperature distributions at selected heights across Sections A-A and

impinged on the opposite wall. Thereupon both an upward motion and a circumferential diversion were generated. (See Fig. 15 for the flow pattern in Section A-A.) This resulted in a temperature depression in the vicinity of the walls (Figs. 13 and 14), as well as along the path that the cold stream traversed (Fig. 14). The top part of the tank was virtually unaffected (at $t = 10.7$ s), but in the lower part a temperature differential of as great as 30°C on the same horizontal plane existed, and this occurred within an extended depth of the storage tank (Figs. 13 and 14).

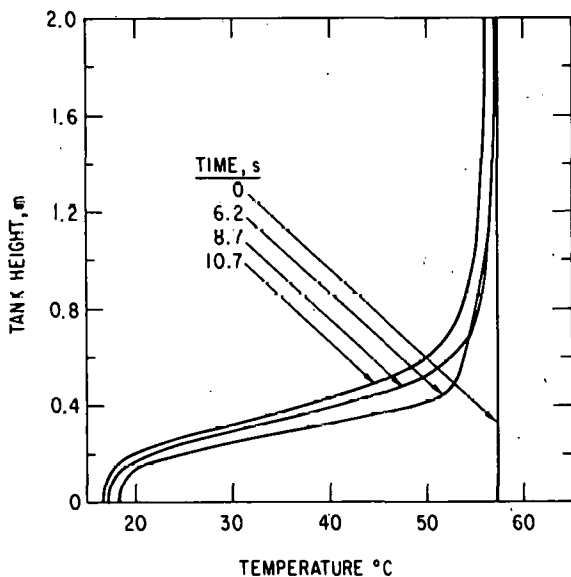
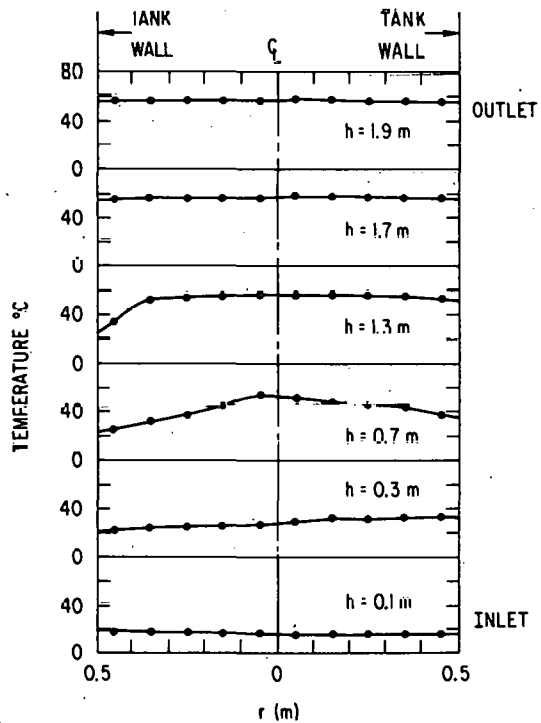


Fig. 12

Temperature Profile at Tank Centerline.
 $6 \times 12 \times 12$ grid, $\Delta r = 0.1$ m, $\Delta \theta = 30^\circ$,
 $\Delta z = 0.2$ m, $V_{in} = 1.0$ m/s, $T_{in} = 15.6^\circ\text{C}$,
 $T_0 = 57.2^\circ\text{C}$.

Fig. 13

Temperature Distribution across
Section A-A at $t = 10.7$ s



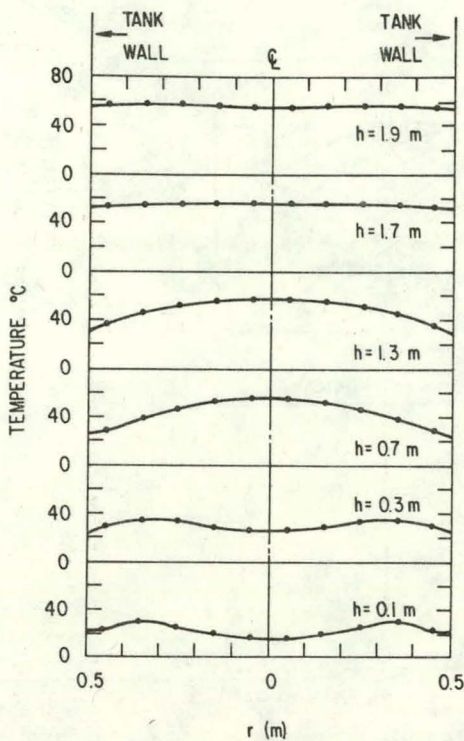


Fig. 14. Temperature Distribution across Section B-B at $t = 10.7$ s

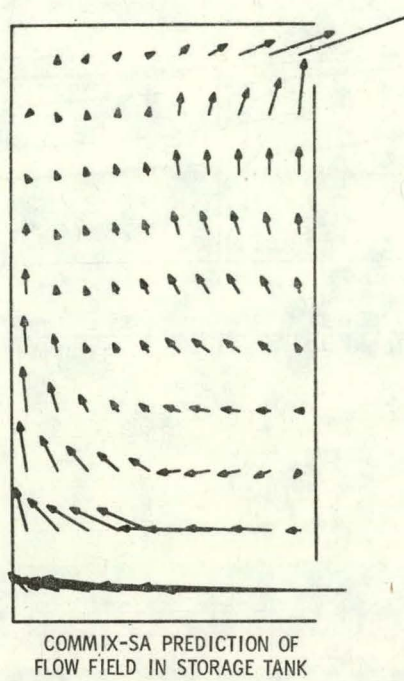


Fig. 15. Flow Pattern across Section A-A at $t = 10.7$ s;
 $V_{in} = 1$ m/s

This example shows that the three-dimensional effect can be important in a cylindrical storage tank. It also shows that large inertia force (high inlet velocity) contributes to extended mixing (which reduces stratification).

A list of the input file and a portion of the computer output follows.

B. Heat Discharge from a VCCB Tank⁷

In this example, vertical concentric cylindrical baffles (VCCB's) are installed in a cylindrical heat-storage water tank, which has a height-to-diameter ratio of 4.0 (see Fig. 16). During heat discharge, hot water flows out at the top of the tank as shown, and cold water is pumped in through an inlet flow distributor at the bottom of the tank. Because of the symmetry in the geometry and flow field, a 15° sector is used in this simulation, the corresponding finite-difference grid layout being shown in Fig. 17, with Δr (from center out) = $9*0.0267$ (m), $\Delta\theta = 3*15^\circ$, Δz (from bottom up) = $2*0.06$, 0.1, 0.136, $7*0.16$, 0.136, 0.1, $2*0.06$ (m). The VCCB's are located between the third and fourth cells, and again between the fourth and fifth cells. They are assumed to be made of nonconducting materials and serve to restrict the mixing region and guide the fluid flow in a way that enhances stratification. The tank has a volume of 64.84 gal (0.245 m 3), and the flow rate is 2.085 gpm (1.315×10^{-4} m 3 /s). The evolution of the temperature profile in the tank during heat discharge is shown in Fig. 18. A list of input file and a portion of the computer output for the analysis of this case also follow.

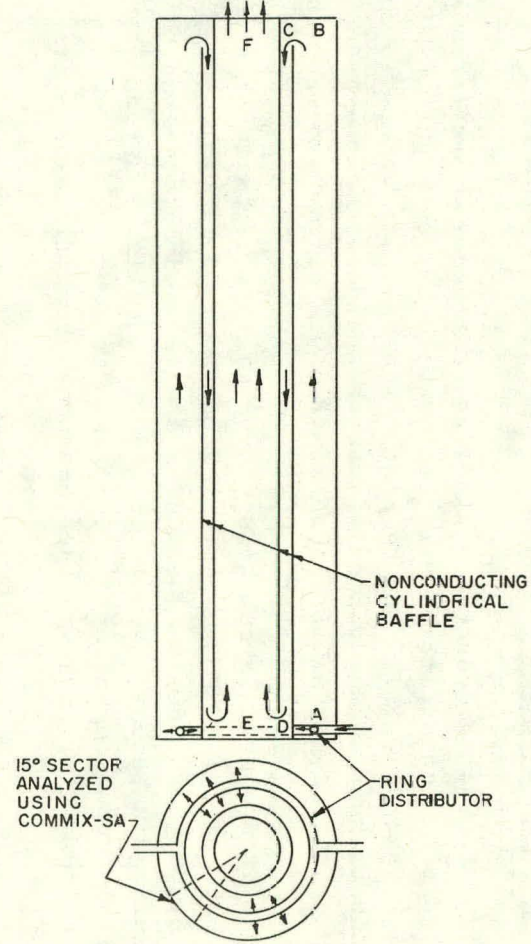


Fig. 16

Storage Tank with Vertical Concentric Cylindrical Baffles (VCCB's) and Ring Distributor

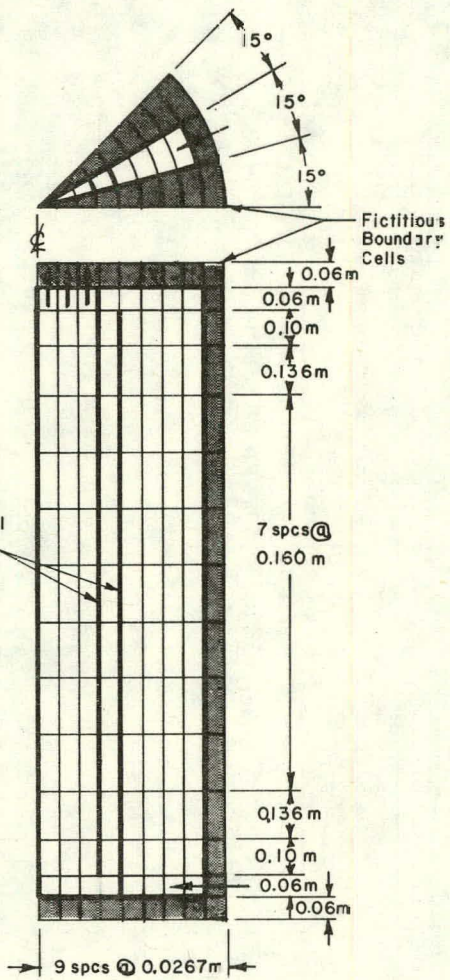


Fig. 17

Finite-difference Grid Layout for 15° Sector of VCCB Tank

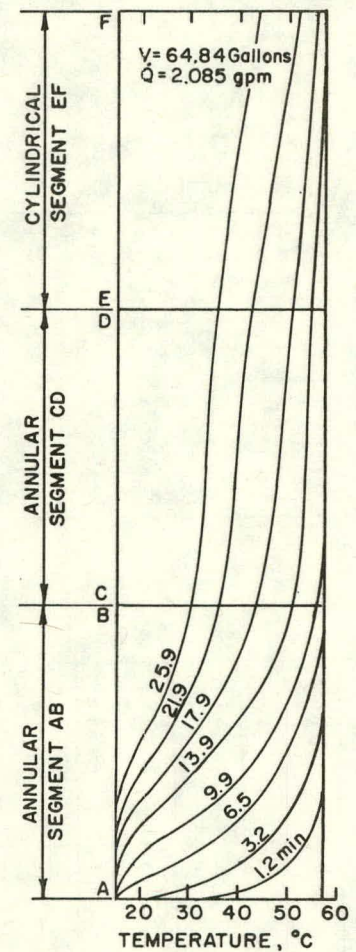


Fig. 18

Evolution of Temperature Profile during Heat Discharge from a Storage Tank (Fig. 16); $Q = 2.085 \text{ gpm}$ ($1.315 \times 10^{-4} \text{ m}^3/\text{s}$)

1
 &STUFF
 ND=3,IEAR=5,JBAR=12,KBAR=10,XMIN=0.0,RIDL=0.0,
 ONEGA=1.7,GX=0.0,GY=0.0,GZ=-9.8,
 ISTPR=1305,2305,3305,4305,5201,6201,6302,7201,7302,8201,8302,
 9105,10302,10306,11104,11306,12104,12306,13104,13306,
 NTHPR=1201,1310,2201,2310,3201,3310,4201,4310,
 5201,5310,6201,6310,8201,8310
 DX=6*0.1,DY=12*30.,DZ=12*.2,
 EPS1=1.0E-5,EPS2=1.0E-7,B0=0.0,A0=0.5,
 TURBV=0.0,TURBC=0.0,
 IFNRG=-10,IFPLOT=-1,
 MAXNT=5,T=0.0,TPRNT=-0.005,
 NDT=20,500,10000,DT=.001,.01,.015,
 NIT=20,50,10000,IT=150,100,30,THETAZ=0.0,
 CHF=0.0,0.0,0.0,0.0,
 CVVEL(1)=-1.0,CVVEL(2)=1.0,NT=1,ISEC=0,
 ICONPR=3,TIMEND=15.0,BAFR=1.0E+25,IFRMB=0,
 &END
 IFLD -1.0 1 6 1 12 1 12
 IFLD 1.0 1 5 1 12 2 11
 IFLD 2.0 1 4 1 12 3 10
 IFLD -6.0 6 6 1 12 1 12
 IFLD -6.0 1 5 1 12 1 1
 IFLD -6.0 1 5 1 12 12 12
 IFLD -4.0 6 6 1 1 2 2
 END
 IFLU -1.0 1 6 1 12 1 12
 IFLU 1.0 1 4 1 12 2 11
 IFLU 0.0 1 4 1 12 1 1
 IFLU 0.0 1 4 1 12 12 12
 IFLU -101.0 5 5 1 1 2 2
 IFLU -102.0 5 5 1 1 11 11
 IFLV -1.0 1 6 1 12 1 12
 IFLV 1.0 1 5 1 12 2 11
 IFLV 0.0 1 5 1 12 1 1
 IFLV 0.0 1 5 1 12 12 12
 IFLV 0.0 6 6 1 12 2 11
 IFLH -1.0 1 6 1 12 1 12
 IFLH 1.0 1 5 1 12 2 10
 IFLH 0.0 6 6 1 12 1 12
 THL 1.0 1 6 1 12 1 12
 P 101325.0 1 6 1 12 1 12
 TL 57.2 1 6 1 12 1 12
 TL .15.6 6 6 1 1 2 2
 END
 MS(I,J,K)

656	657	658	659	660	0
651	652	653	654	655	0
646	647	648	649	650	0
641	642	643	644	645	0
635	637	638	639	640	0
631	632	633	634	635	0
625	627	628	629	630	0
621	622	623	624	625	0

616	617	618	619	620	0
611	612	613	614	615	0
606	607	608	609	610	0
601	602	603	604	605	0

56	57	58	59	60	672
51	52	53	54	55	671
46	47	48	49	50	670
41	42	43	44	45	669
36	37	38	39	40	668
31	32	33	34	35	667
26	27	28	29	30	666
21	22	23	24	25	665
16	17	18	19	20	664
11	12	13	14	15	663
6	7	8	9	10	662
1	2	3	4	5	661

116	117	118	119	120	684
111	112	113	114	115	683
106	107	108	109	110	682
101	102	103	104	105	681
96	97	98	99	100	680
91	92	93	94	95	679
86	87	88	89	90	678
81	82	83	84	85	677
76	77	78	79	80	676
71	72	73	74	75	675
66	67	68	69	70	674
61	62	63	64	65	673

176	177	178	179	180	696
171	172	173	174	175	695
166	167	168	169	170	694
161	162	163	164	165	693
156	157	158	159	160	692
151	152	153	154	155	691
146	147	148	149	150	690
141	142	143	144	145	689
136	137	138	139	140	688
131	132	133	134	135	687
126	127	128	129	130	686
121	122	123	124	125	685

236	237	238	239	240	708
231	232	233	234	235	707
226	227	228	229	230	706
221	222	223	224	225	705

216	217	218	219	220	704
211	212	213	214	215	703
206	207	208	209	210	702
201	202	203	204	205	701
196	197	198	199	200	700
191	192	193	194	195	699
186	187	188	189	190	698
181	182	183	184	185	697

296	297	298	299	300	720
291	292	293	294	295	719
286	287	288	289	290	718
281	282	283	284	285	717
276	277	278	279	280	716
271	272	273	274	275	715
266	267	268	269	270	714
261	262	263	264	265	713
256	257	258	259	260	712
251	252	253	254	255	711
246	247	248	249	250	710
241	242	243	244	245	709

356	357	358	359	360	732
351	352	353	354	355	731
346	347	348	349	350	730
341	342	343	344	345	729
336	337	338	339	340	728
331	332	333	334	335	727
326	327	328	329	330	726
321	322	323	324	325	725
316	317	318	319	320	724
311	312	313	314	315	723
306	307	308	309	310	722
301	302	303	304	305	721

416	417	418	419	420	744
411	412	413	414	415	743
406	407	408	409	410	742
401	402	403	404	405	741
396	397	398	399	400	740
391	392	393	394	395	739
386	387	388	389	390	738
381	382	383	384	385	737
376	377	378	379	380	736
371	372	373	374	375	735
366	367	368	369	370	734
361	362	363	364	365	733

476	477	478	479	480	756
471	472	473	474	475	755
466	467	468	469	470	754
461	462	463	464	465	753
456	457	458	459	460	752
451	452	453	454	455	751
446	447	448	449	450	750
441	442	443	444	445	749
436	437	438	439	440	748
431	432	433	434	435	747
426	427	428	429	430	746
421	422	423	424	425	745

536	537	538	539	540	768
531	532	533	534	535	767
526	527	528	529	530	766
521	522	523	524	525	765
516	517	518	519	520	764
511	512	513	514	515	763
506	507	508	509	510	762
501	502	503	504	505	761
496	497	498	499	500	760
491	492	493	494	495	759
486	487	488	489	490	758
481	482	483	484	485	757

596	597	598	599	600	780
591	592	593	594	595	779
586	587	588	589	590	778
581	582	583	584	585	777
576	577	578	579	580	776
571	572	573	574	575	775
566	567	568	569	570	774
561	562	563	564	565	773
556	557	558	559	560	772
551	552	553	554	555	771
546	547	548	549	550	770
541	542	543	544	545	769

836	837	838	839	840	0
831	832	833	834	835	0
826	827	828	829	830	0
821	822	823	824	825	0
816	817	818	819	820	0
811	812	813	814	815	0
806	807	808	809	810	0
801	802	803	804	805	0
796	797	798	799	800	0
791	792	793	794	795	0
786	787	788	789	790	0
781	782	783	784	785	0

COMMON BLOCK DIMENSIONS

NBU1 - 0	NBU2 - 0	NBU3 - 0	NBU4 - 96	NBU5 - 0	NBU6 - 0
NBV1 - 0	NBV2 - 0	NBV3 - 0	NBV4 - 240	NBV5 - 0	NBV6 - 0
NBW1 - 0	NBW2 - 0	NBW3 - 0	NBW4 - 120	NBW5 - 0	NBW6 - 0
NBF1 - 0	NBF2 - 1	NBF3 - 0	NBF4 - 239	NBF5 - 0	NBC - 240

* INITIALIZATION COMPLETED *

***** BEGINNING OF OUTPUT FOR STEP 0 AT 0.0 SECONDS *****

RESIDUAL MASS (kg/m**3-s) DL

K= 5		DL					
I-->	1	2	3	4	5	6	
12	0.0	0.0	0.0	0.0	0.0	0.0	
11	0.0	0.0	0.0	0.0	0.0	0.0	
10	0.0	0.0	0.0	0.0	0.0	0.0	
9	0.0	0.0	0.0	0.0	0.0	0.0	
8	0.0	0.0	0.0	0.0	0.0	0.0	
7	0.0	0.0	0.0	0.0	0.0	0.0	
6	0.0	0.0	0.0	0.0	0.0	0.0	
5	0.0	0.0	0.0	0.0	0.0	0.0	
4	0.0	0.0	0.0	0.0	0.0	0.0	
3	0.0	0.0	0.0	0.0	0.0	0.0	
2	0.0	0.0	0.0	0.0	0.0	0.0	
1	0.0	0.0	0.0	0.0	0.0	0.0	

U COMPONENT OF VELOCITY (m/s) UL

K= 5		UL					
I-->	1	2	3	4	5	6	
12	0.0	0.0	0.0	0.0	0.0	0.0	
11	0.0	0.0	0.0	0.0	0.0	0.0	
10	0.0	0.0	0.0	0.0	0.0	0.0	
9	0.0	0.0	0.0	0.0	0.0	0.0	
8	0.0	0.0	0.0	0.0	0.0	0.0	
7	0.0	0.0	0.0	0.0	0.0	0.0	
6	0.0	0.0	0.0	0.0	0.0	0.0	
5	0.0	0.0	0.0	0.0	0.0	0.0	
4	0.0	0.0	0.0	0.0	0.0	0.0	
3	0.0	0.0	0.0	0.0	0.0	0.0	
2	0.0	0.0	0.0	0.0	0.0	0.0	
1	0.0	0.0	0.0	0.0	0.0	0.0	
U00X=	0.0	0.0	0.0	0.0	0.0	0.0	0.0
U00Y=	0.0	0.0	0.0	0.0	0.0	0.0	0.0

V COMPONENT OF VELOCITY (m/s) VL

K= 5		VL					
I-->	1	2	3	4	5	6	
12	0.0	0.0	0.0	0.0	0.0	0.0	
11	0.0	0.0	0.0	0.0	0.0	0.0	
10	0.0	0.0	0.0	0.0	0.0	0.0	
9	0.0	0.0	0.0	0.0	0.0	0.0	

8	0.0	0.0	0.0	0.0	0.0	0.0
7	0.0	0.0	0.0	0.0	0.0	0.0
6	0.0	0.0	0.0	0.0	0.0	0.0
5	0.0	0.0	0.0	0.0	0.0	0.0
4	0.0	0.0	0.0	0.0	0.0	0.0
3	0.0	0.0	0.0	0.0	0.0	0.0
2	0.0	0.0	0.0	0.0	0.0	0.0
1	0.0	0.0	0.0	0.0	0.0	0.0

W COMPONENT OF VELOCITY (m/s) WL

PRESSURE (PASCAL)

TEMPERATURE (deg C) TL

9	57.2000	57.2000	57.2000	57.2000	57.2000	57.2000
8	57.2000	57.2000	57.2000	57.2000	57.2000	57.2000
7	57.2000	57.2000	57.2000	57.2000	57.2000	57.2000
6	57.2000	57.2000	57.2000	57.2000	57.2000	57.2000
5	57.2000	57.2000	57.2000	57.2000	57.2000	57.2000
4	57.2000	57.2000	57.2000	57.2000	57.2000	57.2000
3	57.2000	57.2000	57.2000	57.2000	57.2000	57.2000
2	57.2000	57.2000	57.2000	57.2000	57.2000	15.6000
1	57.2000	57.2000	57.2000	57.2000	57.2000	57.2000

TANK WALL TEMPERATURE

0.0

TOTAL HEAT LOSS FROM TANK = 0.0 JOULE

TEMPERATURE (deg C) TL

K= 2	1	2	3	4	5	6
J						
12	57.2000	57.2000	57.2000	57.2000	57.2000	57.2000
11	57.2000	57.2000	57.2000	57.2000	57.2000	57.2000
10	57.2000	57.2000	57.2000	57.2000	57.2000	57.2000
9	57.2000	57.2000	57.2000	57.2000	57.2000	57.2000
8	57.2000	57.2000	57.2000	57.2000	57.2000	57.2000
7	57.2000	57.2000	57.2000	57.2000	57.2000	57.2000
6	57.2000	57.2000	57.2000	57.2000	57.2000	57.2000
5	57.2000	57.2000	57.2000	57.2000	57.2000	57.2000
4	57.2000	57.2000	57.2000	57.2000	57.2000	57.2000
3	57.2000	57.2000	57.2000	57.2000	57.2000	57.2000
2	57.2000	57.2000	57.2000	57.2000	57.2000	57.2000
1	57.2000	57.2000	57.2000	57.2000	57.2000	15.6000

TANK WALL TEMPERATURE

0.0

TOTAL HEAT LOSS FROM TANK = 0.0 JOULE

ENTHALPY (J/kg) HL

J= 1	1	2	3	4	5	6
K						
12	2.3390+05	2.3390+05	2.3390+05	2.3390+05	2.3390+05	0.0
11	2.3390+05	2.3390+05	2.3390+05	2.3390+05	2.3390+05	2.3390+05
10	2.3390+05	2.3390+05	2.3390+05	2.3390+05	2.3390+05	2.3390+05
9	2.3390+05	2.3390+05	2.3390+05	2.3390+05	2.3390+05	2.3390+05
8	2.3390+05	2.3390+05	2.3390+05	2.3390+05	2.3390+05	2.3390+05
7	2.3390+05	2.3390+05	2.3390+05	2.3390+05	2.3390+05	2.3390+05
6	2.3390+05	2.3390+05	2.3390+05	2.3390+05	2.3390+05	2.3390+05
5	2.3390+05	2.3390+05	2.3390+05	2.3390+05	2.3390+05	2.3390+05
4	2.3390+05	2.3390+05	2.3390+05	2.3390+05	2.3390+05	2.3390+05
3	2.3390+05	2.3390+05	2.3390+05	2.3390+05	2.3390+05	2.3390+05
2	2.3390+05	2.3390+05	2.3390+05	2.3390+05	2.3390+05	6.5250+04
1	2.3390+05	2.3390+05	2.3390+05	2.3390+05	2.3390+05	0.0

ENTHALPY (J/kg) HL

K= 2
 I--> 1 2 3 4 5 6
 J
 12 2.3890+05 2.3890+05 2.3890+05 2.3890+05 2.3890+05 2.3890+05
 11 2.3890+05 2.3890+05 2.3890+05 2.3890+05 2.3890+05 2.3890+05
 10 2.3890+05 2.3890+05 2.3890+05 2.3890+05 2.3890+05 2.3890+05
 9 2.3890+05 2.3890+05 2.3890+05 2.3890+05 2.3890+05 2.3890+05
 8 2.3890+05 2.3890+05 2.3890+05 2.3890+05 2.3890+05 2.3890+05
 7 2.3890+05 2.3890+05 2.3890+05 2.3890+05 2.3890+05 2.3890+05
 6 2.3890+05 2.3890+05 2.3890+05 2.3890+05 2.3890+05 2.3890+05
 5 2.3890+05 2.3890+05 2.3890+05 2.3890+05 2.3890+05 2.3890+05
 4 2.3890+05 2.3890+05 2.3890+05 2.3890+05 2.3890+05 2.3890+05
 3 2.3890+05 2.3890+05 2.3890+05 2.3890+05 2.3890+05 2.3890+05
 2 2.3890+05 2.3890+05 2.3890+05 2.3890+05 2.3890+05 2.3890+05
 1 2.3890+05 2.3890+05 2.3890+05 2.3890+05 2.3890+05 6.5250+04

DENSITY (kg/m**3) ROL
 J= 1
 I--> 1 2 3 4 5 6
 K
 12 985.2593 985.2593 985.2593 985.2593 985.2593 0.0
 11 985.2593 985.2593 985.2593 985.2593 985.2593 985.2593
 10 985.2601 985.2601 985.2601 985.2601 985.2601 985.2601
 9 985.2609 985.2609 985.2609 985.2609 985.2609 985.2609
 8 985.2618 985.2618 985.2618 985.2618 985.2618 985.2618
 7 985.2626 985.2626 985.2626 985.2626 985.2626 985.2626
 6 985.2634 985.2634 985.2634 985.2634 985.2634 985.2634
 5 985.2642 985.2642 985.2642 985.2642 985.2642 985.2642
 4 985.2651 985.2651 985.2651 985.2651 985.2651 985.2651
 3 985.2659 985.2659 985.2659 985.2659 985.2659 985.2659
 2 985.2667 985.2667 985.2667 985.2667 985.2667 998.5035
 1 985.2667 985.2667 985.2667 985.2667 985.2667 0.0
 R00= 0.0 0.0 0.0 0.0 0.0 0.0 0.0 0.0 0.0 0.0 0.0 0.0

DENSITY (kg/m**3) ROL
 K= 2
 I--> 1 2 3 4 5 6
 J
 12 985.2667 985.2667 985.2667 985.2667 985.2667 985.2667
 11 985.2667 985.2667 985.2667 985.2667 985.2667 985.2667
 10 985.2667 985.2667 985.2667 985.2667 985.2667 985.2667
 9 985.2667 985.2667 985.2667 985.2667 985.2667 985.2667
 8 985.2667 985.2667 985.2667 985.2667 985.2667 985.2667
 7 985.2667 985.2667 985.2667 985.2667 985.2667 985.2667
 6 985.2667 985.2667 985.2667 985.2667 985.2667 985.2667
 5 985.2667 985.2667 985.2667 985.2667 985.2667 985.2667
 4 985.2667 985.2667 985.2667 985.2667 985.2667 985.2667
 3 985.2667 985.2667 985.2667 985.2667 985.2667 985.2667
 2 985.2667 985.2667 985.2667 985.2667 985.2667 985.2667
 1 985.2667 985.2667 985.2667 985.2667 985.2667 998.5035
 R00= 0.0 0.0 0.0 0.0 0.0 0.0 0.0 0.0 0.0 0.0 0.0

CELL VOID FRACTION THL

I= 5		1	2	3	4	5	6	7	8	9	10	11	12
J	K-->	1.0000	1.0000	1.0000	1.0000	1.0000	1.0000	1.0000	1.0000	1.0000	1.0000	1.0000	1.0000
12		1.0000	1.0000	1.0000	1.0000	1.0000	1.0000	1.0000	1.0000	1.0000	1.0000	1.0000	1.0000
11		1.0000	1.0000	1.0000	1.0000	1.0000	1.0000	1.0000	1.0000	1.0000	1.0000	1.0000	1.0000
10		1.0000	1.0000	1.0000	1.0000	1.0000	1.0000	1.0000	1.0000	1.0000	1.0000	1.0000	1.0000
9		1.0000	1.0000	1.0000	1.0000	1.0000	1.0000	1.0000	1.0000	1.0000	1.0000	1.0000	1.0000
8		1.0000	1.0000	1.0000	1.0000	1.0000	1.0000	1.0000	1.0000	1.0000	1.0000	1.0000	1.0000
7		1.0000	1.0000	1.0000	1.0000	1.0000	1.0000	1.0000	1.0000	1.0000	1.0000	1.0000	1.0000
6		1.0000	1.0000	1.0000	1.0000	1.0000	1.0000	1.0000	1.0000	1.0000	1.0000	1.0000	1.0000
5		1.0000	1.0000	1.0000	1.0000	1.0000	1.0000	1.0000	1.0000	1.0000	1.0000	1.0000	1.0000
4		1.0000	1.0000	1.0000	1.0000	1.0000	1.0000	1.0000	1.0000	1.0000	1.0000	1.0000	1.0000
3		1.0000	1.0000	1.0000	1.0000	1.0000	1.0000	1.0000	1.0000	1.0000	1.0000	1.0000	1.0000
2		1.0000	1.0000	1.0000	1.0000	1.0000	1.0000	1.0000	1.0000	1.0000	1.0000	1.0000	1.0000
1		1.0000	1.0000	1.0000	1.0000	1.0000	1.0000	1.0000	1.0000	1.0000	1.0000	1.0000	1.0000

FIELD VARIABLE MARKER IFIELD

K= 2

I	1	2	3	4	5	6
12	1	1	1	1	1	-6
11	1	1	1	1	1	-6
10	1	1	1	1	1	-6
9	1	1	1	1	1	-6
8	1	1	1	1	1	-6
7	1	1	1	1	1	-6
6	1	1	1	1	1	-6
5	1	1	1	1	1	-6
4	1	1	1	1	1	-6
3	1	1	1	1	1	-6
2	1	1	1	1	1	-6
1	1	1	1	1	1	-4

FIELD VARIABLE MARKER IFIELD

K= 6

I	1	2	3	4	5	6
12	2	2	2	2	1	-6
11	2	2	2	2	1	-6
10	2	2	2	2	1	-6
9	2	2	2	2	1	-6
8	2	2	2	2	1	-6
7	2	2	2	2	1	-6
6	2	2	2	2	1	-6
5	2	2	2	2	1	-6
4	2	2	2	2	1	-6
3	2	2	2	2	1	-6
2	2	2	2	2	1	-6
1	2	2	2	2	1	-6

U VELOCITY FLOW VARIABLE MARKER IFLOWU

I= 4

K	1	2	3	4	5	6	7	8	9	10	11	12
J												
12	0	1	1	1	1	1	1	1	1	1	1	0
11	0	1	1	1	1	1	1	1	1	1	1	0
10	0	1	1	1	1	1	1	1	1	1	1	0
9	0	1	1	1	1	1	1	1	1	1	1	0
8	0	1	1	1	1	1	1	1	1	1	1	0
7	0	1	1	1	1	1	1	1	1	1	1	0
6	0	1	1	1	1	1	1	1	1	1	1	0
5	0	1	1	1	1	1	1	1	1	1	1	0
4	0	1	1	1	1	1	1	1	1	1	1	0
3	0	1	1	1	1	1	1	1	1	1	1	0
2	0	1	1	1	1	1	1	1	1	1	1	0
1	0	1	1	1	1	1	1	1	1	1	1	0

U VELOCITY FLOW VARIABLE MARKER IFLOWU

K= 6

I	1	2	3	4	5	6
J						
12	1	1	1	1	-1	-1
11	1	1	1	1	-1	-1
10	1	1	1	1	-1	-1
9	1	1	1	1	-1	-1
8	1	1	1	1	-1	-1
7	1	1	1	1	-1	-1
6	1	1	1	1	-1	-1
5	1	1	1	1	-1	-1
4	1	1	1	1	-1	-1
3	1	1	1	1	-1	-1
2	1	1	1	1	-1	-1
1	1	1	1	1	-1	-1

V VELOCITY FLOW VARIABLE MARKER IFLOWV

I= 4

K	1	2	3	4	5	6	7	8	9	10	11	12
J												
12	0	1	1	1	1	1	1	1	1	1	1	0
11	0	1	1	1	1	1	1	1	1	1	1	0
10	0	1	1	1	1	1	1	1	1	1	1	0
9	0	1	1	1	1	1	1	1	1	1	1	0
8	0	1	1	1	1	1	1	1	1	1	1	0
7	0	1	1	1	1	1	1	1	1	1	1	0
6	0	1	1	1	1	1	1	1	1	1	1	0
5	0	1	1	1	1	1	1	1	1	1	1	0
4	0	1	1	1	1	1	1	1	1	1	1	0
3	0	1	1	1	1	1	1	1	1	1	1	0

2	0	1	1	1	1	1	1	1	1	1	1	1	0
1	0	1	1	1	1	1	1	1	1	1	1	1	0

V VELOCITY FLOW VARIABLE MARKER IFLOWV

K= 6

I	1	2	3	4	5	6
J						
12	1	1	1	1	1	0
11	1	1	1	1	1	0
10	1	1	1	1	1	0
9	1	1	1	1	1	0
8	1	1	1	1	1	0
7	1	1	1	1	1	0
6	1	1	1	1	1	0
5	1	1	1	1	1	0
4	1	1	1	1	1	0
3	1	1	1	1	1	0
2	1	1	1	1	1	0
1	1	1	1	1	1	0

W VELOCITY FLOW VARIABLE MARKER IFLOWW

I= 4

K	1	2	3	4	5	6	7	8	9	10	11	12
J												
12	-1	1	1	1	1	1	1	1	1	1	-1	-1
11	-1	1	1	1	1	1	1	1	1	1	-1	-1
10	-1	1	1	1	1	1	1	1	1	1	-1	-1
9	-1	1	1	1	1	1	1	1	1	1	-1	-1
8	-1	1	1	1	1	1	1	1	1	1	-1	-1
7	-1	1	1	1	1	1	1	1	1	1	-1	-1
6	-1	1	1	1	1	1	1	1	1	1	-1	-1
5	-1	1	1	1	1	1	1	1	1	1	-1	-1
4	-1	1	1	1	1	1	1	1	1	1	-1	-1
3	-1	1	1	1	1	1	1	1	1	1	-1	-1
2	-1	1	1	1	1	1	1	1	1	1	-1	-1
1	-1	1	1	1	1	1	1	1	1	1	-1	-1

W VELOCITY FLOW VARIABLE MARKER IFLOWW

K= 6

I	1	2	3	4	5	6
J						
12	1	1	1	1	1	0
11	1	1	1	1	1	0
10	1	1	1	1	1	0
9	1	1	1	1	1	0
8	1	1	1	1	1	0
7	1	1	1	1	1	0
6	1	1	1	1	1	0

5	1	1	1	1	1	0
4	1	1	1	1	1	0
3	1	1	1	1	1	0
2	1	1	1	1	1	0
1	1	1	1	1	1	0

***** END OF OUTPUT FOR STEP 0 AT 0.0 SECONDS *****

STEP: 1, T: 0.001, DT: 0.001, ITERATIONS: 150, DLMAX: 5.200+00 AT (1, 1, 2). DCONV: 4.93D-02 1.35D+03 330.17
 STEP: 2, T: 0.002, DT: 0.001, ITERATIONS: 150, DLMAX: 5.32D+00 AT (1, 1, 2). DCONV: 1.07D-01 1.38D+03 305.14
 STEP: 3, T: 0.003, DT: 0.001, ITERATIONS: 150, DLMAX: 1.30D+00 AT (1, 1, 2). DCONV: 1.08D-01 3.38D+02 280.32
 STEP: 4, T: 0.004, DT: 0.001, ITERATIONS: 150, DLMAX: 2.37D-01 AT (1, 1, 2). DCONV: 1.07D-01 6.17D+01 255.14
 STEP: 5, T: 0.005, DT: 0.001, ITERATIONS: 150, DLMAX: 4.50D-01 AT (1, 1, 2). DCONV: 1.07D-01 1.17D+02 230.59

***** MAXIMUM TIME STEP (MAXNT) REACHED. *****

***** RESTART TAPE WRITTEN AFTER TIME STEP 5 *****

***** BEGINNING OF OUTPUT FOR STEP 5 AT 0.0050 SECONDS *****

7

RESIDUAL MASS (kg/m**3-s) DL

J= 1
 I--> 1 2 3 4 5 6

K						
12	0.0	0.0	0.0	0.0	0.0	0.0
11	0.4273	0.2863	0.1787	0.1491	0.1369	0.0
10	0.4069	0.3002	0.1921	0.1624	0.0920	0.0
9	0.4095	0.3015	0.1929	0.1632	0.0924	0.0
8	0.4120	0.3033	0.1940	0.1639	0.0929	0.0
7	0.4162	0.3061	0.1955	0.1650	0.0934	0.0
6	0.4198	0.3089	0.1972	0.1664	0.0941	0.0
5	0.4225	0.3108	0.1986	0.1676	0.0948	0.0
4	0.4250	0.3126	0.1996	0.1685	0.0953	0.0
3	0.4272	0.3141	0.2005	0.1691	0.0956	0.0
2	0.4504	0.3014	0.1874	0.1560	0.1430	0.0
1	0.0	0.0	0.0	0.0	0.0	0.0

RESIDUAL MASS (kg/m**3-s) DL

K= 10
 I--> 1 2 3 4 5 6

J						
12	0.0788	0.3006	0.1924	0.1626	0.0921	0.0
11	0.1256	0.3002	0.1924	0.1626	0.0921	0.0
10	0.2107	0.3005	0.1922	0.1627	0.0922	0.0
9	0.1226	0.3009	0.1926	0.1627	0.0921	0.0
8	0.1460	0.3007	0.1925	0.1630	0.0924	0.0

7	0.2075	0.3004	0.1920	0.1622	0.0920	0.0
6	0.1730	0.3001	0.1919	0.1622	0.0917	0.0
5	0.1978	0.3007	0.1922	0.1625	0.0920	0.0
4	0.2573	0.3006	0.1922	0.1626	0.0921	0.0
3	0.2702	0.3005	0.1923	0.1626	0.0921	0.0
2	0.3211	0.3003	0.1923	0.1626	0.0920	0.0
1	0.4069	0.3002	0.1921	0.1624	0.0920	0.0

U COMPONENT OF VELOCITY (m/s) UL

J= 1		I--> 1 2 3 4 5 6						
K		12	-0.1205	-0.2028	-0.3451	-0.5868	0.0	0.0
12		0.1205	0.2028	0.3451	0.5868	1.0000	0.0	0.0
11		0.0554	0.0877	0.1065	0.0976	0.0	0.0	0.0
10		0.0304	0.0343	0.0335	0.0231	0.0	0.0	0.0
9		0.0129	0.0131	0.0113	0.0069	0.0	0.0	0.0
8		0.0036	0.0035	0.0029	0.0016	0.0	0.0	0.0
7		-0.0334	-0.0033	-0.0027	-0.0016	0.0	0.0	0.0
6		-0.0127	-0.0129	-0.0111	-0.0067	0.0	0.0	0.0
5		-0.0300	-0.0338	-0.0327	-0.0222	0.0	0.0	0.0
4		-0.0551	-0.0869	-0.1049	-0.0917	0.0	0.0	0.0
3		-0.1218	-0.2062	-0.3528	-0.5019	-1.0000	0.0	0.0
2		0.1218	0.2062	0.3528	0.5019	0.0	0.0	0.0
1		U00X= 0.0717	-0.0717	-0.0453	-0.0239	-0.0110	-0.0031	0.0032
		U00Y= 0.0192	-0.0192	-0.0121	-0.0064	-0.0029	-0.0008	0.0009

78

U COMPONENT OF VELOCITY (m/s) UL

K= 10		I--> 1 2 3 4 5 6						
J		12	0.0479	0.0493	0.0418	0.0242	0.0	0.0
12		0.0193	0.0132	0.0069	0.0021	0.0	0.0	0.0
11		-0.0052	-0.0072	-0.0067	-0.0041	0.0	0.0	0.0
10		-0.0215	-0.0172	-0.0118	-0.0060	0.0	0.0	0.0
9		-0.0304	-0.0215	-0.0137	-0.0066	0.0	0.0	0.0
8		-0.0332	-0.0228	-0.0141	-0.0067	0.0	0.0	0.0
7		-0.0304	-0.0215	-0.0137	-0.0066	0.0	0.0	0.0
6		-0.0215	-0.0172	-0.0137	-0.0066	0.0	0.0	0.0
5		-0.0172	-0.0118	-0.0060	0.0	0.0	0.0	0.0
4		-0.0052	-0.0072	-0.0067	-0.0041	0.0	0.0	0.0
3		0.0193	0.0132	0.0069	0.0021	0.0	0.0	0.0
2		0.0479	0.0493	0.0418	0.0242	0.0	0.0	0.0
1		0.0554	0.0877	0.1065	0.0976	0.0	0.0	0.0
U00X=	0.0717	-0.0717	-0.0453	-0.0239	-0.0110	-0.0031	0.0032	0.0111
U00Y=	0.0192	-0.0192	-0.0121	-0.0064	-0.0029	-0.0008	0.0009	0.0030

V COMPONENT OF VELOCITY (m/s) VL

J= 1		I--> 1 2 3 4 5 6						
K		12	0.0283	0.0595	0.1208	0.2270	0.4003	0.0
12		0.0283	0.0595	0.1208	0.2270	0.4003	0.0	0.0

11	-0.0283	-0.0595	-0.1208	-0.2270	-0.4003	0.4003
10	-0.0161	-0.0276	-0.0459	-0.0682	-0.0842	0.0842
9	-0.0078	-0.0111	-0.0155	-0.0195	-0.0209	0.0209
8	-0.0034	-0.0043	-0.0052	-0.0059	-0.0058	0.0058
7	-0.0009	-0.0011	-0.0013	-0.0014	-0.0013	0.0013
6	0.0009	0.0011	0.0012	0.0013	0.0013	-0.0013
5	0.0033	0.0042	0.0051	0.0058	0.0057	-0.0057
4	0.0077	0.0110	0.0153	0.0192	0.0203	-0.0203
3	0.0160	0.0276	0.0458	0.0675	0.0815	-0.0815
2	0.0286	0.0608	0.1241	0.2336	0.3864	-0.3864
1	-0.0286	-0.0608	-0.1241	-0.2336	-0.3864	0.0

V COMPONENT OF VELOCITY (m/s) VL

K= 10

	I--> 1	2	3	4	5	6
J						
12	0.0161	0.0276	0.0459	0.0682	0.0842	-0.0842
11	0.0391	0.0495	0.0573	0.0600	0.0561	-0.0561
10	0.0469	0.0468	0.0437	0.0387	0.0327	-0.0327
9	0.0419	0.0347	0.0285	0.0231	0.0188	-0.0188
8	0.0282	0.0207	0.0157	0.0123	0.0098	-0.0098
7	0.0099	0.0068	0.0050	0.0038	0.0030	-0.0030
6	-0.0099	-0.0068	-0.0050	-0.0038	-0.0030	0.0030
5	-0.0282	-0.0207	-0.0157	-0.0123	-0.0098	0.0098
4	-0.0419	-0.0347	-0.0285	-0.0231	-0.0188	0.0188
3	-0.0469	-0.0468	-0.0437	-0.0387	-0.0327	0.0327
2	-0.0391	-0.0495	-0.0573	-0.0600	-0.0561	0.0561
1	-0.0161	-0.0276	-0.0459	-0.0682	-0.0842	0.0842

79

W COMPONENT OF VELOCITY (m/s) WL

J= 1

	I--> 1	2	3	4	5	6
K						
12	0.0	0.0	0.0	0.0	0.0	0.0
11	0.0	0.0	0.0	0.0	0.0	0.0
10	0.0491	0.0766	0.1343	0.2539	0.4993	-0.4993
9	0.0647	0.0822	0.1089	0.1454	0.1827	-0.1827
8	0.0675	0.0762	0.0868	0.0979	0.1060	-0.1060
7	0.0674	0.0721	0.0769	0.0812	0.0838	-0.0838
6	0.0672	0.0708	0.0742	0.0769	0.0785	-0.0785
5	0.0674	0.0720	0.0767	0.0809	0.0835	-0.0835
4	0.0674	0.0760	0.0865	0.0973	0.1051	-0.1051
3	0.0647	0.0822	0.1088	0.1446	0.1792	-0.1792
2	0.0496	0.0778	0.1374	0.2613	0.4807	-0.4807
1	0.0	0.0	0.0	0.0	0.0	0.0
W00=	0.0	0.0416	0.0588	0.0643	0.0658	0.0661
						0.0659
						0.0644
						0.0589
						0.0415
						0.0
						0.0

W COMPONENT OF VELOCITY (m/s) WL

K= 10

	I--> 1	2	3	4	5	6
--	--------	---	---	---	---	---

12	0.0475	0.0641	0.0852	0.1084	0.1275	-0.1275						
11	0.0441	0.0491	0.0522	0.0536	0.0537	-0.0537						
10	0.0406	0.0386	0.0362	0.0341	0.0329	-0.0329						
9	0.0377	0.0324	0.0287	0.0264	0.0253	-0.0253						
8	0.0358	0.0292	0.0254	0.0232	0.0222	-0.0222						
7	0.0352	0.0283	0.0244	0.0223	0.0214	-0.0214						
6	0.0358	0.0292	0.0254	0.0232	0.0222	-0.0222						
5	0.0377	0.0324	0.0287	0.0264	0.0253	-0.0253						
4	0.0406	0.0386	0.0362	0.0341	0.0329	-0.0329						
3	0.0441	0.0491	0.0522	0.0536	0.0537	-0.0537						
2	0.0475	0.0641	0.0852	0.1084	0.1275	-0.1275						
1	0.0491	0.0766	0.1343	0.2539	0.4993	-0.4993						
WOO=	0.0	0.0416	0.0588	0.0643	0.0658	0.0661	0.0659	0.0644	0.0589	0.0415	0.0	0.0

PRESSURE (PASCAL) P

J= 1		I--> 1 2 3 4 5 6					
K		80082.7	80082.7	80082.7	80082.7	80082.7	80082.7
12		80082.7	80082.7	80082.7	80082.7	80082.7	80082.7
11		83944.7	83960.1	83956.9	83881.1	83568.8	82013.8
10		85607.3	85622.2	85633.7	85637.2	85633.9	83944.9
9		87035.7	87047.0	87057.4	87065.1	87069.4	85876.1
8		88283.5	88290.5	88297.2	88302.5	88305.8	87807.2
7		89418.5	89421.1	89424.0	89426.3	89428.1	89738.3
6		90515.4	90513.4	90512.0	90510.9	90510.7	91669.4
5		91651.7	91644.1	91636.7	91629.8	91625.4	93600.5
4		92903.6	92889.3	92872.3	92850.5	92826.5	95531.6
3		94344.2	94327.7	94302.7	94239.3	94031.0	97462.8
2		96033.2	96042.2	96079.6	96150.1	96206.5	99393.9
1		101325.0	101325.0	101325.0	101325.0	101325.0	80082.7

PRESSURE (PASCAL) P

K= 10		I--> 1 2 3 4 5 6					
J		85606.3	85620.5	85631.9	85640.4	85646.0	83944.9
12		85606.3	85620.5	85631.9	85640.4	85646.0	83944.9
11		85603.7	85612.6	85619.9	85625.4	85628.9	83944.9
10		85600.3	85602.1	85603.3	85604.2	85605.3	83944.9
9		85596.6	85591.9	85587.8	85585.1	85584.2	83944.9
8		85594.0	85584.7	85577.1	85572.1	85570.1	83944.9
7		85592.8	85582.0	85573.2	85567.5	85565.1	83944.9
6		85593.8	85584.4	85576.9	85571.8	85569.8	83944.9
5		85596.4	85591.4	85587.2	85584.5	85583.6	83944.9
4		85599.9	85601.3	85602.4	85603.3	85604.3	83944.9
3		85603.3	85611.6	85618.6	85624.0	85627.6	83944.9
2		85606.0	85619.1	85630.3	85633.7	85644.2	83944.9
1		85607.3	85622.2	85633.7	85637.2	85633.9	83944.9

TEMPERATURE (deg C) TL

J= 1		I--> 1 2 3 4 5 6					
------	--	------------------	--	--	--	--	--

K	12	57.1996	57.1995	57.1996	57.1997	57.1997	57.2000
11	57.1996	57.1995	57.1996	57.1997	57.1997	57.1997	
10	57.1996	57.1996	57.1998	57.1999	57.2001	57.2001	
9	57.1996	57.1996	57.1998	57.1999	57.2000	57.2000	
8	57.1996	57.1996	57.1998	57.1999	57.2000	57.2000	
7	57.1996	57.1996	57.1998	57.1999	57.2000	57.2000	
6	57.1996	57.1996	57.1998	57.1999	57.2000	57.2000	
5	57.1996	57.1996	57.1998	57.1998	57.2000	57.2000	
4	57.1996	57.1996	57.1998	57.1998	57.1999	57.1999	
3	57.1996	57.1997	57.1999	57.1998	57.1885	57.1885	
2	57.1995	57.1998	57.2000	57.1688	54.9201	15.6000	
1	57.1995	57.1998	57.2000	57.1688	54.9201	57.2000	

TANK WALL TEMPERATURE

0.0

TOTAL HEAT LOSS FROM TANK = 0.0 JOULE

TEMPERATURE (deg C) TL

K= 10	I--> 1	2	3	4	5	6	
J	12	57.1997	57.2001	57.2000	57.2000	57.2001	57.2001
11	57.1997	57.1999	57.1999	57.1999	57.2000	57.2000	
10	57.1997	57.1999	57.1999	57.1999	57.2000	57.2000	
9	57.1995	57.1999	57.1999	57.1999	57.2000	57.2000	
8	57.1997	57.1999	57.1999	57.1999	57.2000	57.2000	
7	57.1997	57.1999	57.1999	57.1999	57.2000	57.2000	
6	57.1996	57.1999	57.1999	57.1999	57.2000	57.2000	
5	57.1997	57.1999	57.1999	57.1999	57.2000	57.2000	
4	57.1997	57.1999	57.1999	57.1999	57.2000	57.2000	
3	57.1996	57.1999	57.1999	57.1999	57.2000	57.2000	
2	57.1997	57.1998	57.1999	57.1999	57.2000	57.2000	
1	57.1996	57.1996	57.1998	57.1999	57.2001	57.2001	

TANK WALL TEMPERATURE

0.0

TOTAL HEAT LOSS FROM TANK = 0.0 JOULE

DENSITY (kg/m**3) ROL

J= 1	I--> 1	2	3	4	5	6	
K	12	985.2602	985.2603	985.2602	985.2601	985.2600	0.0
11	985.2602	985.2603	985.2602	985.2601	985.2600	985.2600	
10	985.2609	985.2610	985.2609	985.2608	985.2608	985.2608	
9	985.2616	985.2616	985.2615	985.2615	985.2614	985.2614	
8	985.2621	985.2621	985.2620	985.2620	985.2619	985.2619	
7	985.2626	985.2626	985.2625	985.2625	985.2624	985.2624	
6	985.2631	985.2631	985.2630	985.2630	985.2629	985.2629	
5	985.2636	985.2636	985.2635	985.2635	985.2634	985.2634	
4	985.2642	985.2641	985.2640	985.2640	985.2640	985.2640	
3	985.2648	985.2647	985.2646	985.2646	985.2679	985.2679	
2	985.2655	985.2654	985.2653	985.2745	986.1480	998.5035	
1	985.2655	985.2654	985.2653	985.2745	986.1480	0.0	

ROL= 985.2655 985.2655 985.2648 985.2641 985.2636 985.2631 985.2626 985.2621 985.2615 985.2609 985.2602 985.2602

DENSITY (kg/m**3) ROL

K= 10

I-->

	1	2	3	4	5	6
J						
12	985.2609	985.2607	985.2608	985.2608	985.2608	985.2608
11	985.2609	985.2608	985.2608	985.2608	985.2608	985.2608
10	985.2609	985.2608	985.2608	985.2608	985.2608	985.2608
9	985.2610	985.2608	985.2608	985.2608	985.2608	985.2608
8	985.2609	985.2608	985.2608	985.2608	985.2607	985.2607
7	985.2609	985.2608	985.2608	985.2603	985.2607	985.2607
6	985.2610	985.2608	985.2608	985.2608	985.2607	985.2607
5	985.2609	985.2608	985.2608	985.2608	985.2608	985.2608
4	985.2609	985.2608	985.2608	985.2608	985.2608	985.2608
3	985.2609	985.2608	985.2608	985.2608	985.2608	985.2608
2	985.2609	985.2608	985.2608	985.2608	985.2608	985.2608
1	985.2609	985.2610	985.2609	985.2608	985.2608	985.2608

R00= 985.2655 985.2655 985.2648 985.2641 985.2636 985.2631 985.2626 985.2621 985.2615 985.2609 985.2602 985.2602

***** END OF OUTPUT FOR STEP 5 AT 0.0050 SECONDS *****

```

0
&STUFF
ND=3,IBAR=3,JBAR=1,KBAR=13,XMIN=0.0,RIDL=0.0,
OMEGA=1.8,GX=0.0,GY=0.0,GZ=-9.8,
ISTPR=1202,2202,3202,4202,5202,6202,7202,8202,9202,
10202,11202,12202,13202,
NTHPR=1202,2202,3202,4202,5202,6202,8202,
DX=9*0.0267,
DY=3*15.0*0.02=2*0.06,0.1,0.136,7*0.16,0.136,0.1,2*0.06,
EPS1=1.0E-4,EPS2=1.0E-6,B0=0.0,A0=0.5,
TURBV=0.0,TURBC=0.0,
TPRNT=-0.099,IFNRG=1,IFPLOT=-1,
MAXNT=10,NDT=20,40,50,10000,DT=0.01,0.05,0.1,0.2,T=0.0,
NIT=20,100,300,400,50000,IT=200,100,30,30,30,THETAZ=0.0,
CHF=0.0,0.0,0.0,0.0,0.0,
CVVEL(1)=-0.00163,CVVEL(2)=0.006514,NT=1,ISEC=1,
ICONPR=0,TIMEND=15.0,BAFR=1.E+25,IFRMB=0,
&END
IFLD -1.0 1 9 1 3 1 15
IFLD 1.0 1 8 2 2 2 14
IFLD -6.0 9 9 2 2 1 15
IFLD -6.0 1 8 1 1 1 15
IFLD -6.0 1 8 3 3 1 15
IFLD -6.0 1 8 2 2 1 15
IFLD -6.0 1 8 2 2 15 15
IFLD -4.0 9 9 2 2 2 2
END
IFLU -1.0 1 9 1 3 1 15
IFLU 1.0 1 7 2 2 2 14
IFLU 0.0 1 7 2 2 1 1
IFLU 0.0 1 7 2 2 15 15
IFLU -4.0 1 7 1 1 2 14
IFLU -4.0 1 7 3 3 2 14
IFLU -101.0 8 8 2 2 2 2
IFLU 3.0 3 3 2 2 3 14
IFLU 3.0 4 4 2 2 2 13
IFLV -1.0 1 9 1 3 1 15
IFLV 1.0 1 8 2 2 2 14
IFLW -1.0 1 9 1 3 1 15
IFLW 1.0 1 8 2 2 2 13
IFLW 0.0 9 9 2 2 1 15
IFLW -4.0 1 8 1 1 2 13
IFLW -4.0 1 8 3 3 2 13
IFLW -3.0 1 3 2 2 14 14
THL 1.0 1 9 1 3 1 15
P 101325.0 1 9 1 3 1 15
TL 57.2 1 9 1 3 1 15
TL 15.6 9 9 2 2 2 2
END
MS(I,J,K)

```

८

122	123	124	125	126	127	128	129	121	0
1	2	3	4	5	6	7	8	121	
113	114	115	116	117	118	119	120	0	

139	140	141	142	143	144	145	146	138	0
9	10	11	12	13	14	15	16	138	
130	131	132	133	134	135	136	137	0	

156	157	158	159	150	161	162	163	155	0
17	18	19	20	21	22	23	24	155	
147	148	149	150	151	152	153	154	0	

173	174	175	176	177	178	179	180	172	0
25	26	27	28	29	30	31	32	172	
164	165	166	167	168	169	170	171	0	

190	191	192	193	194	195	196	197	189	0
33	34	35	36	37	38	39	40	189	
181	182	183	184	185	186	187	188	0	

207	208	209	210	211	212	213	214	206	0
41	42	43	44	45	46	47	48	206	
198	199	200	201	202	203	204	205	0	

224	225	226	227	228	229	230	231	223	0
49	50	51	52	53	54	55	56	223	
215	216	217	218	219	220	221	222	0	

241	242	243	244	245	246	247	248	240	0
57	58	59	60	61	62	63	64	240	
232	233	234	235	236	237	238	239	0	

258	259	260	261	262	263	264	265	257	0
65	66	67	68	69	70	71	72	257	

249	250	251	252	253	254	255	256	0
-----	-----	-----	-----	-----	-----	-----	-----	---

275	276	277	278	279	280	281	282	0
73	74	75	76	77	78	79	80	274
266	267	268	269	270	271	272	273	0

292	293	294	295	296	297	298	299	0
81	82	83	84	85	86	87	88	291
283	284	285	286	287	288	289	290	0

309	310	311	312	313	314	315	316	0
89	90	91	92	93	94	95	96	308
300	301	302	303	304	305	306	307	0

326	327	328	329	330	331	332	333	0
97	98	99	100	101	102	103	104	325
317	318	319	320	321	322	323	324	0

0	0	0	0	0	0	0	0	0
334	335	336	337	338	339	340	341	0
0	0	0	0	0	0	0	0	0

COMMON BLOCK DIMENSIONS

NBU1 -	182	NBU2 -	0	NBU3 -	0	NBU4 -	14	NBU5 -	0	NBU6 -	0
NBV1 -	0	NBV2 -	0	NBV3 -	0	NBV4 -	0	NBV5 -	0	NBV6 -	0
NBW1 -	192	NBW2 -	3	NBW3 -	0	NBW4 -	13	NBW5 -	0	NBW6 -	0
NBF1 -	0	NBF2 -	1	NBF3 -	0	NBF4 -	236	NBF5 -	0	MBC -	237

* INITIALIZATION COMPLETED *

***** BEGINNING OF OUTPUT FOR STEP 0 AT 0.0 SECONDS *****

RESIDUAL MASS (kg/m**3-s) DL

J= 2		I-->								
K	1	2	3	4	5	6	7	8	9	
15	0.0	0.0	0.0	0.0	0.0	0.0	0.0	0.0	0.0	0.0
14	0.0	0.0	0.0	0.0	0.0	0.0	0.0	0.0	0.0	0.0
13	0.0	0.0	0.0	0.0	0.0	0.0	0.0	0.0	0.0	0.0
12	0.0	0.0	0.0	0.0	0.0	0.0	0.0	0.0	0.0	0.0
11	0.0	0.0	0.0	0.0	0.0	0.0	0.0	0.0	0.0	0.0
10	0.0	0.0	0.0	0.0	0.0	0.0	0.0	0.0	0.0	0.0
9	0.0	0.0	0.0	0.0	0.0	0.0	0.0	0.0	0.0	0.0
8	0.0	0.0	0.0	0.0	0.0	0.0	0.0	0.0	0.0	0.0
7	0.0	0.0	0.0	0.0	0.0	0.0	0.0	0.0	0.0	0.0
6	0.0	0.0	0.0	0.0	0.0	0.0	0.0	0.0	0.0	0.0
5	0.0	0.0	0.0	0.0	0.0	0.0	0.0	0.0	0.0	0.0
4	0.0	0.0	0.0	0.0	0.0	0.0	0.0	0.0	0.0	0.0
3	0.0	0.0	0.0	0.0	0.0	0.0	0.0	0.0	0.0	0.0
2	0.0	0.0	0.0	0.0	0.0	0.0	0.0	0.0	0.0	0.0
1	0.0	0.0	0.0	0.0	0.0	0.0	0.0	0.0	0.0	0.0

U COMPONENT OF VELOCITY (m/s) UL

J= 2		I-->								
K	1	2	3	4	5	6	7	8	9	
15	0.0	0.0	0.0	0.0	0.0	0.0	0.0	0.0	0.0	0.0
14	0.0	0.0	0.0	0.0	0.0	0.0	0.0	0.0	0.0	0.0
13	0.0	0.0	0.0	0.0	0.0	0.0	0.0	0.0	0.0	0.0
12	0.0	0.0	0.0	0.0	0.0	0.0	0.0	0.0	0.0	0.0
11	0.0	0.0	0.0	0.0	0.0	0.0	0.0	0.0	0.0	0.0
10	0.0	0.0	0.0	0.0	0.0	0.0	0.0	0.0	0.0	0.0
9	0.0	0.0	0.0	0.0	0.0	0.0	0.0	0.0	0.0	0.0
8	0.0	0.0	0.0	0.0	0.0	0.0	0.0	0.0	0.0	0.0
7	0.0	0.0	0.0	0.0	0.0	0.0	0.0	0.0	0.0	0.0
6	0.0	0.0	0.0	0.0	0.0	0.0	0.0	0.0	0.0	0.0
5	0.0	0.0	0.0	0.0	0.0	0.0	0.0	0.0	0.0	0.0
4	0.0	0.0	0.0	0.0	0.0	0.0	0.0	0.0	0.0	0.0
3	0.0	0.0	0.0	0.0	0.0	0.0	0.0	0.0	0.0	0.0
2	0.0	0.0	0.0	0.0	0.0	0.0	0.0	-0.0016	0.0	
1	0.0	0.0	0.0	0.0	0.0	0.0	0.0	0.0	0.0	
U00X=	0.0	0.0	0.0	0.0	0.0	0.0	0.0	0.0	0.0	0.0
U00Y=	0.0	0.0	0.0	0.0	0.0	0.0	0.0	0.0	0.0	0.0
U00Y=	0.0	0.0	0.0	0.0	0.0	0.0	0.0	0.0	0.0	0.0
U00Y=	0.0	0.0	0.0	0.0	0.0	0.0	0.0	0.0	0.0	0.0

V COMPONENT OF VELOCITY (m/s) VL

W COMPONENT OF VELOCITY (m/s) WL

		J= 2								
		I-->								
K	I	1	2	3	4	5	6	7	8	9
15	0.0	0.0	0.0	0.0	0.0	0.0	0.0	0.0	0.0	0.0
14	0.0	0.0	0.0	0.0	0.0	0.0	0.0	0.0	0.0	0.0
13	0.0	0.0	0.0	0.0	0.0	0.0	0.0	0.0	0.0	0.0
12	0.0	0.0	0.0	0.0	0.0	0.0	0.0	0.0	0.0	0.0
11	0.0	0.0	0.0	0.0	0.0	0.0	0.0	0.0	0.0	0.0
10	0.0	0.0	0.0	0.0	0.0	0.0	0.0	0.0	0.0	0.0
9	0.0	0.0	0.0	0.0	0.0	0.0	0.0	0.0	0.0	0.0
8	0.0	0.0	0.0	0.0	0.0	0.0	0.0	0.0	0.0	0.0
7	0.0	0.0	0.0	0.0	0.0	0.0	0.0	0.0	0.0	0.0
6	0.0	0.0	0.0	0.0	0.0	0.0	0.0	0.0	0.0	0.0
5	0.0	0.0	0.0	0.0	0.0	0.0	0.0	0.0	0.0	0.0
4	0.0	0.0	0.0	0.0	0.0	0.0	0.0	0.0	0.0	0.0
3	0.0	0.0	0.0	0.0	0.0	0.0	0.0	0.0	0.0	0.0
2	0.0	0.0	0.0	0.0	0.0	0.0	0.0	0.0	0.0	0.0
1	0.0	0.0	0.0	0.0	0.0	0.0	0.0	0.0	0.0	0.0
HOQ=	0.0	0.0	0.0	0.0	0.0	0.0	0.0	0.0	0.0	0.0
HOQ=	0.0	0.0	0.0							

PRESSURE (PASCAL)

7	94315.0	94315.0	94315.0	94315.0	94315.0	94315.0	94315.0	94315.0	94315.0	94315.0
6	95859.9	95859.9	95859.9	95859.9	95859.9	95859.9	95859.9	95859.9	95859.9	95359.9
5	97404.8	97404.8	97404.8	97404.8	97404.8	97404.8	97404.8	97404.8	97404.8	97404.8
4	98833.9	98833.9	98833.9	98833.9	98833.9	98833.9	98833.9	98833.9	98833.9	98833.9
3	99973.2	99973.2	99973.2	99973.2	99973.2	99973.2	99973.2	99973.2	99973.2	99973.2
2	100745.7	100745.7	100745.7	100745.7	100745.7	100745.7	100745.7	100745.7	100745.7	100745.7
1	101325.0	101325.0	101325.0	101325.0	101325.0	101325.0	101325.0	101325.0	101325.0	84215.3

TEMPERATURE (deg C) TL

J= 2		1	2	3	4	5	6	7	8	9
K	I-->									
15		57.2000	57.2000	57.2000	57.2000	57.2000	57.2000	57.2000	57.2000	57.2000
14		57.2000	57.2000	57.2000	57.2000	57.2000	57.2000	57.2000	57.2000	57.2000
13		57.2000	57.2000	57.2000	57.2000	57.2000	57.2000	57.2000	57.2000	57.2000
12		57.2000	57.2000	57.2000	57.2000	57.2000	57.2000	57.2000	57.2000	57.2000
11		57.2000	57.2000	57.2000	57.2000	57.2000	57.2000	57.2000	57.2000	57.2000
10		57.2000	57.2000	57.2000	57.2000	57.2000	57.2000	57.2000	57.2000	57.2000
9		57.2000	57.2000	57.2000	57.2000	57.2000	57.2000	57.2000	57.2000	57.2000
8		57.2000	57.2000	57.2000	57.2000	57.2000	57.2000	57.2000	57.2000	57.2000
7		57.2000	57.2000	57.2000	57.2000	57.2000	57.2000	57.2000	57.2000	57.2000
6		57.2000	57.2000	57.2000	57.2000	57.2000	57.2000	57.2000	57.2000	57.2000
5		57.2000	57.2000	57.2000	57.2000	57.2000	57.2000	57.2000	57.2000	57.2000
4		57.2000	57.2000	57.2000	57.2000	57.2000	57.2000	57.2000	57.2000	57.2000
3		57.2000	57.2000	57.2000	57.2000	57.2000	57.2000	57.2000	57.2000	57.2000
2		57.2000	57.2000	57.2000	57.2000	57.2000	57.2000	57.2000	57.2000	15.6000
1		57.2000	57.2000	57.2000	57.2000	57.2000	57.2000	57.2000	57.2000	57.2000

TANK WALL TEMPERATURE

0.0

TOTAL HEAT LOSS FROM TANK = 0.0 JCULE

88

ENTHALPY (J/kg) HL

J= 2		1	2	3	4	5	6	7	8	9
K	I-->									
15		2.3890+05	2.3890+05	2.3890+05	2.3890+05	2.3890+05	2.3890+05	2.3890+05	2.3890+05	0.0
14		2.3890+05	2.3890+05	2.3890+05	2.3890+05	2.3890+05	2.3890+05	2.3890+05	2.3890+05	
13		2.3890+05	2.3890+05	2.3890+05	2.3890+05	2.3890+05	2.3890+05	2.3890+05	2.3890+05	
12		2.3890+05	2.3890+05	2.3890+05	2.3890+05	2.3890+05	2.3890+05	2.3890+05	2.3890+05	
11		2.3890+05	2.3890+05	2.3890+05	2.3890+05	2.3890+05	2.3890+05	2.3890+05	2.3890+05	
10		2.3890+05	2.3890+05	2.3890+05	2.3890+05	2.3890+05	2.3890+05	2.3890+05	2.3890+05	
9		2.3890+05	2.3890+05	2.3890+05	2.3890+05	2.3890+05	2.3890+05	2.3890+05	2.3890+05	
8		2.3890+05	2.3890+05	2.3890+05	2.3890+05	2.3890+05	2.3890+05	2.3890+05	2.3890+05	
7		2.3890+05	2.3890+05	2.3890+05	2.3890+05	2.3890+05	2.3890+05	2.3890+05	2.3890+05	
6		2.3890+05	2.3890+05	2.3890+05	2.3890+05	2.3890+05	2.3890+05	2.3890+05	2.3890+05	
5		2.3890+05	2.3890+05	2.3890+05	2.3890+05	2.3890+05	2.3890+05	2.3890+05	2.3890+05	
4		2.3890+05	2.3890+05	2.3890+05	2.3890+05	2.3890+05	2.3890+05	2.3890+05	2.3890+05	
3		2.3890+05	2.3890+05	2.3890+05	2.3890+05	2.3890+05	2.3890+05	2.3890+05	2.3890+05	
2		2.3890+05	2.3890+05	2.3890+05	2.3890+05	2.3890+05	2.3890+05	2.3890+05	2.3890+05	6.5250+04
1		2.3890+05	2.3890+05	2.3890+05	2.3890+05	2.3890+05	2.3890+05	2.3890+05	2.3890+05	0.0

DENSITY (kg/m**3) ROL

CELL VOID FRACTION

85

FIELD VARIABLE MARKER

J= 2

8	1	1	1	1	1	1	1	1	-6
7	1	1	1	1	1	1	1	1	-6
6	1	1	1	1	1	1	1	1	-6
5	1	1	1	1	1	1	1	1	-6
4	1	1	1	1	1	1	1	1	-6
3	1	1	1	1	1	1	1	1	-6
2	1	1	1	1	1	1	1	1	-4
1	-6	-6	-6	-6	-6	-5	-6	-6	10

U VELOCITY FLOW VARIABLE MARKER IFLOWU

J= 2

	I	1	2	3	4	5	6	7	8	9
K	15	0	0	0	0	0	0	-1	0	
14	1	1	3	1	1	1	1	-1	-1	
13	1	1	3	3	1	1	1	-1	-1	
12	1	1	3	3	1	1	1	-1	-1	
11	1	1	3	3	1	1	1	-1	-1	
10	1	1	3	3	1	1	1	-1	-1	
9	1	1	3	3	1	1	1	-1	-1	
8	1	1	3	3	1	1	1	-1	-1	
7	1	1	3	3	1	1	1	-1	-1	
6	1	1	3	3	1	1	1	-1	-1	
5	1	1	3	3	1	1	1	-1	-1	
4	1	1	3	3	1	1	1	-1	-1	
3	1	1	3	3	1	1	1	-1	-1	
2	1	1	1	3	1	1	1	-101	-1	
1	0	0	0	0	0	0	0	-1	0	

V VELOCITY FLOW VARIABLE MARKER IFLOWV

J= 2

	I	1	2	3	4	5	6	7	8	9
K	15	-1	-1	-1	-1	-1	-1	-1	-1	0
14	1	1	1	1	1	1	1	1	1	-1
13	1	1	1	1	1	1	1	1	1	-1
12	1	1	1	1	1	1	1	1	1	-1
11	1	1	1	1	1	1	1	1	1	-1
10	1	1	1	1	1	1	1	1	1	-1
9	1	1	1	1	1	1	1	1	1	-1
8	1	1	1	1	1	1	1	1	1	-1
7	1	1	1	1	1	1	1	1	1	-1
6	1	1	1	1	1	1	1	1	1	-1
5	1	1	1	1	1	1	1	1	1	-1
4	1	1	1	1	1	1	1	1	1	-1
3	1	1	1	1	1	1	1	1	1	-1
2	1	1	1	1	1	1	1	1	1	-1
1	-1	-1	-1	-1	-1	-1	-1	-1	-1	0

W VELOCITY FLOW VARIABLE MARKER IFLOWW

J= 2

I	1	2	3	4	5	6	7	8	9
K									
15	-1	-1	-1	-1	-1	-1	-1	-1	0
14	-3	-3	-3	-1	-1	-1	-1	-1	0
13	1	1	1	1	1	1	1	1	0
12	1	1	1	1	1	1	1	1	0
11	1	1	1	1	1	1	1	1	0
10	1	1	1	1	1	1	1	1	0
9	1	1	1	1	1	1	1	1	0
8	1	1	1	1	1	1	1	1	0
7	1	1	1	1	1	1	1	1	0
6	1	1	1	1	1	1	1	1	0
5	1	1	1	1	1	1	1	1	0
4	1	1	1	1	1	1	1	1	0
3	1	1	1	1	1	1	1	1	0
2	1	1	1	1	1	1	1	1	0
1	-1	-1	-1	-1	-1	-1	-1	-1	0

***** END OF OUTPUT FOR STEP 0 AT 0.0 SECONDS *****

STEP: 1, T: 0.010, DT: 0.010, ITERATIONS: 200, DLMAX: -9.000+00 AT (6, 2, 2). DCONV: 3.01D-03-4.05D+02 114.69
STEP: 2, T: 0.020, DT: 0.010, ITERATIONS: 200, DLMAX: -7.950+00 AT (6, 2, 13). DCONV: 6.33D-03-4.52D+02 111.97
STEP: 3, T: 0.030, DT: 0.010, ITERATIONS: 200, DLMAX: -7.200+00 AT (6, 2, 3). DCONV: 6.25D-03-4.46D+02 109.27
STEP: 4, T: 0.040, DT: 0.010, ITERATIONS: 200, DLMAX: -6.460+00 AT (7, 2, 3). DCONV: 6.26D-03-4.15D+02 106.62
STEP: 5, T: 0.050, DT: 0.010, ITERATIONS: 200, DLMAX: -5.750+00 AT (6, 2, 13). DCONV: 6.26D-03-3.77D+02 103.83
STEP: 6, T: 0.060, DT: 0.010, ITERATIONS: 200, DLMAX: -5.090+00 AT (6, 2, 13). DCONV: 6.71D-03-3.39D+02 101.11
STEP: 7, T: 0.070, DT: 0.010, ITERATIONS: 200, DLMAX: -4.500+00 AT (1, 2, 2). DCONV: 8.08D-03-3.02D+02 98.39
STEP: 8, T: 0.080, DT: 0.010, ITERATIONS: 200, DLMAX: -4.050+00 AT (1, 2, 2). DCONV: 9.36D-03-2.67D+02 95.70
STEP: 9, T: 0.090, DT: 0.010, ITERATIONS: 200, DLMAX: -3.61D+00 AT (1, 2, 2). DCONV: 1.05D-02-2.35D+02 92.86
STEP: 10, T: 0.100, DT: 0.010, ITERATIONS: 200, DLMAX: -3.19D+00 AT (1, 2, 2). DCONV: 1.16D-02-2.05D+02 90.17

***** MAXIMUM TIME STEP (MAXNT) REACHED. *****

***** BEGINNING OF OUTPUT FOR STEP 10 AT 0.1000 SECONDS *****

RESIDUAL MASS (kg/m**3-s) DL

I-->	1	2	3	4	5	6	7	8	9
K									
15	0.0	0.0	0.0	0.0	0.0	0.0	0.0	0.0	0.0
14	-1.9099	-1.9064	-0.8400	-1.7642	-2.9336	-2.9327	-2.9321	-1.4763	0.0
13	-2.0304	-2.0267	-0.8936	-0.2050	-1.7199	-2.9324	-2.9322	-1.4771	0.0
12	-2.1247	-2.1208	-0.8955	-0.1101	-1.6232	-2.8345	-2.8345	-1.3807	0.0
11	-2.2844	-2.2804	-0.9490	-0.0804	-1.5911	-2.8008	-2.8007	-1.3490	0.0
10	-2.4575	-2.4533	-1.0194	-0.0779	-1.5853	-2.7930	-2.7930	-1.3438	0.0
9	-2.6111	-2.6068	-1.0832	-0.0785	-1.5825	-2.7882	-2.7882	-1.3415	0.0
8	-2.7420	-2.7376	-1.1377	-0.0791	-1.5798	-2.7834	-2.7835	-1.3392	0.0
7	-2.8498	-2.8454	-1.1825	-0.0797	-1.5773	-2.7790	-2.7791	-1.3371	0.0

6	-2.9342	-2.9299	-.2177	-.0803	-1.5750	-2.7750	-2.7751	-1.1352	0.0
5	-2.9987	-2.9945	-.2466	-.0842	-1.5762	-2.7747	-2.7749	-1.1367	0.0
4	-3.0669	-3.0628	-.2938	-.1168	-1.6043	-2.8018	-2.8019	-1.3650	0.0
3	-3.1857	-3.1815	-.4035	-.2201	-1.6973	-2.8942	-2.8944	-1.4582	0.0
2	-3.1893	-3.1850	-.4863	-.14863	-1.6956	-2.8922	-2.8923	-2.8923	0.0
1	0.0	0.0	0.0	0.0	0.0	0.0	0.0	0.0	0.0

U COMPONENT OF VELOCITY (m/s) UL

J= 2		1	2	3	4	5	6	7	8	9
K	I-->									
15		0.0000	0.0000	0.0000	0.0022	0.0013	0.0007	0.0003	0.0	0.0
14		-0.0000	-0.0000	-0.0000	-0.0022	-0.0013	-0.0007	-0.0003	0.0	0.0
13		-0.0000	-0.0000	-0.0000	-0.0000	-0.0001	-0.0001	-0.0001	0.0	0.0
12		-0.0000	-0.0000	-0.0000	-0.0000	-0.0000	-0.0000	-0.0000	0.0	0.0
11		-0.0000	-0.0000	-0.0000	-0.0000	-0.0000	-0.0000	-0.0000	0.0	0.0
10		-0.0000	-0.0000	-0.0000	-0.0000	-0.0000	-0.0000	-0.0000	0.0	0.0
9		-0.0000	-0.0000	-0.0000	-0.0000	-0.0000	-0.0000	-0.0000	0.0	0.0
8		-0.0000	-0.0000	-0.0000	-0.0000	-0.0000	-0.0000	-0.0000	0.0	0.0
7		-0.0000	-0.0000	-0.0000	-0.0000	-0.0000	-0.0000	-0.0000	0.0	0.0
6		-0.0000	-0.0000	-0.0000	-0.0000	-0.0000	-0.0000	-0.0000	0.0	0.0
5		-0.0000	-0.0000	-0.0000	-0.0000	-0.0000	-0.0000	-0.0000	0.0	0.0
4		-0.0000	-0.0000	-0.0000	-0.0000	-0.0000	-0.0000	-0.0000	0.0	0.0
3		-0.0001	-0.0001	-0.0000	-0.0000	-0.0001	-0.0001	-0.0001	0.0	0.0
2		-0.0009	-0.0018	-0.0029	-0.0060	-0.0004	-0.0007	-0.0011	-0.0016	0.0
1		0.0009	0.0018	0.0029	0.0060	0.0004	0.0007	0.0011	0.0	0.0
UOOX=		0.0	0.0	0.0	0.0	0.0	0.0	0.0	0.0	0.0
UOOX=		0.0	0.0	0.0						
UOOY=		0.0	0.0	0.0	0.0	0.0	0.0	0.0	0.0	0.0
UOOY=		0.0	0.0	0.0						

V COMPONENT OF VELOCITY (m/s) VL

J= 2		1	2	3	4	5	6	7	8	9
K	I-->									
15		0.0	0.0	0.0	0.0	0.0	0.0	0.0	0.0	0.0
14		0.0	0.0	0.0	0.0	0.0	0.0	0.0	0.0	0.0
13		0.0	0.0	0.0	0.0	0.0	0.0	0.0	0.0	0.0
12		0.0	0.0	0.0	0.0	0.0	0.0	0.0	0.0	0.0
11		0.0	0.0	0.0	0.0	0.0	0.0	0.0	0.0	0.0
10		0.0	0.0	0.0	0.0	0.0	0.0	0.0	0.0	0.0
9		0.0	0.0	0.0	0.0	0.0	0.0	0.0	0.0	0.0
8		0.0	0.0	0.0	0.0	0.0	0.0	0.0	0.0	0.0
7		0.0	0.0	0.0	0.0	0.0	0.0	0.0	0.0	0.0
6		0.0	0.0	0.0	0.0	0.0	0.0	0.0	0.0	0.0
5		0.0	0.0	0.0	0.0	0.0	0.0	0.0	0.0	0.0
4		0.0	0.0	0.0	0.0	0.0	0.0	0.0	0.0	0.0
3		0.0	0.0	0.0	0.0	0.0	0.0	0.0	0.0	0.0
2		0.0	0.0	0.0	0.0	0.0	0.0	0.0	0.0	0.0
1		0.0	0.0	0.0	0.0	0.0	0.0	0.0	0.0	0.0

W COMPONENT OF VELOCITY (m/s) WL

J= 2										
I-->	1	2	3	4	5	6	7	8	9	
K										
15	0.0	0.0	0.0	0.0	0.0	0.0	0.0	0.0	0.0	0.0
14	0.0040	0.0040	0.0040	0.0040	-0.0056	0.0013	0.0009	0.0007	0.0006	-0.0006
13	0.0040	0.0040	0.0040	-0.0056	0.0009	0.0009	0.0008	0.0008	-0.0008	
12	0.0041	0.0041	0.0041	-0.0056	0.0009	0.0009	0.0009	0.0009	-0.0009	
11	0.0041	0.0041	0.0041	-0.0056	0.0009	0.0009	0.0009	0.0009	-0.0009	
10	0.0041	0.0041	0.0041	-0.0056	0.0009	0.0009	0.0009	0.0009	-0.0009	
9	0.0041	0.0041	0.0041	-0.0056	0.0010	0.0009	0.0009	0.0009	-0.0009	
8	0.0042	0.0042	0.0042	-0.0056	0.0010	0.0010	0.0010	0.0010	-0.0010	
7	0.0042	0.0042	0.0042	-0.0056	0.0010	0.0010	0.0010	0.0010	-0.0010	
6	0.0042	0.0042	0.0042	-0.0056	0.0011	0.0011	0.0011	0.0010	-0.0010	
5	0.0042	0.0042	0.0042	-0.0056	0.0011	0.0011	0.0011	0.0011	-0.0011	
4	0.0043	0.0043	0.0043	-0.0056	0.0011	0.0011	0.0011	0.0011	-0.0011	
3	0.0043	0.0043	0.0043	-0.0056	0.0011	0.0011	0.0011	0.0012	-0.0012	
2	0.0038	0.0040	0.0046	-0.0056	0.0009	0.0010	0.0012	0.0015	-0.0015	
1	0.0	0.0	0.0	0.0	0.0	0.0	0.0	0.0	0.0	
WOG=	0.0	0.0035	0.0039	0.0039	0.0039	0.0038	0.0038	0.0038	0.0037	0.0037
WOC=	0.0037	0.0037	0.0							

J= 2		PRESSURE (PASCAL) P								
I-->	1	2	3	4	5	6	7	8	9	
K										
15	84215.3	84215.3	84215.3	84215.3	84215.3	84215.3	84215.3	84215.3	84215.3	84215.3
14	85280.4	85280.4	85280.4	85424.3	85424.8	85425.0	85425.2	85425.2	84794.6	
13	86056.1	86056.1	86056.1	86192.9	86198.0	86198.0	86198.1	86198.1	85567.1	
12	87200.3	87200.3	87200.3	87326.7	87338.2	87338.2	87338.1	87338.1	86706.4	
11	88635.3	88635.3	88635.3	88748.8	88768.1	88768.0	88768.0	88768.0	88135.5	
10	90186.7	90186.7	90186.6	90286.1	90313.8	90313.8	90313.8	90313.7	89680.3	
9	91737.9	91737.9	91737.9	91823.5	91859.4	91859.4	91859.4	91859.4	91225.2	
8	93289.2	93289.2	93289.2	93360.8	93405.0	93404.9	93404.9	93404.9	92770.1	
7	94840.3	94840.3	94840.3	94989.1	94950.4	94950.4	94950.4	94950.4	94315.0	
6	96391.5	96391.4	96391.4	96435.5	96495.8	96495.7	96495.7	96495.7	95859.9	
5	97942.5	97942.5	97942.5	97972.8	98041.0	98041.0	98041.0	98041.0	97404.8	
4	99377.2	99377.1	99377.1	99394.8	99470.3	99470.3	99470.2	99470.2	98833.9	
3	100520.9	100520.9	100520.9	100528.6	100609.8	100609.8	100609.8	100609.8	99973.2	
2	101296.0	101296.2	101296.6	101297.3	101382.3	101382.3	101382.3	101382.3	100745.7	
1	101325.0	101325.0	101325.0	101325.0	101325.0	101325.0	101325.0	101325.0	84215.3	

J= 2		TEMPERATURE (deg C) TL								
I-->	1	2	3	4	5	6	7	8	9	
K										
15	57.2113	57.2040	57.1952	57.2140	57.2038	57.2032	57.2029	57.1880	57.2000	
14	57.2113	57.2040	57.1952	57.2140	57.2038	57.2032	57.2029	57.1880	57.1830	
13	57.2131	57.2053	57.1960	57.2005	57.2158	57.2055	57.2051	57.1902	57.1902	
12	57.2140	57.2056	57.1955	57.2001	57.2154	57.2051	57.2048	57.1898	57.1898	
11	57.2152	57.2060	57.1951	57.2000	57.2154	57.2050	57.2047	57.1897	57.1897	
10	57.2164	57.2065	57.1947	57.2000	57.2153	57.2050	57.2046	57.1896	57.1896	
9	57.2175	57.2069	57.1943	57.2000	57.2154	57.2050	57.2047	57.1896	57.1896	
8	57.2185	57.2074	57.1940	57.2000	57.2154	57.2050	57.2047	57.1896	57.1896	

7	57.2195	57.2077	57.1937	57.2000	57.2154	57.2050	57.2047	57.1896	57.1856
6	57.2203	57.2081	57.1934	57.2000	57.2154	57.2050	57.2047	57.1896	57.1856
5	57.2210	57.2084	57.1932	57.2000	57.2154	57.2050	57.2046	57.1896	57.1856
4	57.2216	57.2085	57.1929	57.1999	57.2153	57.2049	57.2046	57.1895	57.1895
3	57.2219	57.2086	57.1927	57.1998	57.2152	57.2048	57.2044	57.1892	57.1892
2	57.2239	57.2106	57.2079	57.1938	57.2174	57.2070	57.2063	56.9697	55.6000
1	57.2239	57.2106	57.2079	57.1938	57.2174	57.2070	57.2063	56.9697	57.2000

TANK WALL TEMPERATURE

0.0

TOTAL HEAT LOSS FROM TANK = 0.0 JOULE

DENSITY (kg/m³) ROL

J= 2		1	2	3	4	5	6	7	8	9
K	I-->									
15		985.2556	985.2589	985.2628	985.2543	985.2590	985.2592	985.2594	985.2662	0.0
14		985.2556	985.2589	985.2628	985.2543	985.2590	985.2592	985.2594	985.2662	985.2662
13		985.2552	985.2586	985.2628	985.2608	985.2538	985.2586	985.2587	985.2555	985.2655
12		985.2553	985.2590	985.2635	985.2615	985.2545	985.2592	985.2594	985.2662	985.2662
11		985.2554	985.2594	985.2643	985.2621	985.2551	985.2599	985.2600	985.2669	985.2669
10		985.2555	985.2599	985.2651	985.2628	985.2558	985.2605	985.2607	985.2676	985.2676
9		985.2556	985.2603	985.2659	985.2635	985.2564	985.2612	985.2613	985.2682	985.2682
8		985.2558	985.2608	985.2668	985.2641	985.2571	985.2618	985.2620	985.2689	985.2689
7		985.2561	985.2613	985.2676	985.2648	985.2578	985.2625	985.2627	985.2696	985.2696
6		985.2564	985.2618	985.2683	985.2654	985.2584	985.2632	985.2633	985.2702	985.2702
5		985.2567	985.2624	985.2691	985.2661	985.2591	985.2638	985.2640	985.2709	985.2709
4		985.2571	985.2629	985.2698	985.2667	985.2597	985.2645	985.2646	985.2715	985.2715
3		985.2574	985.2633	985.2704	985.2673	985.2603	985.2650	985.2652	985.2721	985.2721
2		985.2568	985.2628	985.2640	985.2703	985.2596	985.2643	985.2646	985.3667	985.5041
1		985.2563	985.2628	985.2640	985.2703	985.2596	985.2643	985.2646	985.3667	0.0
		R00= 985.2568	985.2568	985.2574	985.2571	985.2567	985.2564	985.2561	985.2558	985.2556
		R00= 985.2552	985.2556	985.2556						

END OF OUTPUT FOR STEP 10 AT 0.1000 SECONDS *****

VIII. CONCLUDING REMARKS

The mathematical formulation underlying the COMMIX-SA-1 code has been detailed. COMMIX-SA-1 solves the three-dimensional, time-dependent conservation equations of continuity, momentum, and energy in cylindrical coordinates by a modified ICE finite-difference technique. The finite-difference equations have been presented, along with a hydraulic model to treat impermeable and perforated baffles, and a model that accounts for thermal interaction between fluid and structures (e.g., baffles and wall). The singularity problem encountered at the origin of the cylindrical-coordinate system has been discussed, and an integral treatment of the problem that deals with degenerate control volumes surrounding the origin has been described. The integral treatment resolves the singularity problem rigorously and efficiently, requiring little additional core storage and computer running time. The numerical-solution procedure based on the successive-overrelaxation (SOR) method has also been delineated, the SOR method being shown to be superior to other point-relaxation methods as regards computational efficiency. Treatment of the various boundary conditions as outlined has been greatly facilitated by the use of grouped fictitious boundary cells.

The code structure and input format have been described, and two sample problems presented, to aid users in setting up new problems. As stated earlier, COMMIX-SA-1 has been developed with the original objective of analyzing thermal-stratification phenomena in thermocline storage tanks. Subsequent application has, however, revealed its worth as a versatile design tool. Furthermore, the code is structured in modular format and is a suitable basis for further extension, which includes the ongoing modeling of rock beds and salt-gradient solar ponds. Future improvements on COMMIX-SA-1 are anticipated in the area of computational accuracy and efficiency. Such improvements will be reported in the near future, as will the work on rock beds and salt-gradient solar ponds.

The work presented in this report represents the close cooperation between the United States Nuclear Regulatory Commission (USNRC) and agencies within the United States Department of Energy (USDOE), since COMMIX-SA-1 code is a spin-off of the COMMIX-1 (Ref. 9) and COMMIX-IHX¹⁰ codes. The COMMIX-1 code is sponsored by the Reactor Safety Research Division of USNRC (Contract No. A2045), and the COMMIX-IHX code was developed under the auspices of the Reactor Research and Technology Division of USDOE.

APPENDIX A

A Simple Eddy-diffusivity Turbulence Model

An advanced turbulence model has been developed at ANL-CT, i.e., the three-equation (k - ϵ - g , or turbulence kinetic energy--dissipation rate of turbulence kinetic energy--scalar energy) continuum model.¹⁹ The model has also been implemented in COMMIX-IHX¹⁰ and is currently under study. However, in the range of applications anticipated for COMMIX-SA-1, particularly in the stratified heat-storage area (where stratification requires small flow velocity), turbulent effects are not considered important. Therefore, little effort has been spent on turbulence modeling within COMMIX-SA-1. Nevertheless, a simple eddy-viscosity-turbulence model has been used to serve as a rough guide whenever and wherever needed. Basically, the effective viscosity μ as occurring in Eqs. 9-15 and the effective thermal conductivity as occurring in Eq. 8 are regarded as consisting of two parts: the laminar and turbulent parts; i.e.,

$$\mu = \mu_\ell + \mu_t \quad (A.1)$$

and

$$K = K_\ell + K_t, \quad (A.2)$$

where μ_ℓ and K_ℓ are provided by the water-property package and μ_t and K_t are coded in COMMIX-SA-1 as input variables TURBV and TURBC, respectively. We can estimate μ_t according to⁹

$$\mu_t = 0.007 C_\mu \rho U_{\max} \ell, \quad (A.3)$$

where

$$C_\mu = \begin{cases} 0.1 & \text{Re}_{\max} > 2000 \\ 0.1(0.001\text{Re}_{\max} - 1) & \text{for } 1000 < \text{Re}_{\max} < 2000 \\ 0 & \text{Re}_{\max} < 1000 \end{cases}$$

$$U_{\max} = \max(u, v, w),$$

$$\text{Re}_{\max} = \max(\text{Re}_r, \text{Re}_\theta, \text{Re}_z),$$

and

$$\ell = \max(\Delta r, r \Delta \theta, \Delta z).$$

Once μ_t is known, K_t can be estimated from

$$K_t = \frac{C_\mu \mu_t}{\text{Pr}_t}, \quad (A.4)$$

where Pr_t is the turbulent Prandtl number, whose estimate requires an appropriate experimental correlation.

For future applications or future extensions of COMMIX-SA-1, the advanced turbulence model¹⁹ will be implemented as warranted.

APPENDIX B
Thermophysical Properties of Water

As mentioned in Sec. II.D, the water-properties package as used in COMMIX-SA-1 is the result of a cumulative effort by many individuals. Since the curve fitting on which the package is based was performed over a large pressure range, it is of interest to see how accurate the package is for the rather narrow range ($p = 1-2$ bars, and $T = 0-100^\circ\text{C}$) that concerns solar sensible heat-storage applications.

In the following plots of density (Fig. B.1), viscosity (Fig. B.2), specific heat (Fig. B.3), and conductivity (Fig. B.4), the calculated results from the package are presented as solid curves. These are compared with data points available from Keenan et al.,¹⁴ Eckert and Drake,²⁰ and Schlichting.²¹ As can be seen from the figures, the maximum deviation is 0.4% for density, 0.4% for specific heat, 1.5% for conductivity, and negligible for viscosity. These comparisons should lend confidence to the package being used and provide for convenient graphical references. For convenience, plots for kinematic viscosity (Fig. B.5), thermal diffusivity (Fig. B.6), and Prandtl number (Fig. B.7) are also included.

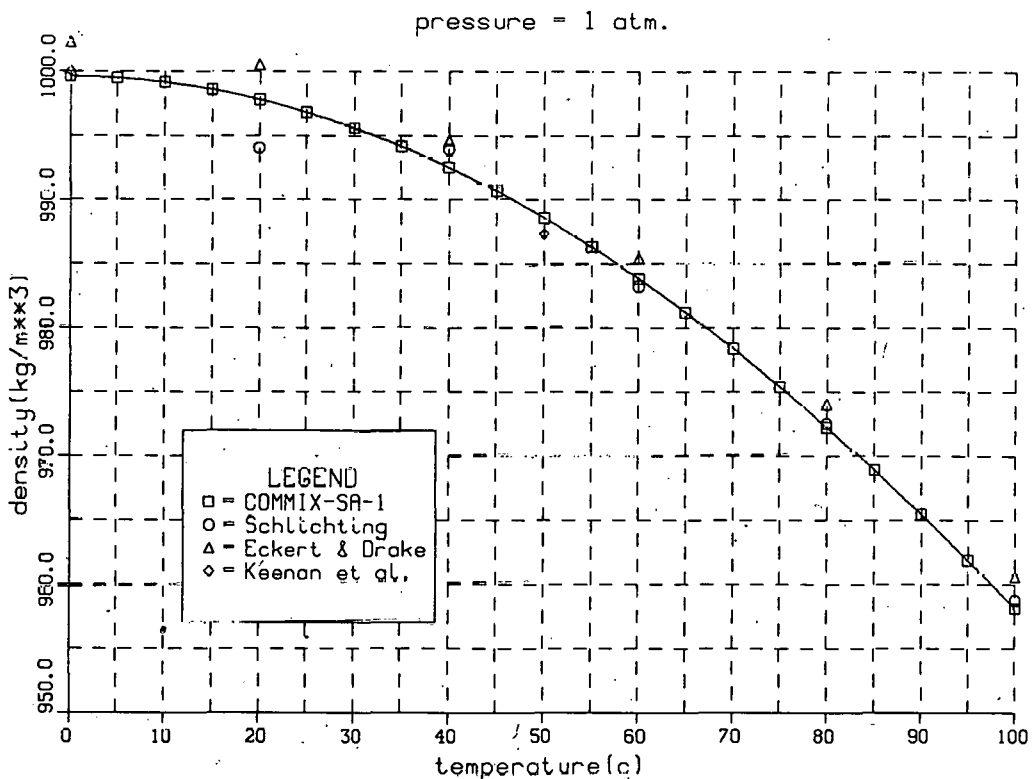


Fig. B.1. Density of Water as a Function of Temperature. Conversion factor: 1 atm = 0.1 MPa.

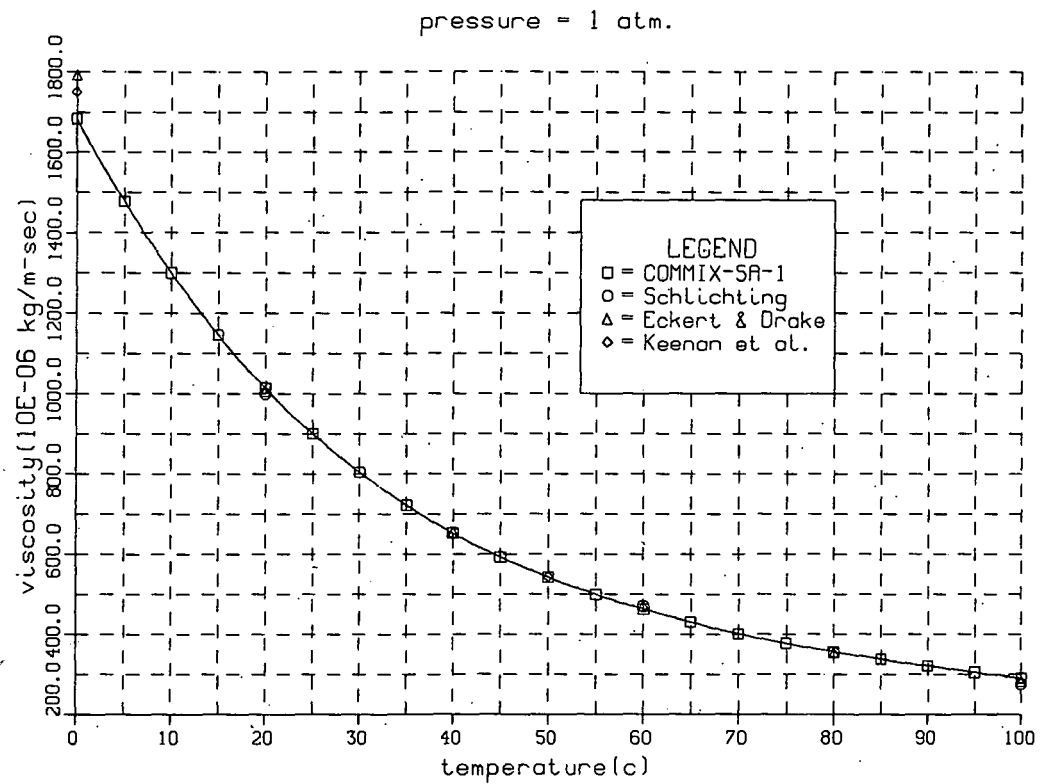


Fig. B.2. Viscosity of Water as a Function of Temperature. Conversion factor: 1 atm = 0.1 MPa.

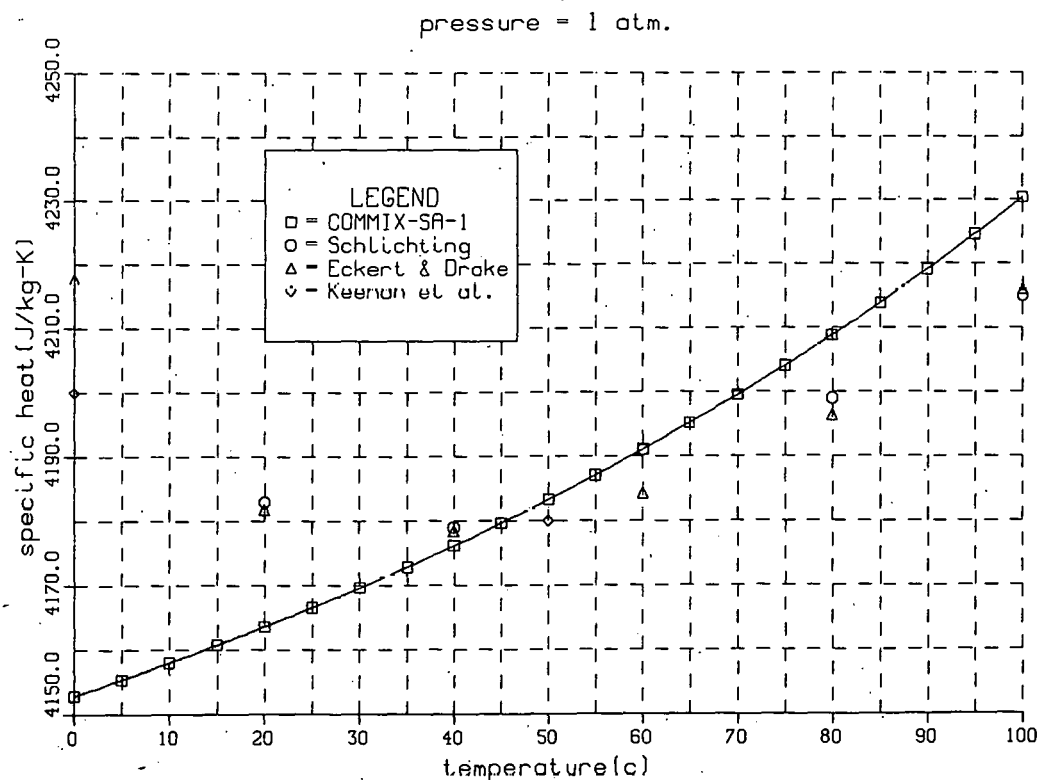


Fig. B.3. Specific Heat of Water as a Function of Temperature.
Conversion factor: 1 atm = 0.1 MPa.

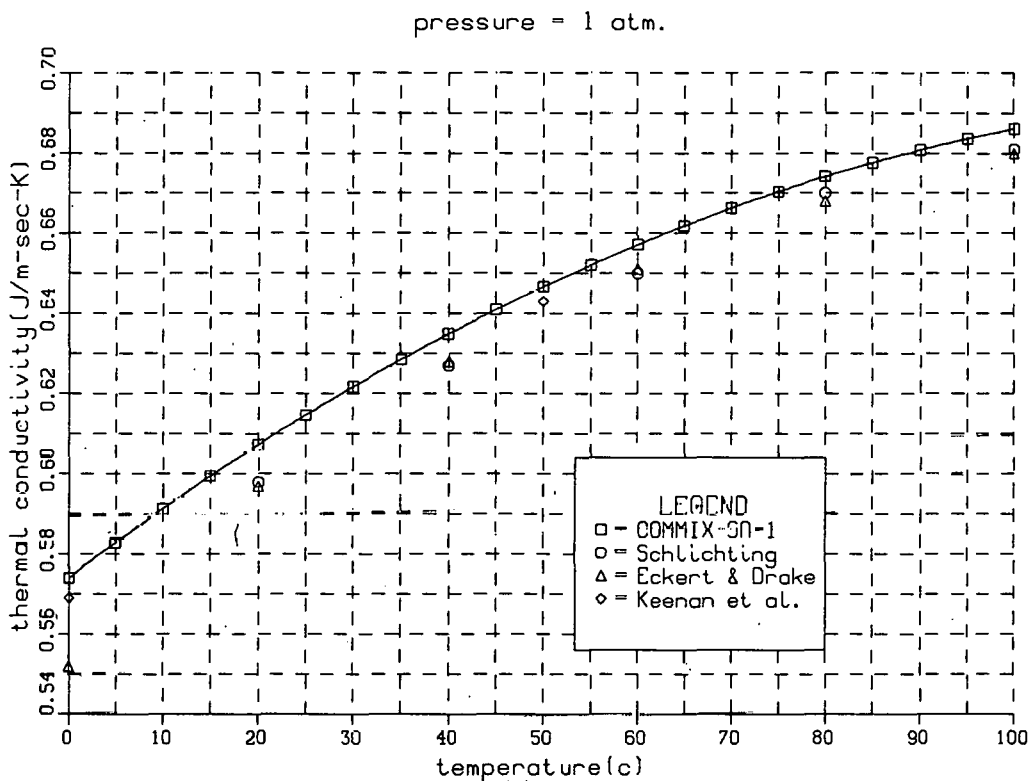


Fig. B.4. Thermal Conductivity of Water as a Function of Temperature.
Conversion factor: 1 atm = 0.1 MPa.

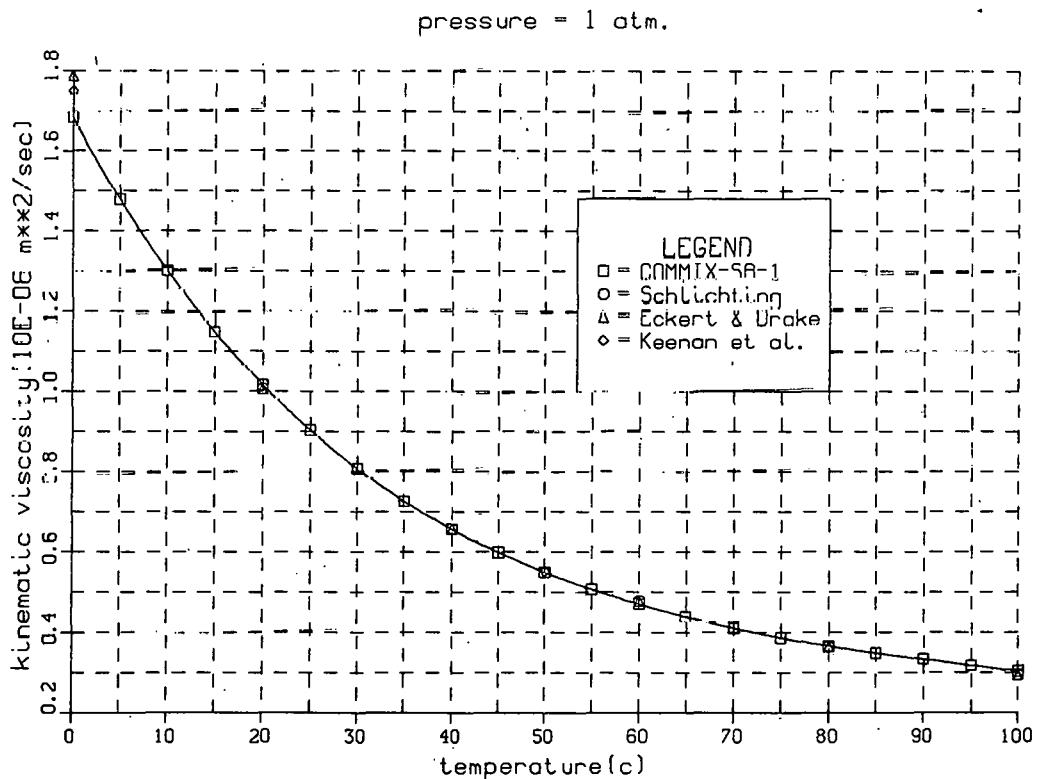


Fig. B.5. Kinematic Viscosity of Water as a Function of Temperature.
Conversion factor: 1 atm = 0.1 MPa.

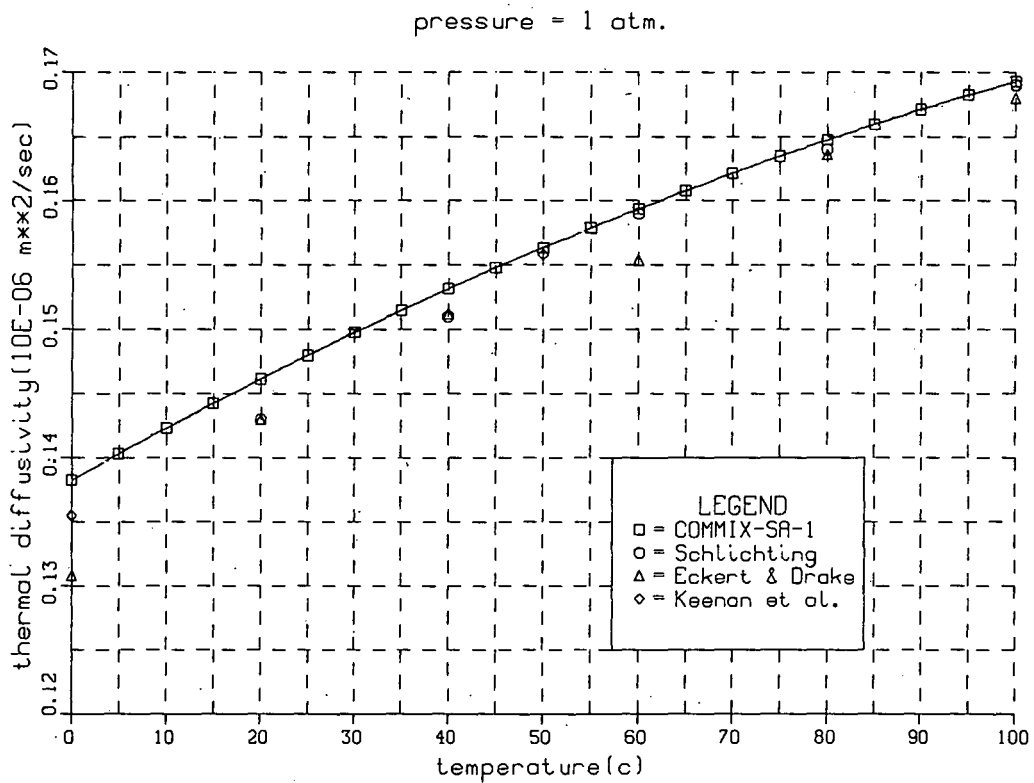


Fig. B.6. Thermal Diffusivity of Water as a Function of Temperature.
Conversion factor: 1 atm = 0.1 MPa.

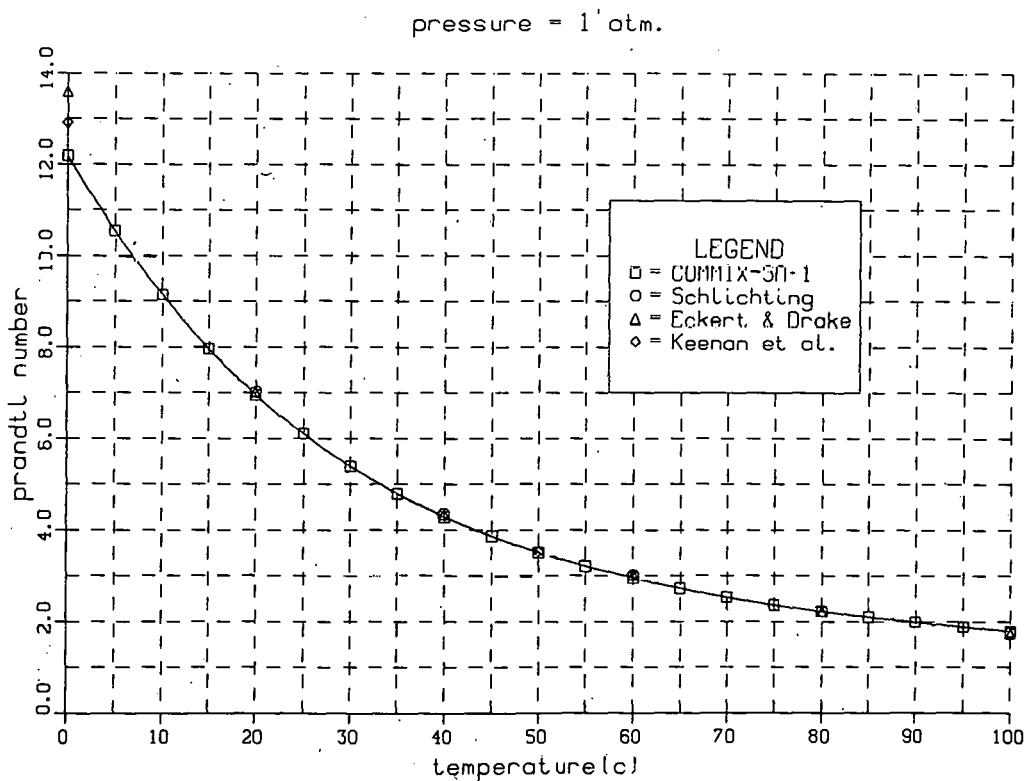


Fig. B.7. Prandtl Number of Water as a Function of Temperature.
Conversion factor: 1 atm = 0.1 MPa.

APPENDIX C

A Modified Successive Overrelaxation Iteration Scheme

The point Jacobi iterative method originally used in conjunction with the ICE finite-difference algorithm in the COMMIX-SA-1 code was demonstrated to possess relatively poor convergence properties. Through a sequence of numerical studies, the point successive overrelaxation (SOR) iterative method was shown to converge significantly faster than does the Jacobi method. A near-optimum overrelaxation parameter was determined for storage-tank geometry that is to be used in a sequence of parametric studies with baffled tanks. Further, a modified SOR method was devised and demonstrated to be superior to the usual SOR method with a near-optimum relaxation parameter. The results are summarized below.

Formally, after the governing PDE's are finite-differenced, a system of linear algebraic equations results:

$$AX = k, \quad (C.1)$$

where X represents the unknown pressure vector, k represents the vector with known components that have been explicitly evaluated by the momentum and continuity equations, and A is a square matrix having as its entries the derivatives of the cell residual masses with respect to pressure. Due to the use of donor-cell differencing in the continuity equation, some of the entries in matrix A may change values from one iteration to the next.

The matrix A can be decomposed as

$$A = D - E - F, \quad (C.2)$$

where D is a diagonal matrix consisting of the diagonal entries of A , and E and F are, respectively, the strictly lower and upper triangular matrices whose entries are the negatives of the entries of A respectively below and above the main diagonal.

The point Jacobi iterative method can then be written as

$$X^{n+1} = D^{-1}(E + F)X^n + D^{-1}k, \quad n \geq 0, \quad (C.3)$$

a procedure to calculate the $(n + 1)$ th iteratives from the n th iteratives of the unknown vector X .

On the other hand, the point successive relaxation method is prescribed by

$$\begin{aligned} X^{n+1} &= (I - \omega L)^{-1}[(1 - \omega)I + \omega U]X^n \\ &+ \omega(I - \omega L)^{-1}D^{-1}k, \quad n \geq 0, \end{aligned} \quad (C.4)$$

where I is the identity matrix, $L \equiv D^{-1}E$, $U \equiv D^{-1}F$, and ω is the relaxation parameter. For the method to work, it is required that $0 < \omega < 2$. With $\omega < 1$, the method is termed "underrelaxation"; with $\omega > 1$, "overrelaxation"; and with $\omega = 1$, "Gauss-Seidel."

In practice, with the Jacobi method, COMMIX-SA-1 would calculate first the residual masses for all cells, then pressure corrections for all cells, and then velocities for all cells, within one iteration. With the SOR method, COMMIX-SA-1 calculates, instead, the residual mass for one cell, the pressure correction for the same cell, and velocities associated with the same cell, and then moves on to the next cell; while performing the same sequence of calculations in the next cell, SOR makes use of the newly calculated pressure and velocities associated with the previous cell. In cylindrical geometry, the order of sweeping is usually first in I (r direction), then in J (θ direction), and then in K (z direction), for both the Jacobi and SOR methods.

However, although the matrix A is diagonally dominant, in cylindrical coordinates the values of its diagonal entries vary substantially. Related to this, it was also observed that residual masses always assume the largest values in the first ring around the center (i.e., $I = 1$). Both observations can be explained if the finite-differenced continuity equation is examined, and the inherent nonuniformity of the $r\Delta\theta$ mesh spacing borne in mind. A modified SOR method then emerged: Sweep first in J (θ direction); repeat the J sweep once or twice for $I = 1$; then sweep in I (r direction); then sweep in K (z direction). This is a simple modification, yet it achieves a better rate of convergence as can be seen from the following results.

Figure C.1 is a plot of the absolute value of the maximum residual mass, $|D_{\max}|$, versus the number of iterations, as obtained from several cylindrical-storage-tank heat-discharge runs. Based on information presented in this figure, the following conclusions are drawn:

1. The SOR method affords a distinctly better rate of convergence than do the Gauss-Seidel and Jacobi methods.
2. The empirically determined optimal value for the overrelaxation factor ω for the tank geometry and the range of parameters in question is near 1.8.
3. The modified SOR method proves to be noticeably better than the usual SOR method and is hence worth recommending.
4. To achieve the same order of accuracy, the Jacobi method needs 4.7-6.5 times more iteration than the modified SOR method.
5. The convergence criteria as shown in Fig. C.1 were calculated based on the maximum velocity in the flow field and some arbitrarily assigned parameters. The fact that most curves in Fig. C.1 level off after about 200 iterations indicates that truncation error is likely a determining factor. Therefore, it seems a more reasonable convergence criterion should be based on the truncation error.

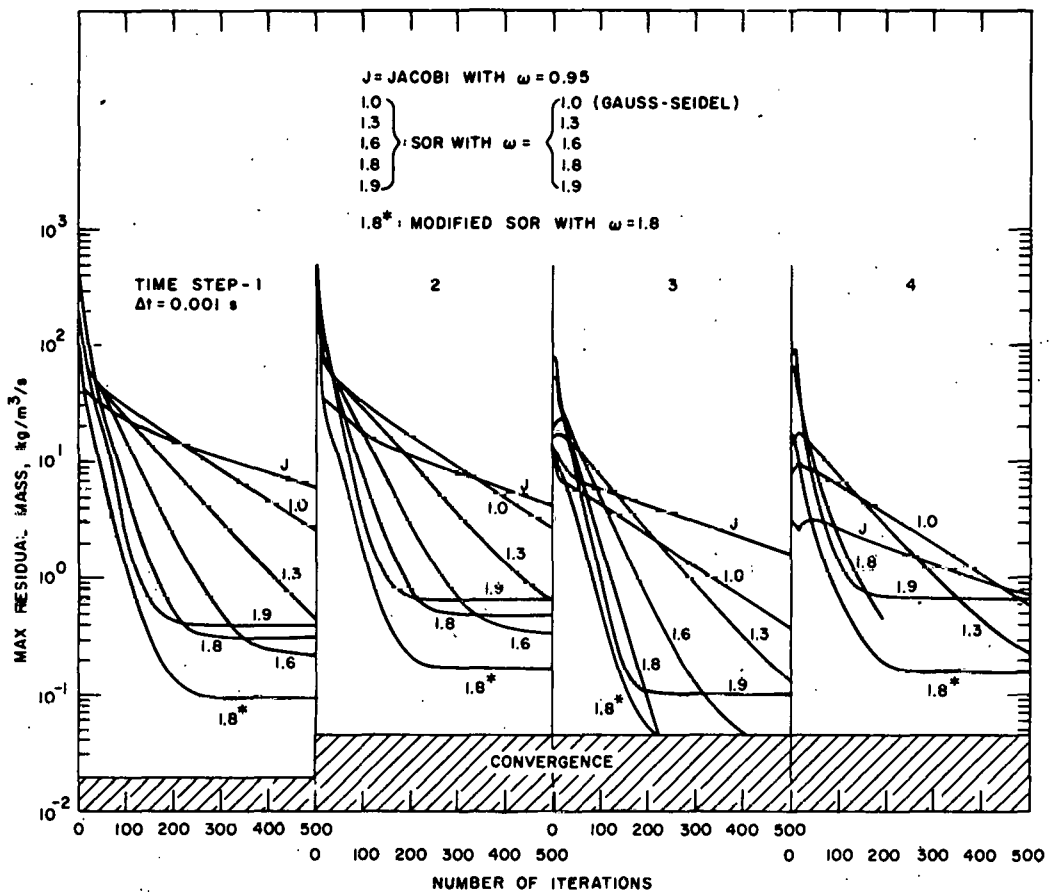


Fig. C.1. Convergence Properties of Various Point-relaxation Methods

All the cases presented in Fig. C.1 were computed with the uniform time step size $\Delta t = 0.001$ s. To see if the use of different time-step sizes would alter the above conclusions, additional cases were run with Δt equal to 0.01, 0.1, and 0.45 s, respectively. The results are presented in Fig. C.2, and it is clear that the effects of time-step size are negligible. These results also point out that it is not necessary to start off a transient calculation with a very small time step; in fact, almost any time step meeting the stability requirements can do equally as well as a very small time step, as far as accuracy is concerned.

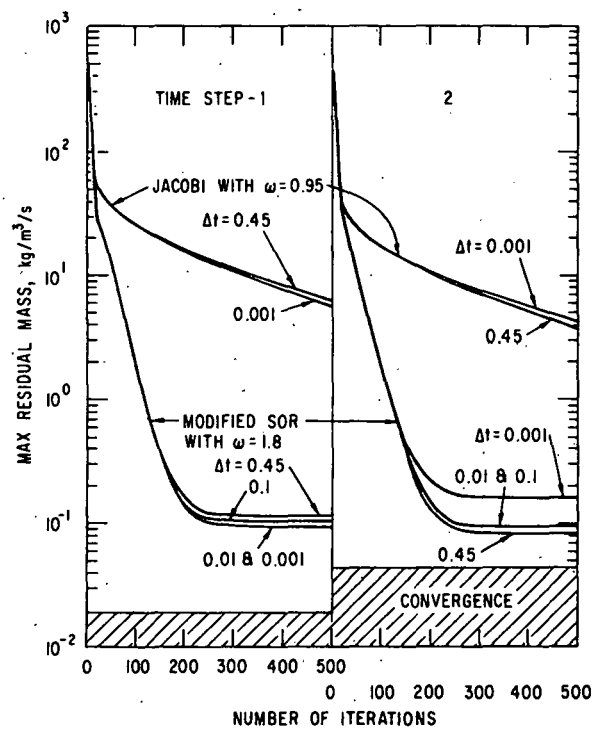


Fig. C.2
Effects of Time-step Size on Convergence Properties of the Jacobi and SOR Methods

ACKNOWLEDGMENTS

We gratefully acknowledge the support and encouragement provided by Mr. J. M. Davis and Dr. S. Sargent of DOE, and Drs. A. I. Michaels, J. J. Peerson, and W. W. Schertz of the Office of Solar Applications, ANL. The developmental work for COMMIX-SA-1 benefited greatly from the COMMIX-1 code, which was sponsored by the Reactor Safety Research Division, USNRC. We are indebted to Drs. R. T. Curtis, C. N. Kelber, and Mr. P. M. Wood of the USNRC for their cooperation. COMMIX-SA-1 was developed under the auspices of the System Development Division, Office of Solar Applications, USDOE.

REFERENCES

1. E. I. H. Lin, W. T. Sha, and A. I. Michaels, "On Thermal Energy Storage Efficiency and the Use of COMMIX-SA for its Evaluation and Enhancement," *Proc. Solar Energy Storage Options Workshop*, San Antonio, Texas, 501-513 (Mar 1979).
2. G. Gutierrez, F. Hincapie, J. A. Duffie, and W. A. Beckman, *Simulation of Forced Circulation Water Heaters; Effects of Auxiliary Energy Supply, Load Type and Storage Capacity*, Sol. Energy 15, 287 (1974).
3. D. J. Close, *A Design Approach for Solar Processes*, Sol. Energy 11, 112 (1967).
4. S. A. Klein et al., *TRNSYS, A Transient Simulation Program*, Engineering Experiment Station Report 38, Solar Energy Laboratory, The University of Wisconsin, Madison (Dec 1976).
5. A. Cabelli, *Storage Tanks--A Numerical Experiment*, Sol. Energy 19, 45-54 (1977).
6. W. T. Sha and E. I. H. Lin, "Three-Dimensional Mathematical Model of Flow Stratification in Thermocline Storage Tanks," *Application of Solar Energy 1978*, ed., S. T. Wu et al., pp. 185-202, UAH Press (1978).
7. E. I. H. Lin and W. T. Sha, "Effects of Baffles on Thermal Stratification in Thermocline Storage Tanks," *Proc. Int. Solar Energy Society Meeting*, Atlanta, Ga. (June 1979).
8. W. T. Sha, R. C. Schmitt, and E. I. H. Lin, *THI3D-1, A Computer Program for Steady-state Thermal-hydraulic Multichannel Analysis*, ANL-77-15 (July 1977).
9. W. T. Sha, H. M. Domanus, R. C. Schmitt, J. J. Oras, and E. I. H. Lin, *COMMIX-1: A Three-dimensional Transient Single-phase Component Computer Program for Thermal-hydraulic Analysis*, ANL-77-96, NUREG/CR-0785 (Sept 1978).
10. W. T. Sha, J. J. Oras, C. I. Yang, H. M. Domanus, R. C. Schmitt, T. T. Kao, H. L. Chou, and S. M. Cho, *COMMIX-IHX: A Three-dimensional, Transient, Single-phase Computer Program for LMFBR-IHX Thermal-hydraulic Analysis*, ANL-79-31 (to be published).

11. R. J. Kee and A. A. McKillop, *A Numerical Method for Predicting Natural Convection in Horizontal Cylinders with Asymmetric Boundary Conditions*, *Comput. Fluids* 5, 1-14 (1977).
12. E. I. H. Lin and W. T. Sha, *On Singularities in the Three-dimensional Navier-Stokes Equations*, *Trans. Am. Nucl. Soc.* 30, 212 (1978).
13. F. H. Harlow and A. A. Amsden, *A Numerical Fluid Dynamics Calculation Method for All Flow Speeds*, *J. Comp. Phys.* 8, 197 (1971).
14. J. H. Keenan, F. G. Keyes, P. G. Hill, and J. G. Moore, *Steam Tables*, John Wiley & Sons, Inc. (1969).
15. W. B. Jordan, *Fits to Thermodynamic Properties of Water*, KAPL-M-6734 (1967).
16. Engineering Sciences Data Item No. 72010, *Pressure Losses Across Perforated Plates, Orifice Plates and Cylindrical Tube Orifices in Ducts*, Engineering Sciences Data Unit Ltd., U.K. (1972).
17. W. M. Rohsenow and H. Y. Choi, *Heat, Mass and Momentum Transfer*, Prentice-Hall (1961).
18. A. A. Amsden and F. H. Harlow, *KACHINA: an Eulerian Computer Program for Multifield Fluid Flows*, LA-5680 (1974).
19. W. T. Sha and B. E. Launder, *A General Model for Turbulent Momentum and Heat Transport in Liquid Metals*, ANL-77-78 (Mar 1979).
20. E. R. G. Eckert and R. M. Drake, Jr., *Analysis of Heat and Mass Transfer*, McGraw-Hill (1972).
21. H. Schlichting, *Boundary-Layer Theory*, McGraw-Hill (1968).

Distribution for ANL-80-8Internal:

W. E. Massey	J. F. Schumar	R. C. Schmitt
J. J. Roberts	R. Mueller	Y. S. Cha
W. W. Schertz	K. Nield	J. G. Bartzis
A. I. Michaels	R. S. Zeno	M. R. Sims
J. J. Peerson	G. S. Rosenberg	A. B. Krisciunas
R. L. Cole	P. R. Huebotter	ANL Contract File
P. Chopra	W. T. Sha (21)	ANL Libraries (2)
K. A. Reed	E. I. H. Lin	TIS Files (6)
	K. V. Liu	

External:

DOE-TIC, for distribution per UC-62 (301)
 Manager, Chicago Operations and Regional Office, DOE
 Chief, Office of Patent Counsel, DOE-CORO
 F. Claski, DOE-CORO
 D. Kung, DOE-CORO
 S. Sargent, DOE-CORO
 President, Argonne Universities Association
 Components Technology Division Review Committee:

F. W. Buckman, Consumers Power Co.
 R. A. Greenkorn, Purdue U.
 W. M. Jacobi, Westinghouse Electric Corp., Pittsburgh
 M. A. Schultz, North Palm Beach, Fla.
 J. Weisman, U. Cincinnati
 J. Andrews, Brookhaven National Lab.
 J. D. Balcomb, Los Alamos Scientific Lab.
 F. Baylin, Solar Energy Research Inst.
 W. A. Beckman, U. Wisconsin-Madison
 C. Bishop, Solar Energy Research Inst.
 R. C. Bourne, Solar Concept Development, Davis, Calif.
 H. M. Curran, Hittman Associates, Inc., Columbia, Md.
 J. M. Davis, Office of Solar Applications, DOE
 F. de Winter, ATLAS Corp., Santa Cruz
 W. Dickinson, Lawrence Livermore Lab.
 J. Dollard, Office of Solar Applications, DOE
 D. M. Eissenberg, Oak Ridge National Lab.
 J. Gahimer, Office of Solar Applications, DOE
 L. H. Gordon, NASA Lewis Research Center
 L. Groome, Solar Energy Research Inst.
 W. R. Haas, Martin Marietta Corp., Denver
 J. Hale, Office of Solar Applications, DOE
 T. D. Harrison, Sandia Lab., Albuquerque
 M. Holtz, Solar Energy Research Inst.
 W. Kahan, Singer Corp., Fairfield, N. J.
 S. Karaki, Colorado State U.
 R. J. Kedl, Oak Ridge National Lab.
 M. K. Kim, Harvard U.
 F. Kreith, Solar Energy Research Inst.
 J. K. Kuhn, Boeing Computer Services, Tukwila, Wash.
 Z. Lavan, Illinois Inst. Technology

G. Lof, Colorado State U.
H. G. Lorsch, Franklin Research Center, Philadelphia
M. Maybaum, Office of Solar Applications, DOE
R. N. Misra, Ohio Agricultural R&D Center, Wooster
J. W. Mitchell, U. Wisconsin-Madison
F. Morse, Office of Solar Applications, DOE
D. Neerer, Los Alamos Scientific Lab.
C. E. Nielsen, Ohio State U.
P. Offenhartz, EIC Corp., Newton, Mass.
S. Paolucci, Sandia Lab., Livermore
L. E. Shaw, Solaron Corp., Denver
B. Shelpuk, Solar Energy Research Inst.
T. H. Short, Ohio Agricultural R&D Center, Wooster
C. J. Swet, Mt. Airy, Md.
M. Wahlig, Lawrence Berkeley Lab.
B. Winters, Sandia Lab., Livermore
L. J. Wittenberg, Monsanto Research Corp., Miamisburg
N. Woodley, Solar Energy Research Inst.
K. T. Yang, U. Notre Dame
R. J. Youngberg, Nebraska State Solar Office, Lincoln
F. C. Hooper, U. Toronto, Canada
T. R. Tamblyn, Engineering Interface, Ltd., Willowdale, Canada
J. Claesson, U. Lund, Sweden